Report No. K-TRAN: KSU-04-6
FINAL REPORT

DEVELOPMENT OF STIFFNESS-BASED SPECIFICATIONS FOR IN-SITU EMBANKMENT COMPACTION QUALITY CONTROL

James S. Petersen
Stefan A. Romanoschi, Ph.D., P.E.
Mustaque Hossain, Ph.D., P.E.
Kansas State University
Manhattan, KS

August 2007

A COOPERATIVE TRANSPORTATION RESEARCH PROGRAM
BETWEEN:

KANSAS DEPARTMENT OF TRANSPORTATION
KANSAS STATE UNIVERSITY
UNIVERSITY OF KANSAS

1 Report No. K-TRAN: KSU-04-6	2 Government Accession No.	3 Recipient Catalog No.
4 Title and Subtitle DEVELOPMENT OF STIFFNESS-BASED SPECIFICATIONS FOR IN-SITU EMBANKMENT COMPACTION QUALITY CONTROL		5 Report Date August 2007 6 Performing Organization Code
7 Author(s) James S. Petersen, Stefen A. Romanoschi, Ph.D., P.E., Mustaque Hossain, Ph.D., P.E.		8 Performing Organization Report No.
9 Performing Organization Name and Address Kansas State University Department of Civil Engineering 2118 Fiedler Hall Manhattan, KS 66506-2905		10 Work Unit No. (TRAIS) 11 Contract or Grant No. C1402
12 Sponsoring Agency Name and Address Kansas Department of Transportation Bureau of Materials and Research 700 SW Harrison Street Topeka, Kansas 66603-3745		13 Type of Report and Period Covered Final Report Summer 2006 - Spring 2007 14 Sponsoring Agency Code RE-0341-01
15 Supplementary Notes For more information write to address in block 9.		

16 Abstract

Compaction of embankment soils is a key factor influencing premature pavement distresses and bridge approach settlement. The current specifications of the Kansas Department of Transportation (KDOT) address embankment compaction in terms of density and moisture content. However, the implementation of performance-based specifications would require measuring mechanical properties of soil, such as stiffness, in addition to density. This is needed because soil stiffness is the parameter used to characterize the embankment soil in the design of pavement structures.

The objectives of this study were to investigate the use of the Light Falling Weight Deflectometer (L-FWD) to measure in-situ soil stiffness and to investigate the feasibility of developing a stiffness-based specification for embankment soil compaction quality control. To achieve these objectives, soil stiffness values were measured at multiple locations along nine KDOT embankment projects using the Prima 100 L-FWD. Concurrent density and moisture measurements were also taken at select locations. Bulk soil samples were collected and remolded soil samples were used to measure the resilient moduli of the soils in the laboratory at varying density and moisture contents. For each soil, and at each combination moisture content and dry density level used in the laboratory tests, a constitutive model was derived from the laboratory resilient modulus data to capture the stress-dependent behavior of the soil. The constitutive model was then implemented in a finite element model of a semi-infinite soil half-space to compute the deflection at the surface of the half-space for a circular load. An equivalent elastic modulus for the soil half-space was back-estimated with the Boussinesque formula, for each combination moisture content and dry density. A regression model was then developed to relate the equivalent elastic modulus of the soil half-space to the dry density and moisture content of the soil. The regression model was used to predict the equivalent elastic moduli for the in-situ moisture contents and dry density values recorded during the field L-FWD tests. The predicted equivalent moduli were then compared to the moduli measured by the L-FWD.

It was found that the equivalent moduli predicted from the results of the laboratory resilient modulus tests do not correlate with the in-situ soil stiffness measured with the L-FWD. This prevented the development of a quality control scheme based on laboratory measured resilient moduli. The high degree of spatial variability obtained for the in-situ moduli measured with the L-FWD prevented the development of a quality control scheme based on a control test strip.

17 Key Words	18 Distribution Statement
Light Falling Weight Deflectometer, pavement, embankment soils, stiffness tests, soil compaction	No restrictions. This document is available to the public through the National Technical Information Service, Springfield, Virginia 22161

19 Security Classification (of this report)	20 Security Classification (of this page)	21 No. of pages	22 Price
Unclassified	Unclassified	120	

Form DOT F 1700.7 (8-72)

DEVELOPMENT OF STIFFNESS-BASED SPECIFICATIONS FOR IN-SITU EMBANKMENT COMPACTION QUALITY CONTROL

Final Report

Prepared for

Kansas Department of Transportation

by

James S. Petersen
Stefan A. Romanoschi, Ph.D., P.E.
Mustaque Hossain, Ph.D., P.E.

Department of Civil Engineering
2118 Fiedler Hall
Kansas State University
Manhattan, KS 66506-2905

August 2007

A Report on Research Sponsored By

THE KANSAS DEPARTMENT OF TRANSPORTATION
TOPEKA, KANSAS

PREFACE

The Kansas Department of Transportation's (KDOT) Kansas Transportation Research and New-Developments (K-TRAN) Research Program funded this research project. It is an ongoing, cooperative and comprehensive research program addressing transportation needs of the state of Kansas utilizing academic and research resources from KDOT, Kansas State University and the University of Kansas. Transportation professionals in KDOT and the universities jointly develop the projects included in the research program.

NOTICE

The authors and the state of Kansas do not endorse products or manufacturers. Trade and manufacturers' names appear herein solely because they are considered essential to the object of this report.

This information is available in alternative accessible formats. To obtain an alternative format, contact the Office of Transportation Information, Kansas Department of Transportation, 700 SW Harrison, Topeka, Kansas 66603-3745 or phone (785) 296-3585 (Voice) (TDD).

DISCLAIMER

The contents of this report reflect the views of the authors who are responsible for the facts and accuracy of the data presented herein. The contents do not necessarily reflect the views or the policies of the state of Kansas. This report does not constitute a standard, specification or regulation.

ABSTRACT

Compaction of embankment soils is a key factor influencing premature pavement distresses and bridge approach settlement. The current specifications of the Kansas Department of Transportation (KDOT) address embankment compaction in terms of density and moisture content. However, the implementation of performance-based specifications would require measuring mechanical properties of soil, such as stiffness, in addition to density. This is needed because soil stiffness is the parameter used to characterize the embankment soil in the design of pavement structures.

The objectives of this study were to investigate the use of the Light Falling Weight Deflectometer (L-FWD) to measure in-situ soil stiffness and to investigate the feasibility of developing a stiffness-based specification for embankment soil compaction quality control. To achieve these objectives, soil stiffness values were measured at multiple locations along nine KDOT embankment projects using the Prima 100 L-FWD. Concurrent density and moisture measurements were also taken at select locations. Bulk soil samples were collected and remolded soil samples were used to measure the resilient moduli of the soils in the laboratory at varying density and moisture contents. For each soil, and at each combination moisture content and dry density level used in the laboratory tests, a constitutive model was derived from the laboratory resilient modulus data to capture the stress-dependent behavior of the soil. The constitutive model was then implemented in a finite element model of a semi-infinite soil half-space to compute the deflection at the surface of the half-space for a circular load. An

equivalent elastic modulus for the soil half-space was back-estimated with the Boussinesque formula, for each combination moisture content and dry density. A regression model was then developed to relate the equivalent elastic modulus of the soil half-space to the dry density and moisture content of the soil. The regression model was used to predict the equivalent elastic moduli for the in-situ moisture contents and dry density values recorded during the field L-FWD tests. The predicted equivalent moduli were then compared to the moduli measured by the L-FWD.

It was found that the equivalent moduli predicted from the results of the laboratory resilient modulus tests do not correlate with the in-situ soil stiffness measured with the L-FWD. This prevented the development of a quality control scheme based on laboratory measured resilient moduli. The high degree of spacial variability obtained for the in-situ moduli measured with the L-FWD prevented the development of a quality control scheme based on a control test strip.

TABLE OF CONTENTS

LIST OF TABLES

LIST OF FIGURES

CHAPTER ONE - INTRODUCTION

1.1 Introduction

The pavement foundation layers perform several functions both during construction and while in-service. They reduce the stresses transmitted to the subgrade to acceptable levels, particularly when used as a temporary haul road during construction, and constitute the construction platform so that overlying pavement layers can be adequately compacted/consolidated. In the long term the foundation must provide sufficient support to prevent premature flexural fatigue cracking in the structural layers. In order to fulfill these functions, the foundation materials must have adequate strength and resistance to permanent deformation or, in other words, to prevent the accumulation of permanent strain within the materials.

The specifications of the Kansas Department of Transportation (KDOT) for the construction of unbound foundation layers for pavements contain requirements for the compaction level, expressed in terms of relative density (the ratio between the dry density and the maximum dry density) at a certain range of moisture content and layer thickness. This process does not necessarily guarantee the performance of the materials, but it is assumed to be adequate based on past experience and engineering judgment. However, for some cases it can be inefficient, since the specified values do not appropriately address the use of stabilized, recycled or marginal materials. It also does not indicate what measures need to be taken to assure the future performance of the foundations layer and of the pavement structure (e.g., how much influence the as-built foundation layer quality has on the thickness of the overlaying pavement structure). If a performance-based specification that takes directly into account the required

material performance parameters can be implemented, the many previously untried materials can be readily introduced. In addition, by directly measuring the performance parameters of the foundation materials as they are being constructed, greater assurance of the design and efficiency of site operations is anticipated.

The objectives of in-situ assessment of foundation layers are to ensure that the overlying layers can be adequately compacted and that acceptable trafficking performance will be achieved during and after construction (i.e. control of rutting/material disturbance). This requires the assessment of both the stiffness and the resistance to permanent deformation of the composite foundation under construction.

Research has been undertaken over the past few years to develop dynamic stiffness measuring devices that can quickly measure the stiffness of the subgrade and other foundation layers during construction. The PRIMA 100 device measures a composite stiffness under a transient load pulse, which is applied to the ground by dropping a weight onto a bearing plate via a rubber buffer. This portable device is a Light Falling Weight Deflectometer (L-FWD), named so because it is based on the same principle as the Falling Weight Deflectometer (FWD). The deflection of the ground is measured and combined with the applied load, which is either measured or is assumed to be constant (by means of a constant drop height), to calculate the stiffness using conventional Boussinesq static analysis.

However, research is needed to develop an efficient methodology for using the stiffness of the foundation layers, as measured by the L-FWD, to estimate the performance of these layers during construction and during the service of the pavement.

1.2 Problem Statement

The current Kansas Department of Transportation (KDOT) specification for the construction of soil embankments contains requirements for the compaction level at a certain range of moisture contents and layer thicknesses, where compaction is expressed in terms of percent compaction computed from the dry density determined in AASHTO T99. While this has proved to be an acceptable method for governing the construction of soil embankments since it reduces the possibility of detrimental settlements, it does not guarantee the performance of the embankment during in-service conditions and that the layer stiffness assumed in the structural design of the pavement is achieved. By directly measuring the stiffness of the soil embankment, it can be assured that the embankment compaction reaches the assumed stiffness value used in the pavement design. This will ensure a proper support to the pavement structure during service conditions.

1.3 Objectives

The objectives of this research are:

• To investigate the suitability of L-FWD for in-situ measurement of foundation layer(s) stiffness;

• To develop a correlation between the measured stiffness, compaction level, and the performance of the layers as support for the upper layers during construction and during regular service;

• To develop recommended stiffness values for the foundation layers to ensure adequate performance during construction and in service for use in performance-based specifications.

CHAPTER TWO - BACKGROUND

2.1 Introduction

Unsatisfactory compaction of the embankment layer of a pavement system can lead to a variety of pavement failures in the future. The subgrade plays a critical role in prevention of these failures. The development of a performance based compaction specification could assure that the subgrade is constructed with adequate strength to prevent early failure of the pavement system. This chapter discusses the testing methods currently used for compaction quality control, the associated testing equipment, and the quality control schemes.

2.2 Embankment Compaction

The compaction of the lower layers of a pavement system has a direct influence on the performance of the pavement throughout its life. The methods used to measure the quality of soil compaction of the various components of a pavement system are discussed in this section.

2.2.1 Components of a Pavement System

Pavements are layered structures composed of a combination of subbase, base course, and surface course atop a subgrade. Each of these components plays a specific role in the performance of a pavement system. A cross section of a basic pavement system can be seen in Figure 2.1.

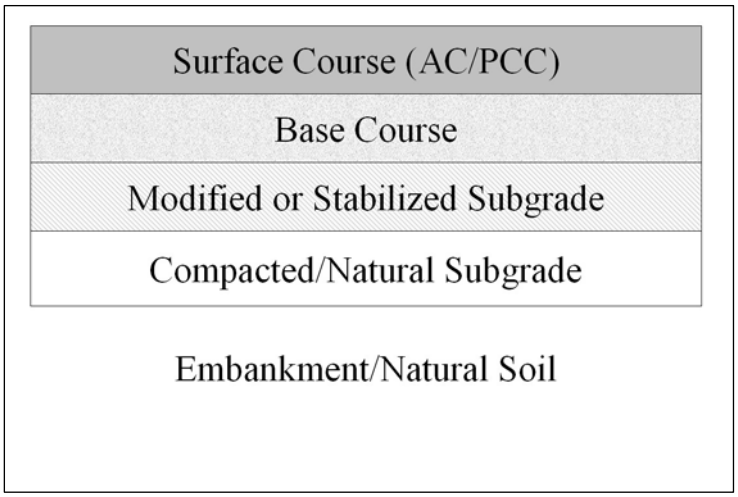

Figure 2.1: Components of a Basic Pavement System

The layer of focus for this project is the subgrade. The subgrade provides a platform on which the pavement is constructed and supports the pavement with a foundation that resists undue deflection that could affect pavement performance. When pavements are constructed in a cut or at-grade, the subgrade consists of the natural in-situ soil. The top layer of this soil may be compacted and/or stabilized in order to increase the layer's strength, stiffness, and stability. For a pavement constructed on embankment fills, the subgrade consists of compacted borrow material.

Immediately on top of the subgrade is the subbase. The subbase consists of a layer or layers of materials placed to provide support for the base. Subbases are most common when subgrade materials are of inferior quality and/or suitable base materials are hard to come by. The subbase layer also prevents fine-grained subgrade soils from entering the base layer, minimizes the damage of frost action, provides drainage for free water within the pavement system, and provides a working platform for construction of the upper layers when the subgrade soil does not have sufficient strength to provide support.

The next component is the base layer. The base layer consists of a layer or layers of specific materials designed to provide uniform and stable support for the surface courses. Typically the base layer consists of high quality aggregates such as crushed stone, gravel, or sand. The base layer provides a large percentage of the structural capacity in a flexible pavement system, and enhances the foundation stiffness in a rigid pavement system.

The top layer in a pavement system is the surface course. The surface course is designed to accommodate the traffic load and distribute the stresses safely to the underlying pavement layers. The surface course is made up of either asphalt in flexible pavements or Portland cement concrete in rigid pavements. It provides the remainder of the structural capacity of the pavement, in addition to preventing the infiltration of surface water, providing a smooth, uniform, skid-resistant driving surface, and protecting the pavement system against traffic abrasion and climate.

Other geotechnical components of a pavement system can include: surfacing aggregate, unbound granular base, unbound granular subbase, and mechanically and/or chemically stabilized subgrade. Aggregate and geosynthetics used in drainage systems, graded granular aggregate and geosynthetic used to separate filtration layers, and the roadway embankment foundation are also geotechnical components of the pavement system (FHWA, 2005).

2.2.2 Influence of Foundation Layers on the Performance of Pavements Structures

Each component of a pavement system plays a critical role in the overall performance of the pavement. If any component is improperly designed or constructed, the pavement will likely suffer from reduced serviceability and premature failure.

Pavement failure can occur due to a variety of reasons. These reasons include: intrusion of subgrade soils into the granular base, excessive loads that cause shear failure in the subgrade, base course, or surface, surface fatigue and excessive settlement. The changing volume of the subgrade due to moisture fluctuation or freezing and thawing can also cause pavement distress. These problems are most often due to inadequate drainage.

For the geotechnical components of a pavement system, the main factors leading to pavement distress are the stiffness and strength of the unbound materials. If the subgrade and/or base of a pavement system have insufficient stiffness and strength, the pavement will be likely to fail. The cause of failure due to the subgrade and base varies between flexible pavements, rigid pavements, and composite pavements, i.e. an asphalt overlay over Portland cement concrete.

In flexible pavements, the subgrade stiffness is very important in preventing fatigue cracking, rutting, and roughness over time. If the subgrade stiffness is insufficient, these problems will be more prevalent. The base also contributes to guarding against failure in flexible pavements. Insufficient base stiffness and strength can lead to fatigue cracking, rutting, corrugations, depressions, and roughness.

For rigid pavements, the subgrade and base also play a key role in prolonging the life of the pavement. An insufficient subgrade can lead to premature fatigue cracking, in addition to pumping. A poorly constructed base can also contribute to premature fatigue cracking, punch outs, faulting, and roughness.

The subgrade and base are also important to the performance of rehabilitated pavements. A base with an insufficient strength and/or stiffness can lead to reflection cracking and increased roughness of the pavement surface (FHWA 2005).

2.2.3 Laboratory Compaction Tests

Compaction of soil is defined as the application of mechanical forces to increase the density of the soil matrix through the removal of air from the soil. Increased strength, reduced permeability and reduced settlement are the desired characteristics of a properly compacted soil.

The Proctor test, which was developed in the early 1930's by R.R. Proctor, is the standard laboratory compaction procedure to simulate field compaction. The tests provide a basis for which the field testing results are compared. The Standard Proctor test uses a 943.89 cm3 mold which is 0.102 m in diameter. Soil is added to the mold in 3 equal lifts and compacted by 25 blows of a 2.495 kg hammer falling 0.305 m per lift. This test applies 593 kJ/m3 of compaction energy into the molded soil (Das, 1998).

Following the development of heavier rollers, Proctor developed a revised version of his standard test called the Modified Proctor Test. This test attempted to simulate the compaction forces of the newer heavier compaction equipment. The Modified Proctor test applies more compaction energy by adding soil in 5 lifts, and compacting the soil using 25 blows per lift of a 4.536 kg hammer falling 0.457 m. With

these changes, the compaction energy imparted onto the molded soil is increased to 2,693 kJ/m^3 (Das, 1998).

Proctor developed moisture density relationships for soil by testing a series of soil specimens. From these tests, he was able to draw the parabolic moisture density graphs as shown in Figure 2.2.

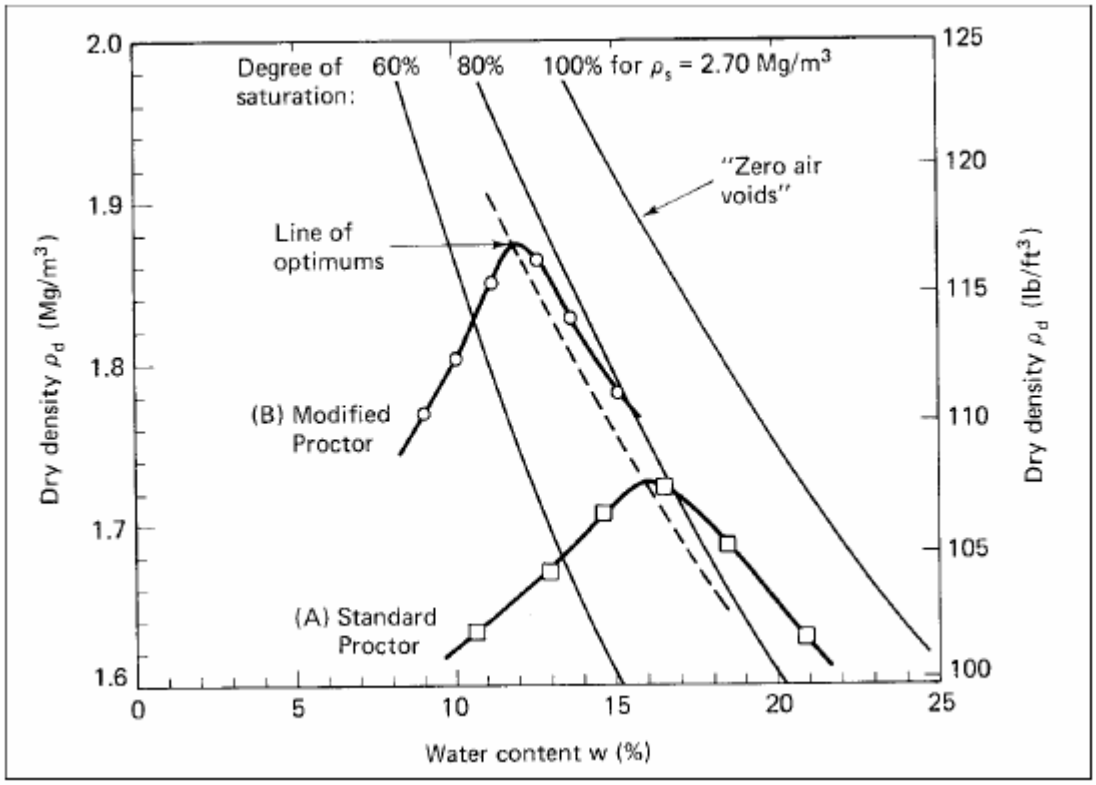

Figure 2.2: Moisture - Density Curves (Holtz and Kovacs 1981)

2.2.4 Factors Influencing Embankment Compaction

Three important factors effect the compaction of soils. The first of these factors is the moisture content of the soil being compacted. Compaction is also affected by soil type, which includes grain size distribution, particle shape, specific gravity of the soil solids, and the clay minerals present. The amount of compaction force applied is another important factor in soil compaction (Das, 1998).

The moisture content of the soil being compacted plays an important role in achieving optimum dry density. Moisture within the soil functions as a lubricant between the grains and aids in the compaction process. Figure 2.2 shows that, under uniform compaction energy, a soil's dry density increases with the addition of moisture until it reaches an optimum moisture content for which the dry density is maximized. This is considered the optimum moisture content for that soil. Any additional moisture beyond this point interferes with the particle packing and reduces the maximum dry density that can be achieved. Soil compaction at optimum moisture allows for the maximum dry density to be achieved but can also minimize potential for shrinkage and swell problems. While most clayey soils exhibit the bell shaped moisture density relationship, other relationships can occur resulting in one and one-half peak, double peak and odd-shaped curves with no defined peaks (Das, 1998).

Another important component determining the effects of compaction is soil type. Soils can be divided into three basic categories: cohesive, granular, and organic soils. Each of these soil types behave differently when subjected to compaction forces. Cohesive soils consist of fine grained materials such as silts and clays. When compacted, the permeability, compressibility, and strength of cohesive soils tend to

change. It has been shown that the hydraulic conductivity decreases as the moisture content of a cohesive soil increases, reaching a minimum at the optimum moisture content. The compressibility of cohesive soils varies with both compaction pressure and moisture content. When compacted at low pressures, cohesive soils with moisture contents above optimum are more compressible than those with moisture contents below optimum; however, when compacted at high pressures, the exact opposite is true. The strength of compacted cohesive soils decreases with increasing moisture content. Some cohesive soils exhibit a drastic drop in strength as the optimum moisture content is exceeded (Das, 1998).

Granular soils, such as sands and gravels, are more resistant to water absorption. These soils can generally be compacted to higher unit weights than cohesive soils; however, uniformly graded sands do not pack well. In many cases, cohesive and granular soils mix, creating a soil with properties different from those of either cohesive or granular soils. Often times these soil mixtures are well graded, making it possible to obtain a more dense state of compaction.

Organic soils are typically not considered suitable for construction purposes; however, in some situations the use of these materials may be warranted. In situations such as these, it is important to ensure that the organic content of the soil does not exceed 8 to 10%. As the organic content of the soils surpasses 10%, the maximum dry unit weight begins to rapidly decrease along with the maximum unconfined compression strength of the soil. Optimum moisture content of organic soils tends to rise with increasing organic content (Das, 1998).

Compaction curves and optimum moisture content vary with soil. Figure 2.3 illustrates compaction curves of eight different soil types ranging from well-graded loamy sand to poorly graded sand.

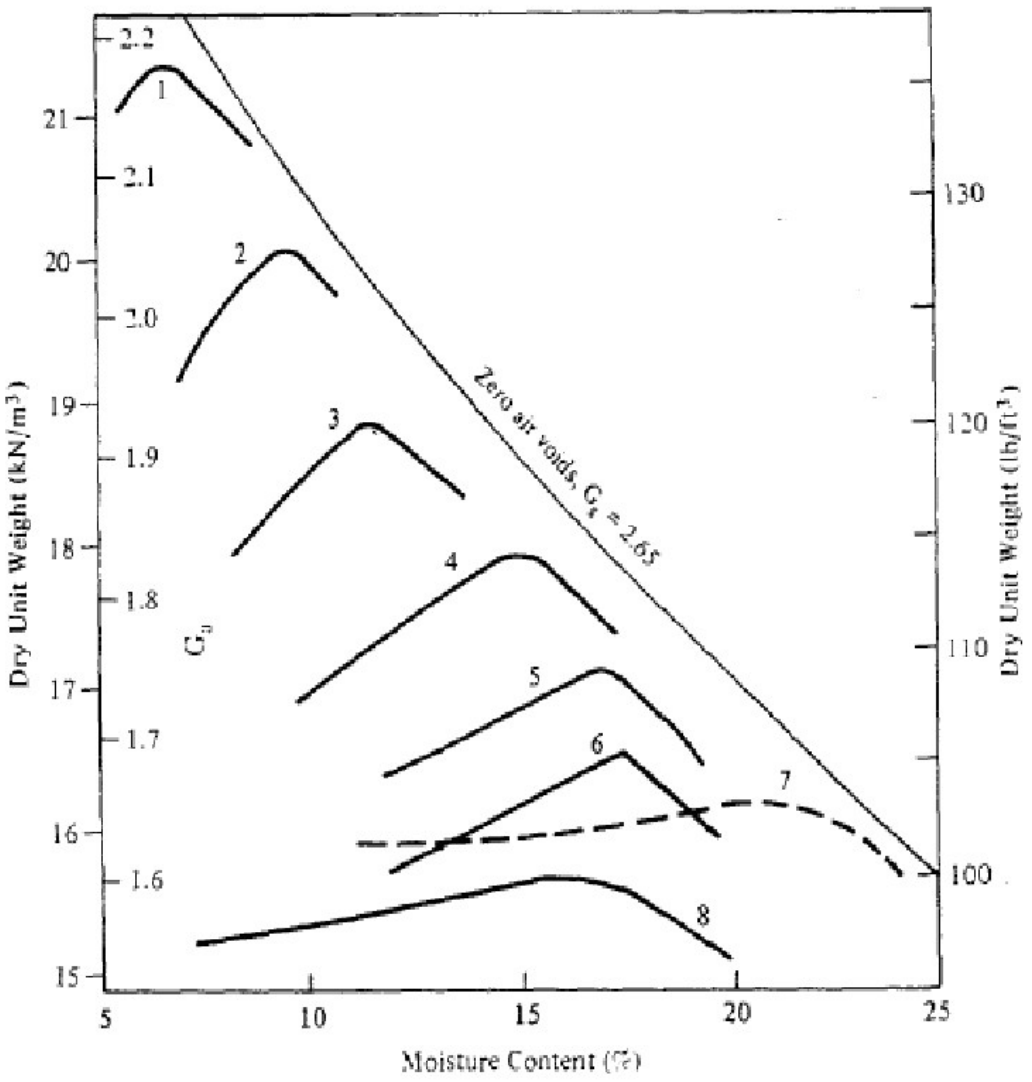

Soil Texture and Plasticity Data

No.	Description	Sand	Silt	Clay	LL	PI
1	Well-graded loamy sand	88	10	2	16	NP
2	Well-graded sandy loam	78	15	13	16	NP
3	Medium-graded sandy loam	73	9	18	22	4
4	Lean sandy silty clay	32	33	35	28	9
5	Lean silty clay	5	64	31	36	15
6	Loessial silt	5	85	10	26	2
7	Heavy clay	6	22	72	67	40
8	Poorly graded sand	94				NP

Figure 2.3: Effect of Soil Type on the Moisture – Density Curves (Spangler and Handy, 1982)

2.2.5 Embankment Compaction Methods

Compaction energy and type of compaction influences the degree of compaction that can be achieved. Soil compaction can be divided into four categories including impact compaction, pressure compaction, kneading compaction, and vibratory compaction. Selection of compaction type is dependent upon both the soil type and the extent of the area which requires compaction.

Impact compaction uses falling weight to increase the compaction forces being applied to the soil surface, similar to the Proctor tests. The amount of energy exerted into the soil is a function of the weight, height and number of drops that occur in each location. This method of compaction is generally limited to small areas.

Pressure compaction is achieved by applying static weight to the soil surface using mechanical rollers or surcharges. Mechanical rollers apply pressure to the soil lifts on each pass, extruding air from the soil and increasing the in place dry density. When compaction time is not a factor and the volume of soil to be compacted is small, surcharges can be placed on top of the soil to provide a natural static load. With time, the extra weight will consolidate and compact the underlying soil at which point the excess can be removed and construction can continue.

Kneading compaction is achieved through the use of tamping foot designed compactors. This method manipulates the soil particles with the use of the sheepsfoot tamping feet. The tamping feet protrude from the roller drum to penetrate the top soil lift to compact the underlying soil, as shown in Figure 2.4.

Figure 2.4: Padded Drum Compactor

This kneading method is important in stratified clay soils to properly compact separated layers together (Caterpillar, 1990).

The last major compaction type used in most earthwork projects is vibratory compaction. Vibratory compaction uses rapid sequences of pressure waves to break up particle bonds to allow the particles to re-orientate in a more dense arrangement (Caterpillar, 1990). This method of compaction is generally created through the rotation of an eccentric weight within the compaction device. This vibratory action is generally defined with three components: amplitude, frequency and centrifugal force.

Amplitude in compaction is defined as the peak to peak vertical movement of the compaction equipment during one cycle. Changing the amplitude of compaction allows the operator to vary the amount of energy being imparted into the soil. Frequency is determined by the number of rotations the eccentric weight rotates around its axis in a

given period of time. Centrifugal force is created by the rotation of the eccentric weight. These parameters along with the soil characteristics create complex interactions.

Modern compaction equipment uses multiple methods to improve the compaction performance of their machines.

2.3 Current KDOT Compaction Specifications

The Kansas Department of Transportation currently uses both density and moisture requirements for embankment quality control. These values are based off the standard Proctor test's optimum dry density and moisture values. Compaction requirements are broken into the following four categories:

- Type AAA Compaction Density ≥ 100% Standard Density
- Type AA Compaction Density ≥ 95% Standard Density
- Type A Compaction Density ≥ 90% Standard Density
- Type B Visual Inspection
- Type C Visual Inspection

Type B requires compaction such that the tamping or sheepsfoot roller will walk out of the compacted material and ride on top of the lift. Low-plastic and non-plastic fine-grained soils require compaction until additional passes of the roller fail to bring the compactor feet closer to the surface of the soil lift.

Type C compaction requires the moisture content to be brought to a satisfactory level during the placement and shaping of the soil lift. Upon completion of the compaction, visual inspection is performed by the field engineer to ensure satisfactory compaction is obtained (KDOT, 1990).

Moisture content requirements are selected based on soil type, application, and location. Moisture content requirements are broken into the following five ranges:

- Moisture Range 0 - 5 (MR-0-5)

  This moisture range requires the moisture content of soil at the time of compaction to be uniform, at or above optimum moisture content, but not to exceed five percent higher than optimum moisture. If the soil is unstable at this moisture range the field engineer will lower the maximum moisture content to the point the soil becomes stable.

- Moisture Range 3-3 (MR-3-3)

  This moisture range requires the moisture content of soil at the time of compaction to be uniform and between three percent below and three percent above the optimum moisture content.

- Moisture Range 5-5 (MR-5-5)

  This moisture range requires the moisture content of the soil at the time of compaction to be uniform and between five percent below and five percent above optimum moisture content.

- Moisture Range 90 (MR-90)

  This moisture range requires the moisture content of the soil at the time of compaction to be such that the required compaction specified can be achieved (KDOT Special Provision 90P-255-R2, 1990).

2.4 Current Field Tests for Measuring In-Situ Subgrade Properties

Density and moisture content are the current basis for quality control of soil compaction. In most highway applications the target values are determined using the standard Proctor test and a relative density. The relative density is computed as the ratio between the dry density and the maximum dry density obtained in the standard Proctor test, as is normally expressed in percentage.

For density measurements in the field, the nuclear density test is the primary test method used by an on-site technician. The secondary method for in-situ density measurement is either the volumetric balloon tester or the sand cone. These devices determine the wet density of the soil; the dry density is computed from the wet density and the in-situ moisture content.

Moisture content on a project is measured along with the wet density. Nuclear density testers are capable of determining the in-situ moisture during testing. This method is generally used as the primary method in the field. Secondary methods include the Speedy moisture tester and retaining samples for determination in the laboratory.

2.4.1 Nuclear Density Test

Nuclear density testing devices are widely used to perform both moisture and density testing in the field. To perform the test on embankment soils, an area large enough for the gauge is first leveled and all loose material is removed. Next, all voids are filled with native fines. An americium-beryllium source is then inserted into the soil and moisture readings are taken. The moisture concentration of the soil is determined by measuring the speed at which neutrons emitted from the source at the end of the rod

reach the underside of the unit. Figure 2.5 shows the nuclear density gauge performing a test in the field. Various models of the nuclear gauges are available for commercial use.

Figure 2.5: Nuclear Density Gauge

The nuclear density gauge is a valuable tool in quality control of compaction due to the speed with which results can be obtained; however, there are disadvantages to using this method. One of these disadvantages is that the measurements are performed only for the top 0.2 m of soil since this is the maximum depth the americium-beryllium source is inserted in the soil. The second disadvantage is related to the strict regulations addressing the transport of the unit because of the nuclear source, in addition to the health risks to the technician due to exposure to radiation. Other disadvantages include: incorrect readings due to poor preparation of the testing area,

incorrect readings caused by placing the unit too close to a vertical wall, and degeneration of the nuclear source (Rollings and Rollings, 1996).

2.4.2 Speedy Moisture Test

The Speedy moisture tester is a commonly used method for determining moisture content of embankment soil. The test involves placing equal amounts of calcium carbide reagent and soil into a pressure vessel. Steel balls are then added and the vessel is sealed and inverted in order to bring the reagent and the soil into contact. The device is then shaken for 10 seconds and allowed to sit for 20 seconds. The process is repeated for 1 to 3 minutes depending on the characteristics of the soil. This ensures that the free moisture in the soil and the calcium carbide reagent react completely. The steel balls help to break up any lumps in the soil sample. After the reaction is complete, the specimen weight and the values are recorded. Calibration curves and conversion charts are then used to determine the moisture content of the soil. A picture of a Speedy moisture tester can be seen in Figure 2.6.

Figure 2.6: Speedy Moisture Testing Kit (durhamgeo.com)

The Speedy moisture test is very useful in the field since it provides rapid results; however, soil samples should also be collected for oven-drying to ensure that the speedy moisture results are accurate. Problems such as old calcium carbide reagent, incomplete break-down of soil lumps, an improperly sealed test vessel, and insufficient time for the chemical reaction are the most common sources for erroneous results.

2.5 Performance Based Tests

A variety of performance based tests are used in pavement design and construction. Each of the more common testing methods are summarized here.

2.5.1 California Bearing Ratio

The California Bearing Ration (CBR) test is a simple test used to indicate the strength of subgrade soils, subbases, and base course materials in pavement systems. The test is used mainly to determine the required thicknesses of flexible pavements.

The test is usually performed on compacted specimens, but may also be conducted on undisturbed soils in the field. Test specimens may be compacted to their maximum unit weights at optimum moisture contents if the CBR is desired at 100 percent maximum dry unit weight and optimum moisture content. The tests can also be performed at specific desired unit weights and moisture contents. Soil specimens are tested by soaking them in water for 96 hours prior to the test in order to simulate poor soil conditions.

The CBR is defined as the ratio obtained by dividing the penetration stress required to cause a piston with a diameter of 49-mm to penetrate 1-cm into the soil by a standard penetration stress of 6.900-kPa. This stress is roughly what is required to cause the same piston to penetrate 1-cm into a mass of crushed rock, so the CBR is basically the strength of the soil relative to that of crushed rock.

If the CBR is desired at an optimum water content and some percentage of the maximum dry unit weight, three specimens should be prepared from the soil to within ± 0.5% of the optimum moisture content. A different compaction effort should be used for each specimen so that the dry unit weights of the specimens vary above and below the desired value. The CBR's for the three specimens should then be plotted against their corresponding dry unit weights, and the CBR for the desired dry unit weight can be interpolated (Murad, 2004).

2.5.2 Dynamic Cone Penetrometer

The dynamic cone penetrometer (DCP) is a test used to measure the in-situ resistance to penetration of soils. The test has been used throughout the United States for site characterization of pavement layers and subgrades. The DCP is an effective

tool for assessing the in-situ strength, stiffness, and uniformity of pavements and subgrades, and is also a useful tool for QA/QC applications in highway construction.

The DCP consists of a fixed upper 575-mm travel rod with either a 4.6- or 8-kg falling weight (the lighter weight being used for weaker soils). It also has a lower rod containing the anvil and a replaceable 20-mm diameter cone with an apex angle of 60°. The DCP test is conducted by dropping the weight from a height of 575-mm and recording the number of blows versus the depth of penetration. From this data, the penetration rate is calculated. The DCP test can verify the level and uniformity of compaction, making it a useful tool for quality control applications. The DCP test is also capable of determining the thickness of the tested layer. The subgrade resilient modulus can also be predicted directly from the DCP results (Murad 2004). A photo and diagram of a dynamic cone penetrometer can be seen in Figure 2.7.

To assess the structural properties of the pavement subgrade, the DCP values are often correlated with the CBR test results in order to asses the structural properties of the pavement layers. The following correlations were developed from the results of several studies.

$\log CBR = 2.62 - 1.27 \log PR$ (Kleyn, 1975)

$\log CBR = 2.56 - 1.15 \log PR$ (Smith and Pratt, 1983)

$\log CBR = 2.2 - 0.71 (\log PR)^{1.5}$ (Livneh and Ishia, 1987)

$\log CBR = 2.56 - 1.16 \log PR$ (for PR values > 10) (Harrison, 1986)

$\log CBR = 2.70 - 1.12 \log PR$ (for PR values < 10) (Harrison, 1986)

$\log CBR = 2.465 - 1.12 \log PR$ (U.S. Army Corps of Engineers)

$CBR = 292/PR^{1.12}$ (U.S. Army Corps of Engineers)

The subgrade resilient modulus can also be determined from the results of the DCP test. The resilient modulus can be determined from either the relationship between the subgrade modulus (E_s) and the CBR value obtained from the equations listed above, or determined directly from the DCP test results. The following equations relate the resilient modulus to the calculated CBR values.

M_R (MPa) = 10.34CBR (for CBR values < 10) (Huekelom and Klomp, 1962)

M_R (MPa) = 17.58 × $CBR^{0.64}$ (Powell, 1984)

The equations shown below relate the resilient modulus directly to the PR value determined from the DCP test.

$\log (E_s) = 3.25 - 0.89 \log (PR)$ (Pen, 1990)

$\log (E_s) = 3.652 - 1.17 \log (PR)$ (Pen, 1990)

$\log (E_s) = B - 0.4 \log (PR)$ (where B is dependent on soil type) (Chua, 1981)

$\log (E_s) = 3.05 - 1.07 \log (PR)$ (DeBeer, 1990)

An equation was also developed by Chen to relate the resilient modulus back-calculated from the FWD test to the results of the DCP test.

$M_{FWD} = 338 (PR)^{-0.39}$ (for 10 < PR < 60) (Chen et al., 1995)

The DCP testing equipment is simple, rugged, and inexpensive and can be operated by one or two people. Site access is not an issue due to the portability of the equipment. The test produces continuous measurements of the in-situ strength and stiffness of pavement layers and subgrade, and is non-destructive. The DCP test can also be performed in pavement core holes. The test results are accurate in many soil types including weak rocks, and are fairly reliable.

One drawback to the use of the DCP test is its limited depth. The test is only good to about 1-meter; however, this depth is adequate for most rehab projects. The test also exhibits high variability and uncertainty in gravelly soils. Another disadvantage is that the test yields only index results and does not measure a fundamental soil property such as shear strength or resilient modulus. Extraction of the cone can be difficult, and the test does not obtain a sample (FHWA 2005).

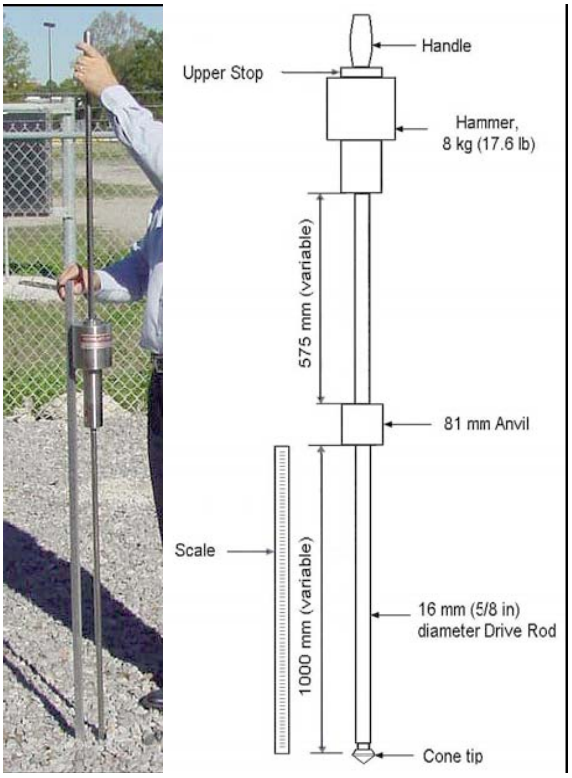

Figure 2.7: Dynamic Cone Penetrometer (Murad 2004)

2.5.3 Falling Weight Deflectometer

One of the most common geophysical testing methods is the Falling Weight Deflectometer (FWD). This test is used to determine the variation of the pavement layer and the subgrade stiffness along a length of pavement. For geotechnical components,

the data gathered can be used to back-calculate the resilient modulus of the subgrade and base layers to identify weak points where further testing is needed.

The FWD testing unit consists of a drop weight mounted on a vertical shaft. The unit can be pulled by a conventional vehicle. A schematic of the testing unit can be seen in Figure 2.8.

The FWD applies an impulse load to the roadway surface by dropping a 4 to 107 kN weight onto a plate resting on the pavement surface. The drop weight is lifted to a predetermined height of 50 to 510 mm hydraulically. The weight is then dropped onto a 300 or 450 mm loading plate, which, in turn, is resting on a rubber buffer. The buffer improves the uniformity of the stress distribution throughout the loading plate area. The impact of the falling weight produces an impact load with a pulse time ranging from 25

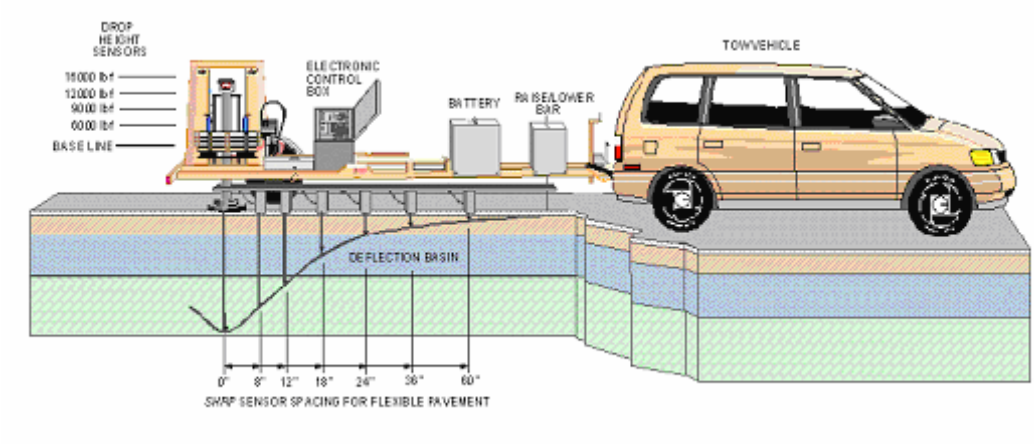

Figure 2.8: FWD Testing System (Murad 2004)

to 40 milliseconds. The impact load usually ranges from 6.7 to 155.7 kN, varying depending on the mass of the drop weight and the drop height. The peak impact force is measured using a load cell. The FWD also records the pavement deflection at the center of the applied load using seven geophones. The geophones are located at 0,

305, 457, 610, 914, 1219, and 1524 mm measured radially from the center. These values are then used to back-calculate the effective stiffness of the pavement layers.

To perform the FWD analysis, the elastic modulus and Poisson's ratio of the materials in each layer should be known. Also, the thickness of each pavement layer must be known. The back-calculation procedure involves the calculation of theoretical deflections under the applied load using assumed pavement moduli. The theoretical deflections are then compared to the measured deflections. The assumed moduli are then adjusted using an iterative process until the values converge. The moduli determined using this method represent the pavement response to the load application.

There are several advantages to using the FWD. Its portability, durability of the equipment, and nondestructive nature of the test make it easy to use in a variety of locations. Also, the repeatability of the tests provides a greater statistical sample for the analysis of the pavement. The FWD is also effective at simulating a moving traffic load. In addition to these advantages, the FWD allows for a direct evaluation of the design resilient modulus values.

The use of the FWD also has some disadvantages. The static method requires the test vehicle to stop between readings, thus requiring traffic control when testing is taking place. The FWD can be impractical for evaluating the pavement structure during construction of subgrades, subbases, and base layers. The uneven surface can cause the geophones to tilt, leading to inaccurate deflection measurements that can not be used in back-calculation. Also, the test requires the pavement section to have a well defined layer thickness. Deep features such as water tables and bedrock, asphalt concrete layers with thicknesses less than 75 mm, and temperature can also affect the

results of the test. In addition, resilient modulus values can be determined to be higher than the predicted values (FHWA, 2005).

Figure 2.9: GeoGauge Testing Device

2.5.4 GeoGauge

The GeoGauge measures the in-place stiffness of compacted soil. The equipment consists of a small 10 kg unit. The GeoGauge is cylindrical in shape with a height of 270 mm and a diameter of 280 mm. The unit has a circular ring that contacts the soil surface. The GeoGauge is placed and seated on the soil surface by pressing and rotating the unit. Local fines are used to provide adequate contact with the circular ring when the surface is rough.

The GeoGauge has a shaker that generates a small dynamic force at 25 specific frequencies ranging from 100 to 196 Hz. During the test sequence the GeoGauge

records the small deflections caused by the vibration of the unit using a geophone sensor within the body of the gauge. Based on the vibration forces and deflections, the machine calculates the GeoGauge stiffness (H_{SG}) based on the average of 25 stiffness values recorded at 25 different frequencies. The elastic modulus of the soil or Young's Modulus (E) can then be computed. The equation used in calculating the elastic stiffness modulus is:

$E_G = H_{SG}[(1-\upsilon^2)/(1.77R)]$ (Humboldt, 2000)

Where E_G is the elastic stiffness modulus in MPa, H_{SG} is the Geogauge stiffness reading in MN/m, υ is Poisson's ratio, and R is the radius of the GeoGauge plate. Humboldt Ltd., the manufacturer of the GeoGauge, recommends that the test only be used up to an H_{SG} value of 23-MN/m, because the test loses accuracy at high stiffness values.

Equations have been developed to relate the GeoGauge stiffness to the modulus back-calculated FWD test results.

$M_{FWD} = 37.65\ H_{SG} – 261.96$ (Lenke, 2003)

Where M_{FWD} is expressed in MPa, and H_{SG} is the Geogauge stiffness in MN/m.

Equations have also been developed by CNA Consulting Engineers to relate the GeoGauge stiffness with the stiffness determined from the Plate Load Test.

$E_{(PLT)r} = 0.8962\ (E_G) + 25.9$ with $R^2 = 0.23$

$E_{(PLT)u} = 0.6158\ (E_G) + 10.3$ with $R^2 = 0.27$

$E_{(PLT)i} = 0.3388\ (E_G) + 84.7$ with $R^2 = 0.66$

Where $E_{(PLT)r}$, $E_{(PLT)u}$, and $E_{(PLT)i}$ are the reloading, unloading, and initial elastic moduli, determined from the Plate Load Test expressed in MPa (Murad 2004). Figure 2.9 is a photograph of the GeoGauge device during a stiffness measurement.

2.5.5 Light Falling Weight Deflectometer

The Light Falling Weight Deflectometer is a portable FWD developed in Germany as an alternative to the plate load test. An L-FWD device consists of four major parts: the sensor body, loading plate, buffer system and sliding weight. The sensor body encloses both the load cell and the central geophone. The geophone is spring mounted at the center of the load plate. Some models allow the use of additional geophones during testing. The geophones measure the surface deflection at the top of the embankment under the impact load produced by the falling weight by measuring the acceleration. The deflection is computed from the acceleration data using numerical integration. During the test, the center deflection (δc) of the loading plate is recorded and used to estimate the L-FWD elastic stiffness modulus using software provided with the L-FWD. The equation used to determine the L-FWD elastic stiffness modulus is similar to the one used to calculate the surface modulus of a layered material assuming a uniform Poisson's ratio and constant loading, known as the Boussineq equation:

$$E_{LFWD} = \frac{2(1-\upsilon^2)\sigma \times R}{\delta_c}$$

Where σ is the applied stress, and R is the plate radius.

The L-FWD consists of a load plate, buffer system and sliding weight attached to a sensor body. Load plates of varying sizes can be attached to the L-FWD depending on the test conditions. The buffer system is attached to the top of the sensor body. The buffer system consists of a series of rubber buffers. Individual buffers can be removed

to create multiple buffer configurations. The handle and sliding weight are also attached to a steel tube connected to the top of the housing. The tube acts as a guide for the falling weight and allows the operator to stabilize the machine during testing on irregular surfaces. The data recorded during testing is transmitted via radio signal or cable to a laptop computer which displays and saves the test data. An L-FWD device is shown in Figure 2.10.

Figure 2.10: Prima 100 Light Falling Weight Deflectometer (Murad, 2004)

The L-FWD device allows the user to vary the drop height, drop weight, plate diameter and buffer configuration. The L-FWD weight drop height can be varied to allow the user to increase or decrease the impact load. The L-FWD device is supplied with multiple weights which can be attached in different configurations. Additional drop weight increases the stress exerted by the plate. By changing the size of the loading

plate diameter, the area over which the force is applied can be changed. This allows the user to change the stress imparted onto the sub-grade soil.

The German Code recommends the following equation to relate the German Dynamic Plate Test results with those of the L-FWD (Murad, 2004).

$$E_{(PLT)R2} = 600 - \frac{300}{300 - E_{LFWD}}$$

Equations have also been developed to correlate the modulus determined from the FWD test with the results of the L-FWD test (Murad, 2004).

$$M_{FWD} = 1.031\ E_{LFWD}$$

2.5.6 Static Plate Load Test

The Static Plate Load Test (PLT) is an effective method for testing the pavement structure layers in both rigid and flexible pavements. The test involves loading a circular plate resting on the layer to be tested, and measuring the deflection of the layer under varying load increments. For roadway testing, the plates are typically 30.5 cm in diameter. The load is applied to the plate by a hydraulic jack. The plate must be loaded continually until all measured settlement has subsided so that the actual deflection for each load increment is obtained. The amount of time required for the preliminary settlement to take place is determined by plotting a time-deformation curve during the test. At the point when the curve becomes horizontal, or when the rate of deformation nears 0.0025-cm/min, the next load increment is applied. According to the ASTM D1195-93 testing method, the test should continue until a peak load is reached or until the ratio of load increment to settlement increment reaches a minimum, steady magnitude.

The modulus obtained from the PLT test reflects the composite modulus of the tested layers rather than their true modulus. One method for predicting pavement stress and deflection is the Odemark method, or the Method of Equivalent Thickness (MET). This method involves transforming layers of different stiffnesses to an equivalent layer of the same stiffness, then applying Boussinesq's equation to predict the stress and deflection.

2.6 Laboratory Soil Resilient Modulus

The resilient modulus for embankment soils is determined in the laboratory using a repeating or cyclical load triaxial cell. This test and the factors affecting the results of the laboratory resilient modulus test are described in the following paragraphs.

2.6.1 Factors Affecting the Laboratory Resilient Modulus

Laboratory resilient modulus is mostly dependent on three factors: stress conditions, moisture content, and dry density. The main factor affecting laboratory resilient modulus is the deviator stress. Resilient modulus increases with increasing confining stress for all soils, fine and coarse grained. However, the resilient modulus of fine grained subgrade soils, especially clay soils, is less affected by the confining stress than by the deviator stress. Resilient modulus is also influenced by the number of stress repetitions, but will tend to become constant with increasing number of stress repetitions.

The second factor affecting soil resilient modulus is moisture content. However, when considering the effect of moisture content variation on the resilient modulus, the third factor affecting resilient modulus, dry density, must also be considered. Moisture content variation can influence the resilient modulus differently, depending on the

variation of the dry density. An increase in moisture content will typically lead to a significant decrease in soil stiffness (Burczyk, 1994). At lower moisture contents, the resilient modulus will increase as dry density increases, while at higher moisture contents, the resilient modulus decreases with increasing dry density (Li, 1994).

2.6.2 Laboratory Resilient Modulus Testing Procedure

The resilient modulus for embankment soils is determined in the laboratory using a repeating or cyclical load triaxial cell. The triaxial cell itself varies from 100 mm in diameter and 200 mm and up in height depending upon the minimum required sample size. Soil samples can be taken from the field and trimmed to size or compacted in the laboratory using a variety of methods. Soil specimens for fine grained soils have a minimum diameter of 71 mm. The height of the specimen is limited to a minimum of 2 times the diameter (AASHTO, 2000).

Deformation of the sample can be measured using two LVDT's attached to either side of the soil specimen. If soil samples are too soft for LVDT mounting or the triaxial cell does not permit internal mounting, an LVDT can be mounted externally on the loading piston. The load cell is located at the top of the specimen or within the loading machine. The typical triaxial setup can be seen in Figure 2.11.

The loading piston can be powered pneumatically or hydraulically depending upon the equipment. In addition, computer controller and data acquisition equipment is required to properly load specimens and record test data.

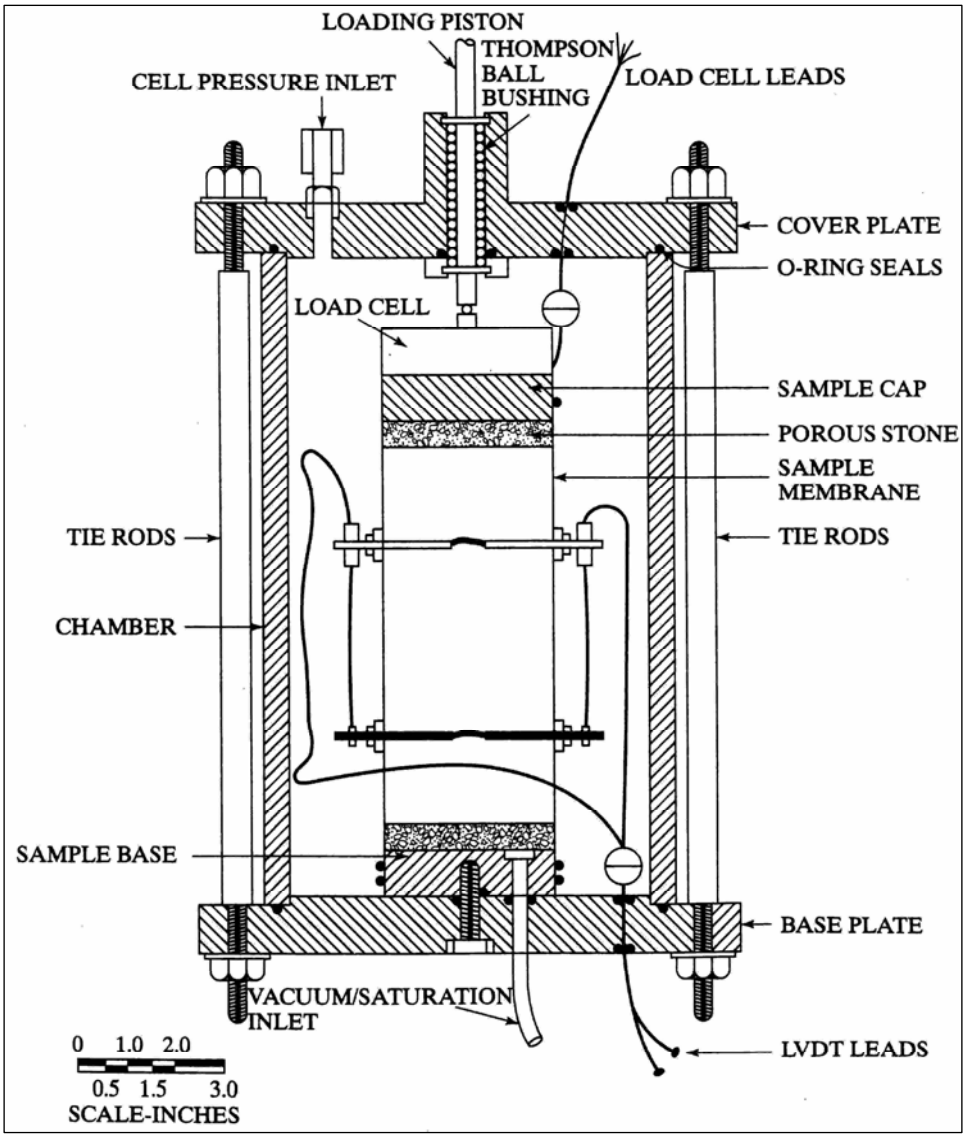

Figure 2.11: Typical Triaxial Test Setup (Haung, 2004)

CHAPTER THREE - RESEARCH METHODOLOGY

3.1 Introduction

The goal of this research project is to investigate the possibility of developing a stiffness based specification for the compaction of embankments in highway construction projects utilizing an L-FWD device to measure stiffness. To achieve this goal, field testing was performed to measure stiffness at nine different highway embankment construction sites with the L-FWD and other stiffness measuring devices. The data collected at these sites was analyzed in order to determine the feasibility of using the L-FWD as a tool for measuring stiffness. Soil samples were also analyzed in the laboratory to determine the tri-axial resilient modulus to study the correlation between the L-FWD stiffness measurements and the laboratory measured stiffness. This chapter presents the equipment and methodology used in collecting and analyzing the field stiffness and laboratory data.

3.2 Field Test Sections

A major component of the research methodology was the in-situ field determination of embankment soil stiffness using the L-FWD. The test sections for this project were selected based upon soil type, availability, and location. The test sections were recommended by the Kansas Department of Transportation based upon these criteria.

Test sections ranged from 153 to 534 meters in length, depending upon site conditions and the contractor's ongoing work. All test sections required contractor grading of the testing area to provide a uniform contact surface for the L-FWD. Tests were taken at 7.62 or 15.24 meter intervals depending upon the length of the test

section. Shorter test sections required tests to be performed at more frequent intervals in order to obtain a sufficient number of test points. Table 3.1 summarizes the size and location of the nine field test sections where the L-FWD tests were performed.

Table 3.1: Test Section Summary

Location	Route	County	Test Section Length (m)	Test Spacing (m)	AASHTO Soil Classification	Description
Abilene	I-70	Dickinson	153	7.62	A-2-4	East bound I-70
Doniphan Co.	K-7	Doniphan	229	7.62	A-4	South bound K-7 North of 36 Highway
Garden City	US-50	Finney	275	7.62	A-2-4	US-50 Southeast of Garden City
Hill City	US-283	Norton	313	7.62	A-6	US-283 North of Hill City
Manhattan	K-18	Riley	229	7.62	A-7-6	US-18 South-West Manhattan
Marysville	US-77	Marshall	534	15.24	A-4	South of Marysville East of US-
Sabetha	US-75	Brown	275	7.62	A-7-6	US-75 East of Sabetha
Salina 1	I-70	Saline	381	15.24	A-6	East bound I-70 West of Salina
Salina 2	I-70	Saline	237	7.62	A-4	Ramp onto I-70 North of Salina

3.3 In-Situ L-FWD Testing

The Prima 100 light-weight FWD equipment used in this project is manufactured and marketed by Carl Bro Consultants in Glostrup, Denmark. The Prima 100 L-FWD device consists of four major parts: the sensor body, loading plate, buffer system and sliding weight (Figure 3.1). The sensor body encloses both the load cell and the central geophone. The geophone is spring mounted at the center of the load plate. Two additional geophones along with a mounting bar were provided with the machine; they were used at the Abilene and Manhattan test sites. The geophones measure the deflection at the top of the embankment under the impact load by measuring the acceleration. The deflection is computed from the acceleration data using numerical integration.

The load plate, buffer system and sliding weight all attach to the sensor body. The sensor body itself acts as a 100 mm load plate. Two additional plates, 200 and 300 mm in diameter, are provided with the device and can be attached to the bottom of the sensor housing. Figure 3.1 shows the sensor body with a 300 mm load plate attached. The 300 mm load plate was used in all tests performed for this project.

The buffer system is attached to the top of the sensor body. The buffer system consists of four conical solid rubber buffers which screw into the sensor body. Individual buffers can be removed to create four, three and two buffer configurations. The rubber buffers can be seen in Figure 3.1.

The handle and sliding weight are attached to a steel tube connected to the top of the housing. The tube acts as a guide for the falling weight and provides a conduit for the electronic cables. The tube handle also allows the operator to stabilize the machine during testing on irregular surfaces. The handle and sliding weight configuration can be seen in Figure 3.2.

The digital GPS controller is mounted on the top of the tube and is connected to the electronics and sensors via a cable that runs through the center of the slide tube. The digital controller displays and controls the test point drop number, test recording and data saving. Figure 3.3 shows the digital controller. The recorded data is transmitted via radio signal or cable to a laptop computer which displays and saves the test data.

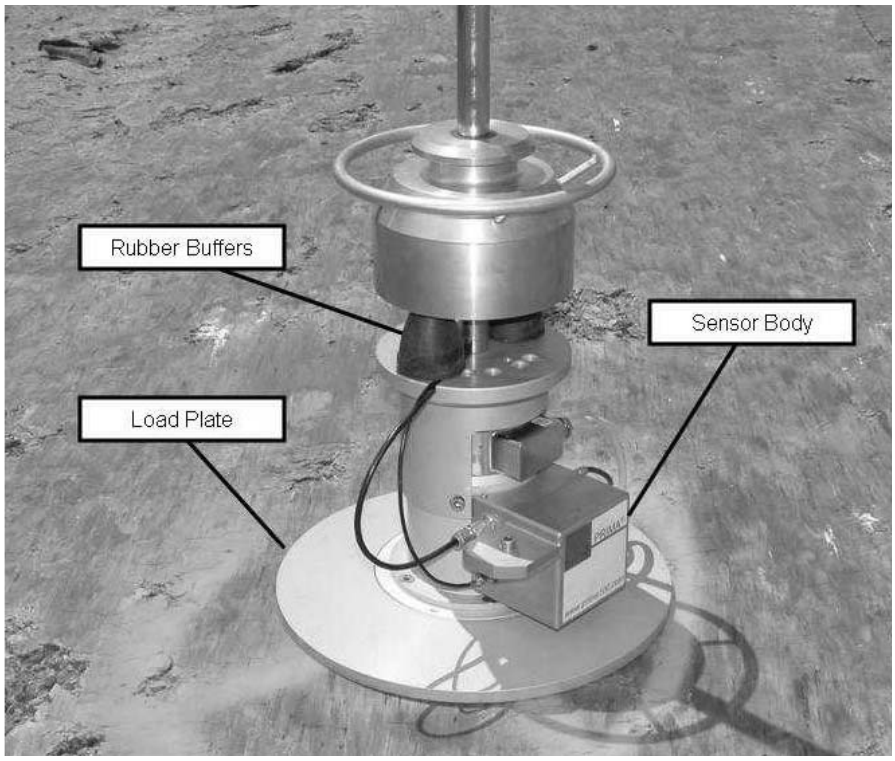

Figure 3.1: L-FWD Sensor Body, Loading Plate and Rubber Buffers

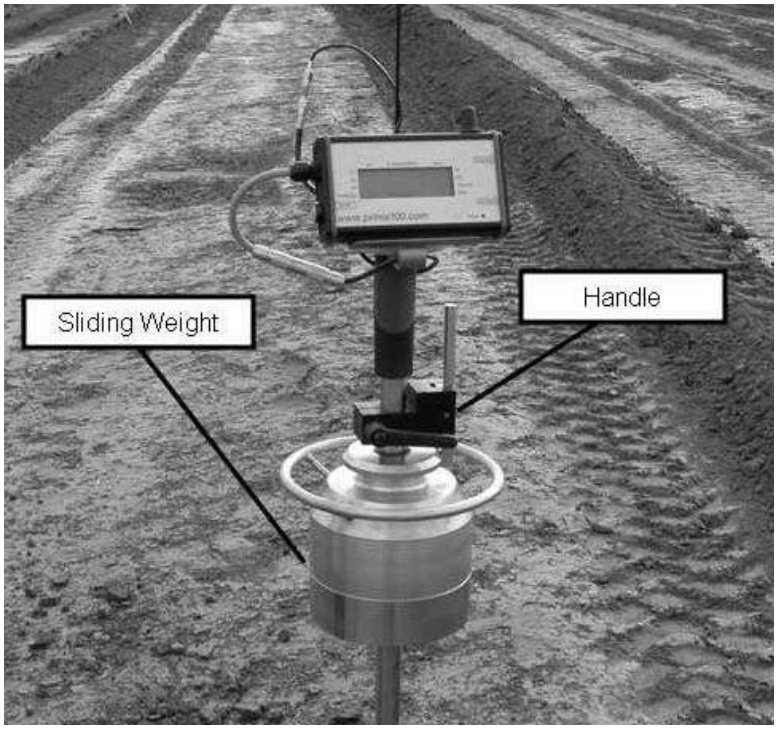

Figure 3.2: L-FWD Handle and Sliding Weight

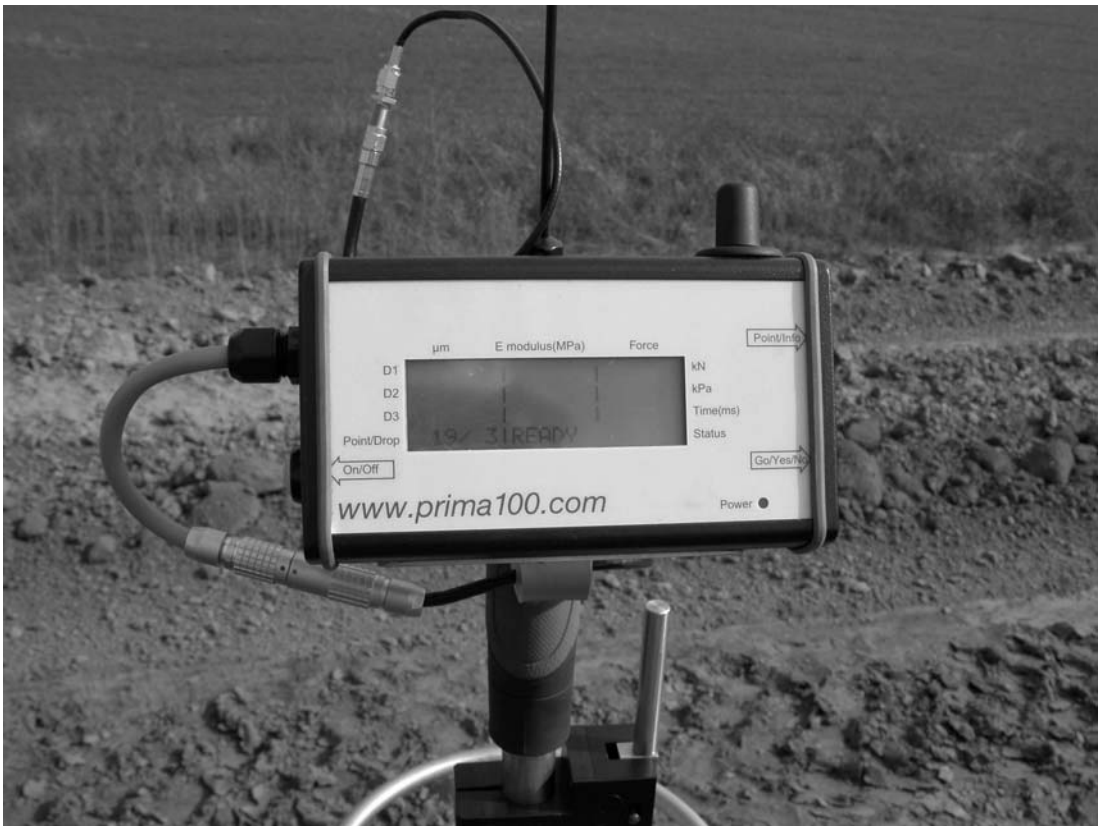

Figure 3.3: L-FWD Digital GPS Unit

The Prima 100 L-FWD device allows the user to vary the drop height, drop weight, plate diameter and buffer configuration. The L-FWD weight drop height can vary up to 85 cm. The Prima device is supplied with a standard 10 kg weight along with two additional 5 kg weights. Adjusting the drop height, drop weight, and plate diameter allows the user to change the amount of stress imparted on the soil.

The number of rubber buffers on the Prima 100 L-FWD can be adjusted to alter the length of the load impact pulse. During the initial L-FWD testing, four buffers were used. This configuration created short pulse times of 17 to 18 seconds and caused the machine to move after impact. It was observed that this affected the accuracy of the deflection measurement. Following a trial at the Marysville site, the configuration was changed to two buffers to attenuate the moving of the device. This reduced the shaking

and moving of the machine during testing and increased the pulse time noticeably to 19 to 22 milliseconds.

3.4 In-situ Stiffness Measurements with the Geo-Gauge

The Humboldt GeoGauge was used along with the L-FWD at some project locations. GeoGauge tests were performed at the Marysville, Doniphan, and Manhattan test sites. The tests were performed at the same locations as the L-FWD tests along each project. Figure 3.4 shows the GeoGauge performing a test at the Marysville test site.

Figure 3.4: Geo-Gauge Testing Device

3.5 In-place Density and Moisture Content Tests

Following the L-FWD soil stiffness measurements, density and moisture data were collected at every fifth testing point along each test section, in the same location that the stiffness measurements were performed.

A nuclear density gauge was used to determine the in-situ density and moisture at all of the test sites. All the nuclear density measurements were performed by trained personnel from either KDOT or the earth work contractor. Various models of Troxler nuclear gauges were used for this project. Figure 3.5 shows the nuclear density gauge performing a moisture test in the field.

Figure 3.5: Nuclear Density Gauge

A volumetric balloon tester was used along with the nuclear gauge on the first test section, Salina 1, to determine the in-situ density of the soil. Both methods are considered standard test methods (AASHTO T238, T205). The collected density data suggested that the balloon method was less precise. Because the balloon method test was also found to be cumbersome, this test was not used on the remaining test sites.

The moisture content was measured at the same locations as density along the test section. Moisture content was measured using three different methods depending upon the project. On all projects, soil samples were sealed in jars and retained for moisture determination in the laboratory. These samples were later dried in the lab to determine the moisture content. This test was performed following the AASHTO T265 specification. The other two methods which were performed only in the field included the nuclear gauge moisture reading and the Speedy moisture content test. The Speedy test was conducted at the Sabetha test site following the AASHTO T217-02 specification.

3.6 Sampling of Soils for Laboratory Resilient Modulus Tests

Soil samples from each site were collected in the same general area as the test locations and stored in sealed five-gallon buckets. The collected soil was visually inspected to ensure that the collected soil and the in-situ tested soil were the same soil type. The soil samples from each site were then transported back to the KSU laboratory for processing. In the laboratory, the soil samples were divided into pans and oven dried. Once dry, the soil was then mechanically ground and stored in sealed five gallon buckets.

3.7 Laboratory Tests on Soil

After the soil gathered in the field was transported back to the laboratory, tests were performed to further analyze the soil. These tests included soil classification analysis and resilient modulus testing. These tests are described in detail below.

3.7.1 Soil Classification Analysis

The soil at each project site was classified according to the AASHTO soil classification system. For the Salina 1, Salina 2, Garden City, Sabetha, and Marysville test sites, soil classification data was provided by the Kansas Department of Transportation. For the Hill City and Doniphan sites, the tests needed for soil classifications were performed in the laboratory. In addition, standard Proctor tests were preformed to obtain optimum moisture and density values.

Table 3.2: Soil Description and Classification Summary

Location	Max Dry Density (kg/m^3)	Optimum Moisture (%)	LL (%)	PI (%)	AASHTO Classification	Description
Abilene	1,811	11.6	12.5	NP	A-2-4	Sandy Soil
Doniphan Co.	1,714	17.4	33.4	6.3	A-4	Silty Soil
Garden City	2,034	9.8	21	5	A-2-4	Sandy Soil
Hill City	1,780	15.0	34	14	A-6	Clay Soil
Manhattan	1,676	20.4	44.4	18.3	A-7-6	Clay Soil
Marysville	1,719.6	15.7	23	NP	A-4	Silty Soil
Sabetha	1,716.5	18.0	43	28	A-7-6	Clay Soil
Salina 1	1,856	13.8	30	15	A-6	Clay Soil
Salina 2	1,744	15.4	23	4	A-4	Silty Soil

3.7.2 Resilient Modulus Tests

The resilient modulus of each soil sample was determined in the laboratory using a repeated load tri-axial testing machine. The Universal Testing Machine (UTM) manufactured by Industrial Process Controls of Melbourne, Australia was used for this

purpose. The test protocol for determining the resilient modulus followed the AASHTO T 292-97 test method (2000).

The UTM test configuration consisted of four main components: the Computer Data Acquisition System (CDAS), the hydraulic system, a PC, and the tri-axial cell. The CDAS records the signals from the transducers, digitizes the information, and then passes the information along to the PC. The CDAS also controls the testing frame and transducers, along with adjusting and applying the load through the actuator. The hydraulic system allows for strict control of the loading, and therefore, precise control of the stresses incurred by the sample. The hydraulic system is connected to the actuator through an electrically controlled hydraulic servo valve. The force applied to the sample is determined using a load cell mounted in line with the loading shaft. The tri-axial cell consists of an air-tight chamber, a loading arm, and a sample platform. The UTM testing machine can be seen in Figure 3.6.

Figure 3.6: Universal Testing Machine (www.k-state.edu/pavements/)

The tri-axial cell used in these tests was 150-mm in diameter and 300-mm tall. Confining pressure for the tri-axial test was provided by means of pressurized air. A separate air tank with a servo value was connected to the tri-axial cell. Using the pressure sensor, the computer system maintained a static pressure during the testing. Figure 3.7 shows the tri-axial cell used to determine the resilient modulus of the soil samples.

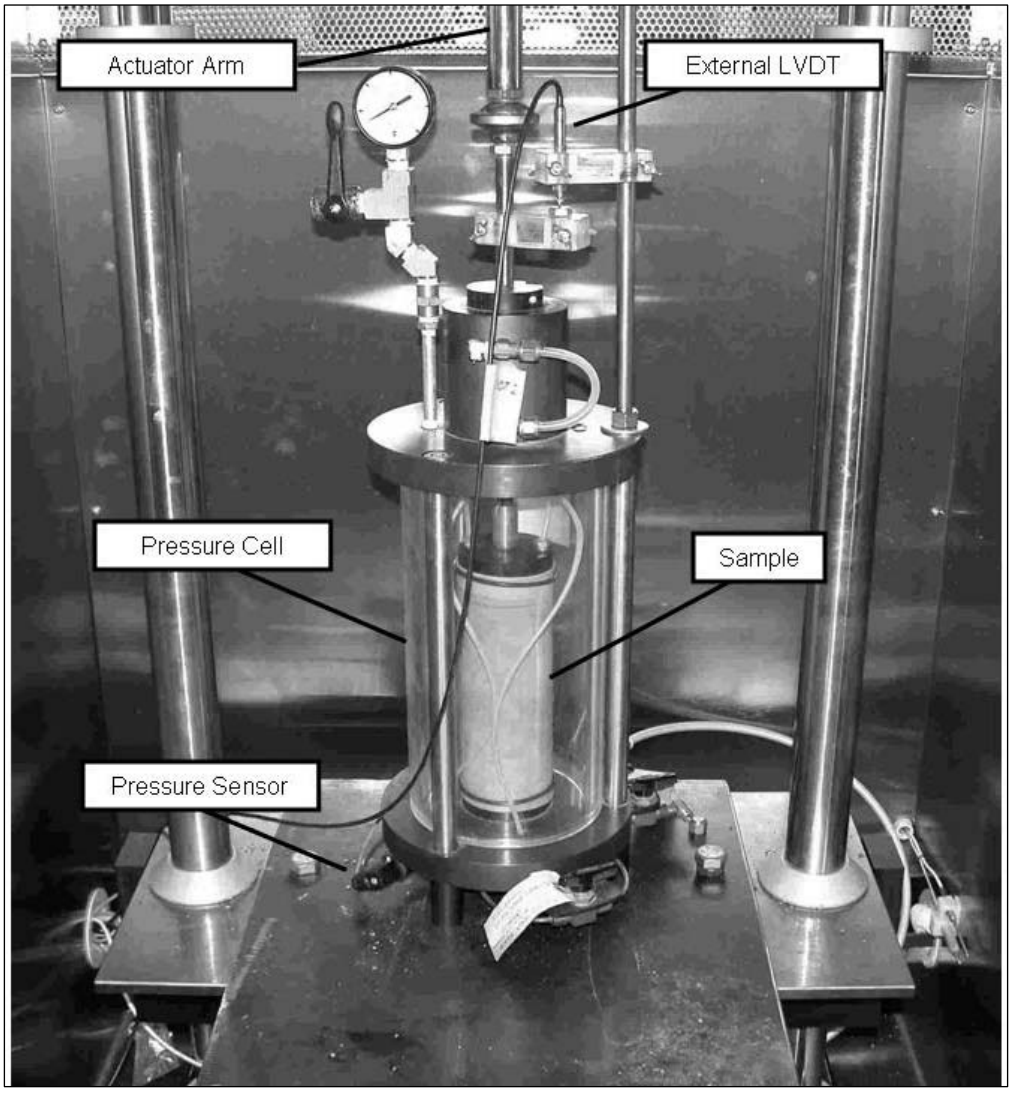

Figure 3.7: Tri-axial Test Setup

Soil samples were prepared at three levels of compaction, 90%, 95%, and 100% of the soil maximum dry density. Three samples were prepared at each level of compaction with three moisture contents each for a total of nine samples per soil, as shown in Table 3.3

Table 3.3: Density-Moisture Combinations for Tri-Axial Testing

Test Site	Moisture Content		
Doniphan	-5% OMC	OMC	+3%,+5%
Garden City	-5% OMC	OMC	+2% OMC
Hill City	-5% OMC	OMC	+2% OMC
Manhattan	-5% OMC	OMC	+2% OMC
Marysville	-5% OMC	OMC	+5% OMC
Sabetha	-5% OMC	OMC	+2% OMC
Salina I	-5% OMC	OMC	+5% OMC
Salina II	-5% OMC	OMC	+2% OMC

After the soil had been dried and mechanically ground, the soil and water quantities needed to obtain the desired moisture content and compaction level were determined. This was done by first testing the moisture content of the ground soil (although it had been dried and stored in sealed containers, some moisture might have been present). Next, the weight of water and the weight of soil required for each sample was calculated based on the volume of the sample in addition to the level of compaction and moisture content of each individual sample. Each sample was then mixed thoroughly and compacted.

The samples were compacted in three lifts, as specified in the T 292-97 (2000) protocol. A Satec 5000 testing machine was used to compact the samples by static loading. The samples were compacted in steel tubes, and then carefully extracted

using a hydraulic jack. The final sample size was 71 mm in diameter with a height of 144 mm. The sample size was selected based on the size of the tri-axial cell components available, and the load capacity of compaction equipment.

Once the samples had been extracted, they were placed in a rubber membrane. The covered sample was then placed in the tri-axial cell and porous stones were placed above and below the specimen. Figures 3.8 through 3.10 show the sample preparation process.

Figure 3.8: Sample Compaction

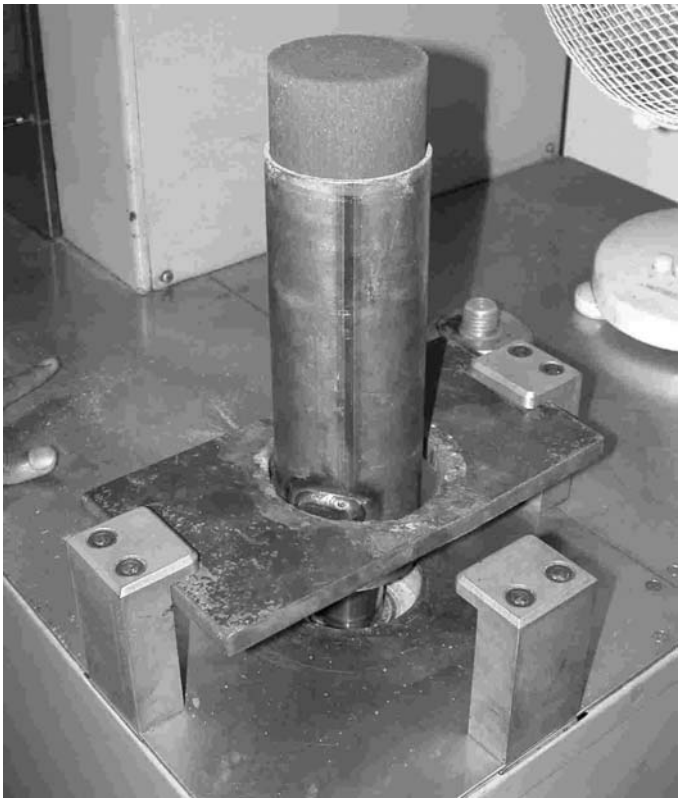

Figure 3.9: Sample Extraction

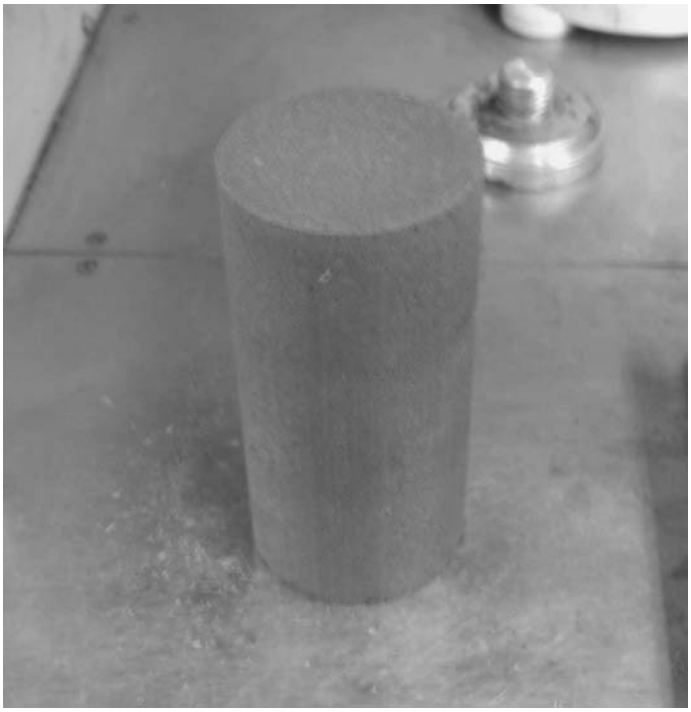

Figure 3.10: Soil Sample Prepared for the Resilient Modulus Test

After the sample was placed in the tri-axial cell, the tri-axial cell was sealed and placed inside the UTM. With the cell inside the UTM, the hydraulic actuator was connected to the loading arm of the tri-axial cell. After the actuator was adjusted to contact the specimen, the external LVDT was placed and adjusted to ensure maximum stroke availability.

The testing procedure for all samples followed the AASHTO T 292-97 (2000) protocol. Each sample was conditioned prior to the testing sequence. The sample was conditioned for 1,000 load repetitions using a deviator stress of 21 kPa and a confining pressure of 21 kPa. After the initial conditioning, each sample was tested at five levels of deviator stresses; 21 kPa, 34 kPa, 48 kPa, 69 kPa and 103 kPa. A static confining pressure of 21 kPa was applied for all test sequences. During each of the five deviator stress test sequences, 100 load repetitions were applied to the sample. The values recorded for the last five repetitions were averaged to calculate the resilient modulus for each stress/loading sequence. Figures 3.11 and 3.12 show the typical UTM set up and testing screens with the resilient modulus graphed, respectively.

Figure 3.12 shows the typical test results for one of the soil samples. For each test, resilient modulus, resilient strain, permanent strain, confining pressure, cyclical stress, and contact stress were recorded for each load repetition. Only the values corresponding to the 96^{th} to 100^{th} loading cycles were used in calculating the final resilient modulus at each stress condition.

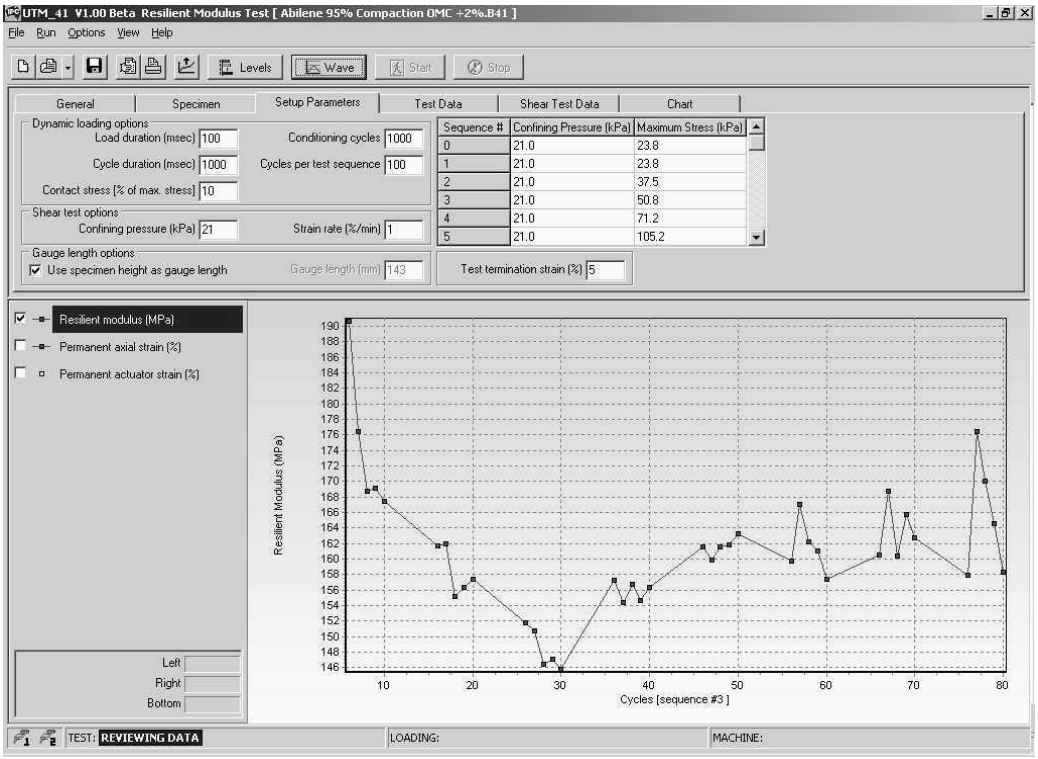

Figure 3.11: Resilient Modulus Test Setup Screen

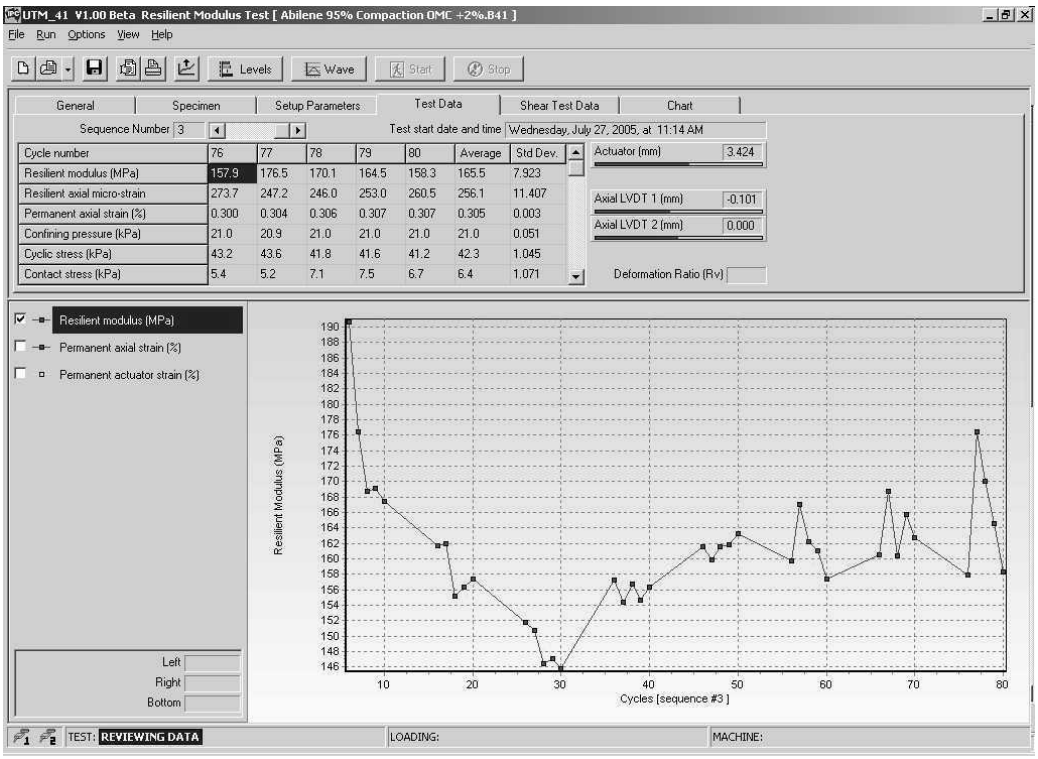

Figure 3.12: Resilient Modulus Test Result Screen

CHAPTER FOUR - RESULTS AND DISCUSSION

4.1 Introduction

This chapter discusses the results of the experiments performed in this research. The methodology used in both the field and laboratory tests is described in Chapter 3. The data collected during testing was used to determine the stiffness moduli, spatial variability and resilient modulus of each soil. This data was then used to develop a correlation between the laboratory resilient modulus and the field moisture and density.

4.2 L-FWD Test Results

The measured center deflection, corresponding to the average of a minimum of three drops, was used to estimate the dynamic stiffness using the Boussinesq equation:

$$E_{LFWD} = \frac{K \cdot \left(1 - \mu^2\right) \cdot P \cdot r}{\delta_c} \tag{4.1}$$

where,

E_{LFWD} = LFWD dynamic stiffness

K = π/2 and 2 for rigid and flexible plates, respectively.

δ_c = Central deflection

P = Applied Stress

: = Poisson's ratio

r = Radius of the plate.

In this study, the plate was assumed to be rigid and the Poisson's ratio was assumed to be 0.35. Using this information, Equation (4.1) can then be rewritten as:

$$E_{LFWD} = \frac{\pi \cdot \left(1 - 0.35^2\right) \cdot P \cdot r}{2 \cdot \delta_c} \tag{4.2}$$

Table 4.1 summarizes the test data of each project. The project location, soil type, number of points tested, and spatial test intervals. The average stiffness results obtained by back-calculation of L-FWD results are also given.

Table 4.1: Summary of L-FWD Stiffness Moduli

Site	Route	Soil Type	No. of Test Points	Spacing (m)	Moduli (MPa)		
					Avg.	Std. Dev.	Coeff. of Variation (%)
Abilene	I-70	A-2-4/ SC-SM	21	7.62	35	12	34.0
Doniphan Co.	K-7	A-6/CL	31	7.62	29	15	51.7
Garden City	US-50	A-2-4/ SC-SM	36	7.62	97	25	25.8
Hill City	US-283	A-6/CL	41	7.62	90	34	37.8
Manhattan	US-18	A-7-6/CL	31	7.62	36	18	50.0
Marysville	US-77	A-4/ML	35	15.24	59	20	33.9
Sabetha	US-75	A-7-6/CL	36	7.62	57	24	42.1
Salina 1	I-70	A-6/CL	25	15.24	37	14	37.8
Salina 2	I-70	A-4/ML	31	7.62	35	14	40.0

4.2.1 Spatial Variability of L-FWD Stiffness Modulus

Figures 4.1 through 4.7 and Table 4.1 show the spatial variability of the L-FWD measured modulus of the embankment soil in the nine projects. All soils exhibited a very high variability of the measured stiffness; the coefficient of variation ranged between 25.8 and 51.7 percent. Because of this high variability, it is not possible to develop a quality control scheme for in-situ stiffness measurements based on a control test strip.

The Garden City, Hill City, and Sabetha projects showed no consistent trend between stiffness readings. Projects such as Doniphan Co. and Salina 2 had

noticeable trends, while the remaining projects, Marysville, Salina 1, Abilene, and Manhattan, had no visible trends.

The Doniphan Co. project had stiffness values mainly between 15 and 25 MPa the first 150 m. The GeoGauge and FWD were also used to test stiffness on the Doniphan Co. project. Little correlation was seen between the GeoGauge and the L-FWD results. However, the L-FWD and FWD results correlated well; the stiffnesses measured by the two equipments in the same location were very close.

The Salina 2 soil had variable stiffness values until about 100 m into the project when the values started increasing steadily. At 180 m the stiffness values began to decrease and continued to fall through the end of the project.

The Marysville project showed a slight increasing stiffness trend from the beginning of the project to about 100 m. At this point the stiffness values started to fluctuate and no trend could be seen. The GeoGauge was also used at the Marysville test site, although poor correlation was seen between the L-FWD stiffness values and the GeoGauge stiffness values.

The Abilene test site also showed no apparent trend in stiffness until near the end of the test locations. From about 130 m until the end of the project, the stiffness values showed a slight increasing pattern.

The Manhattan project showed fairly steady stiffness values ranging from 20 to 40 MPa for the first 115 m. The GeoGauge was also used at the Manhattan test site to measure stiffness. No noticeable correlation was seen between the L-FWD and the GeoGauge stiffness values.

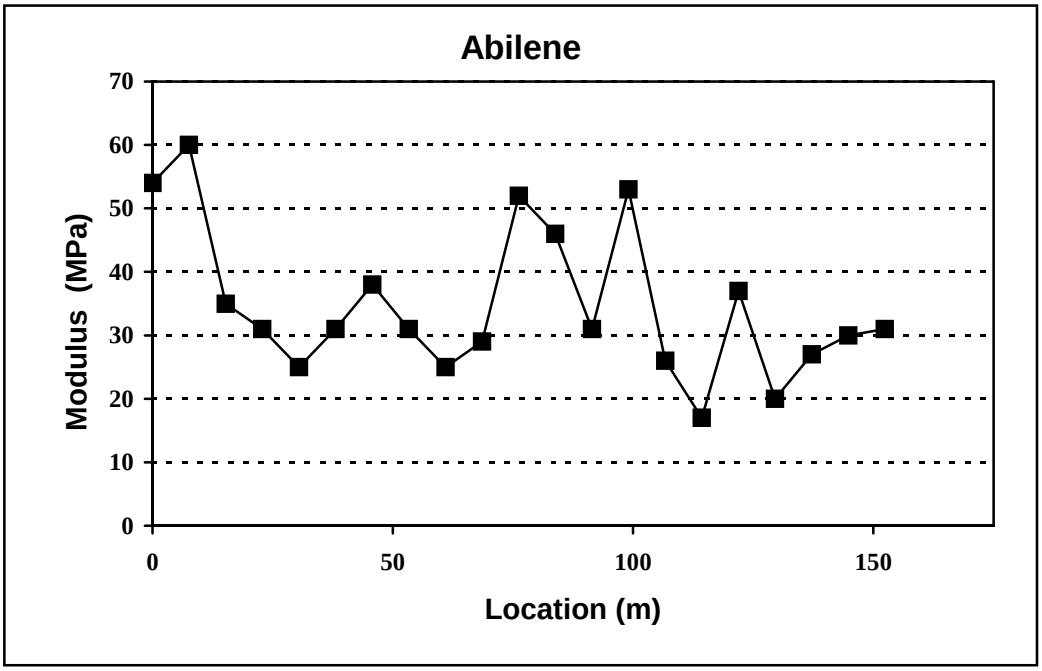

Figure 4.1: In-situ Measured Stiffness - Abilene

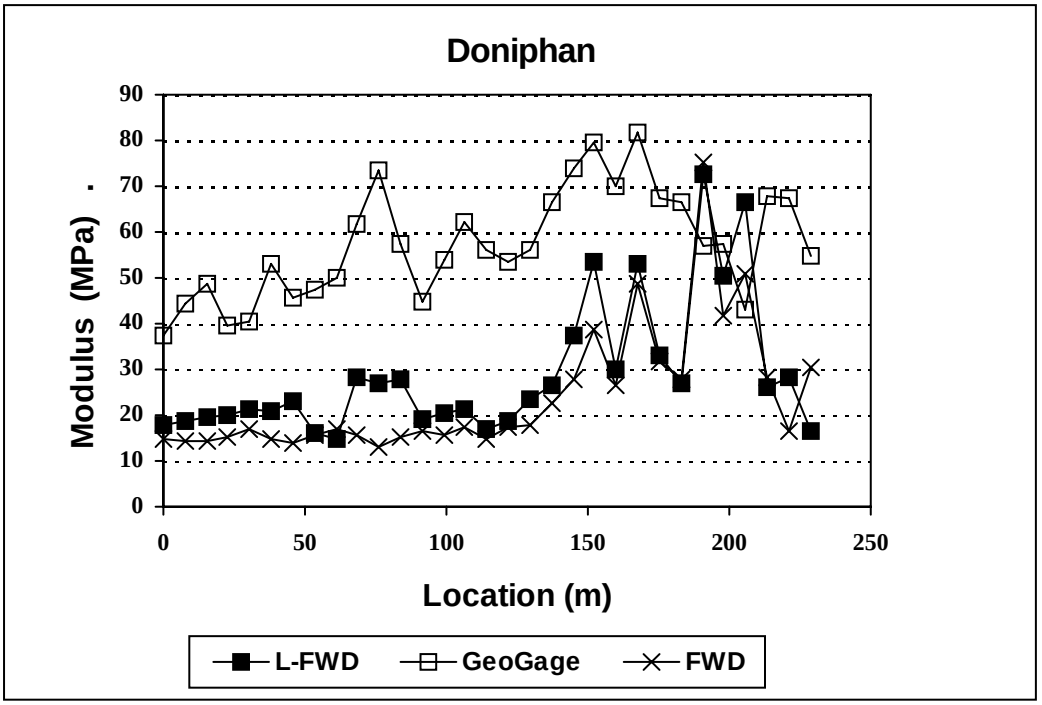

Figure 4.2: In-situ Measured Stiffness - Doniphan Co.

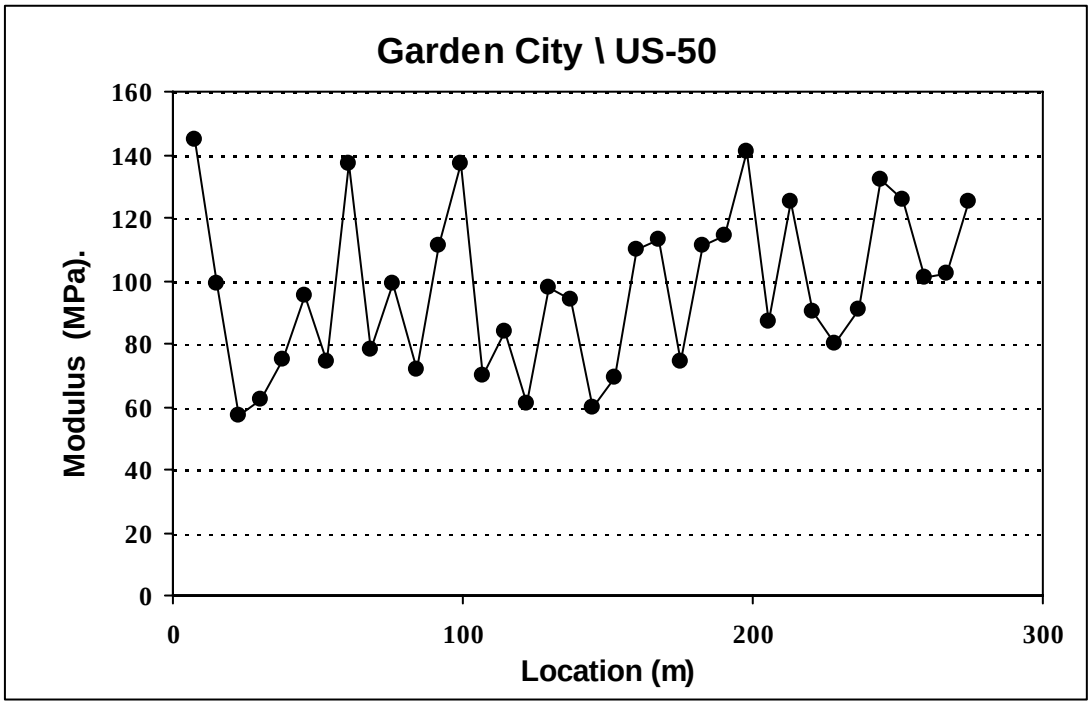

Figure 4.3: In-situ Measured Stiffness - Garden City

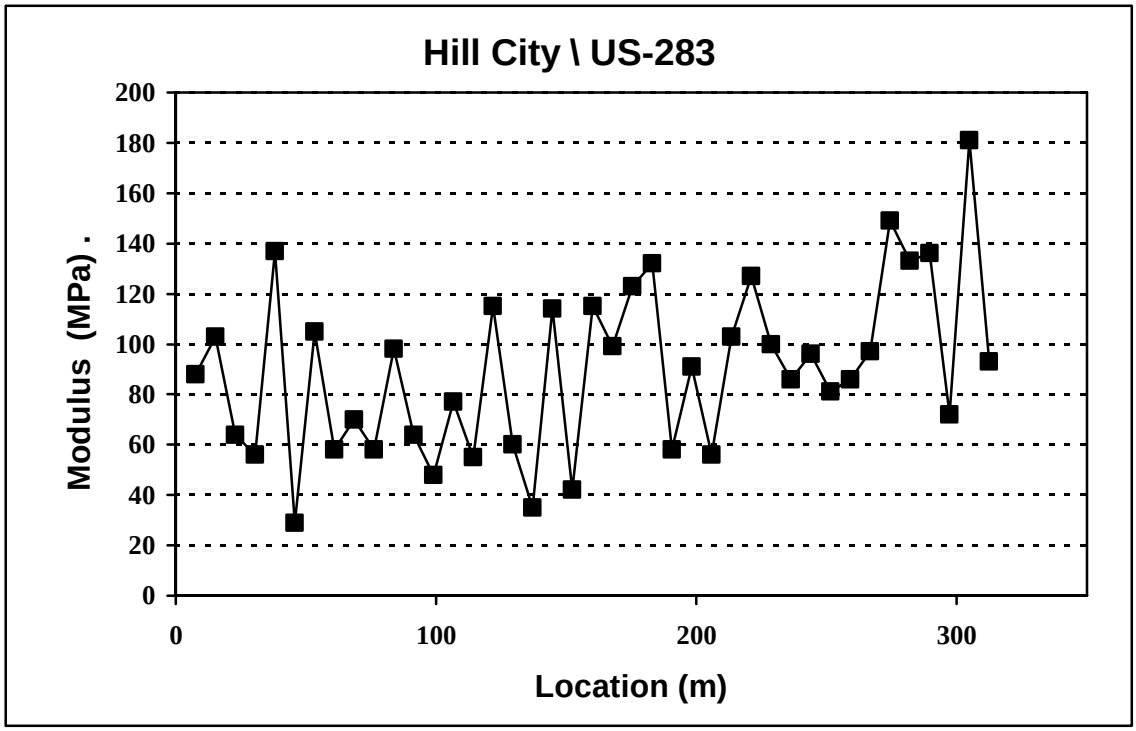

Figure 4.4: In-situ Measured Stiffness - Hill City

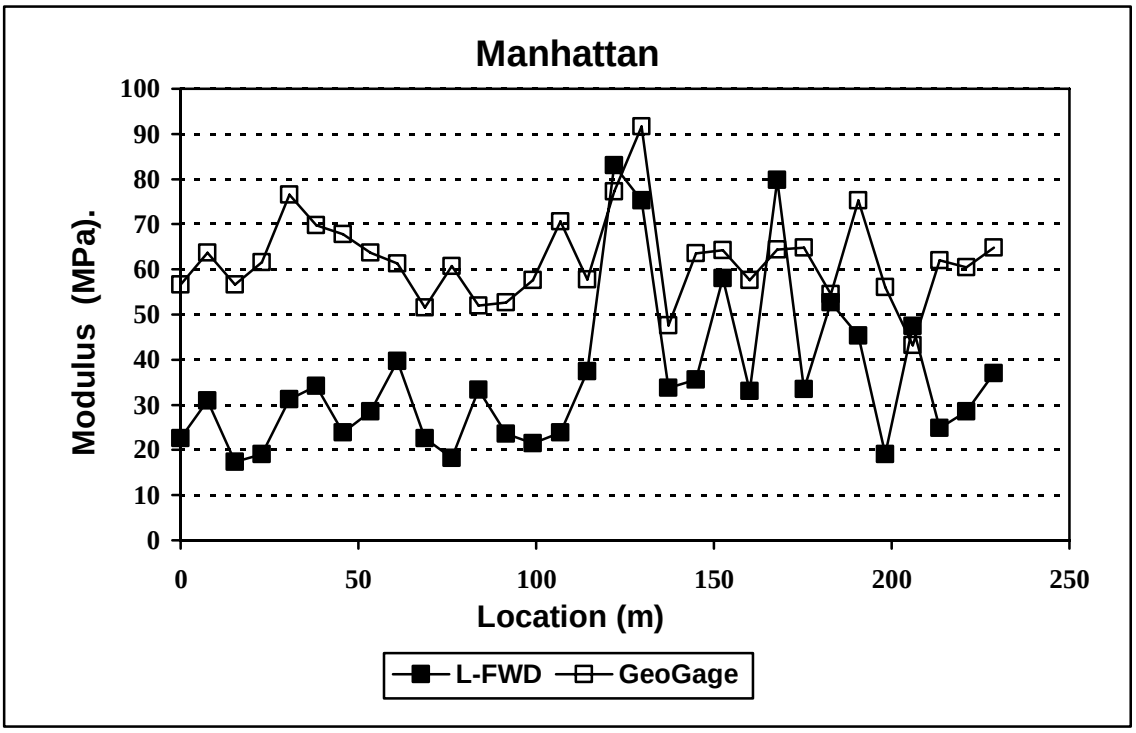

Figure 4.5: In-situ Measured Stiffness – Manhattan

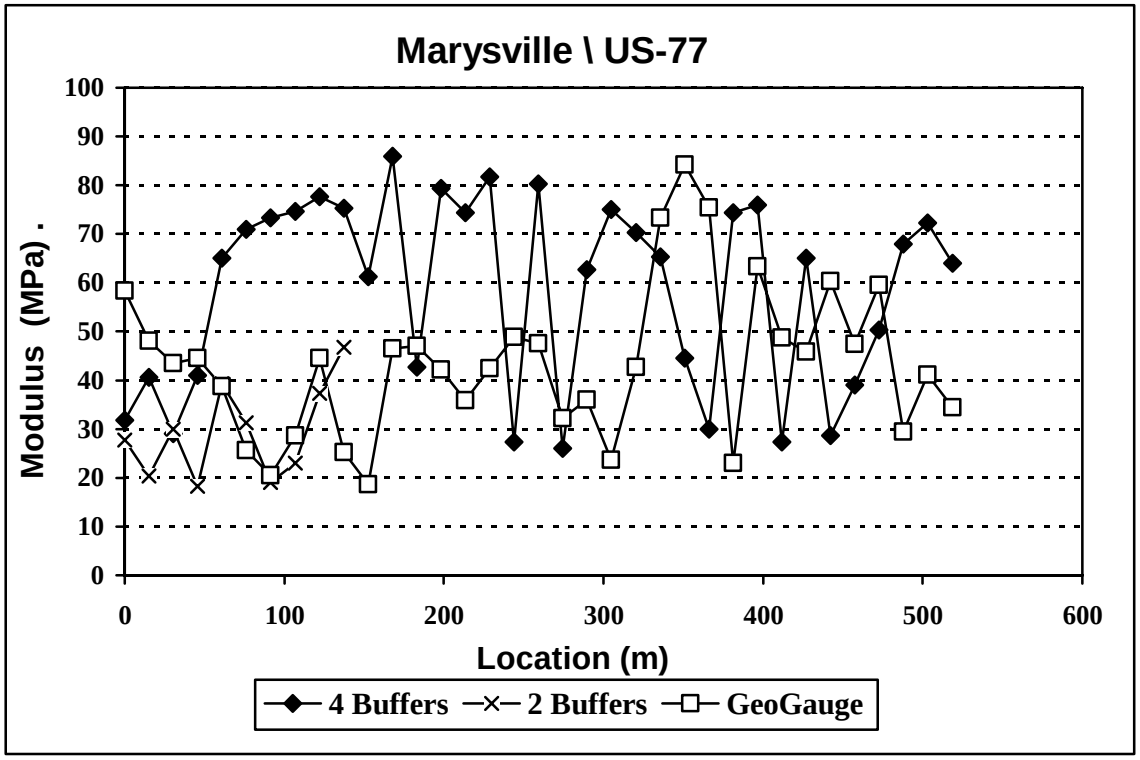

Figure 4.6: In-situ Measured Stiffness - Marysville

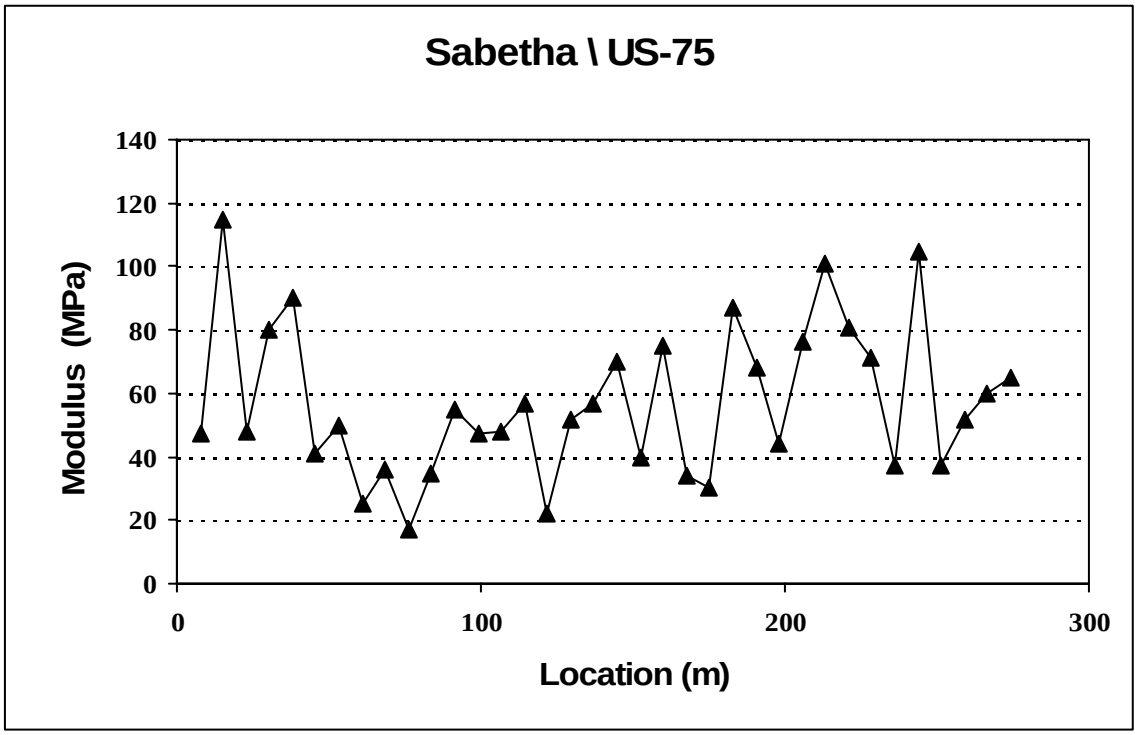

Figure 4.7: In-situ Measured Stiffness – Sabetha

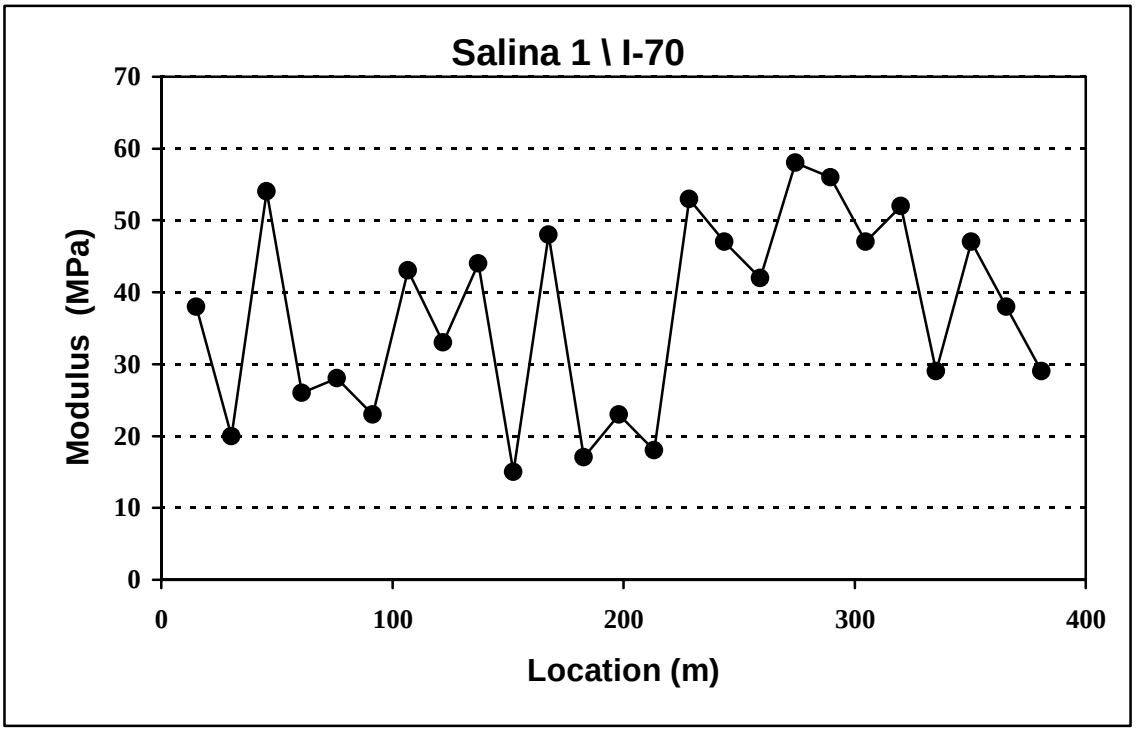

Figure 4.8: In-situ Measured Stiffness - Salina 1

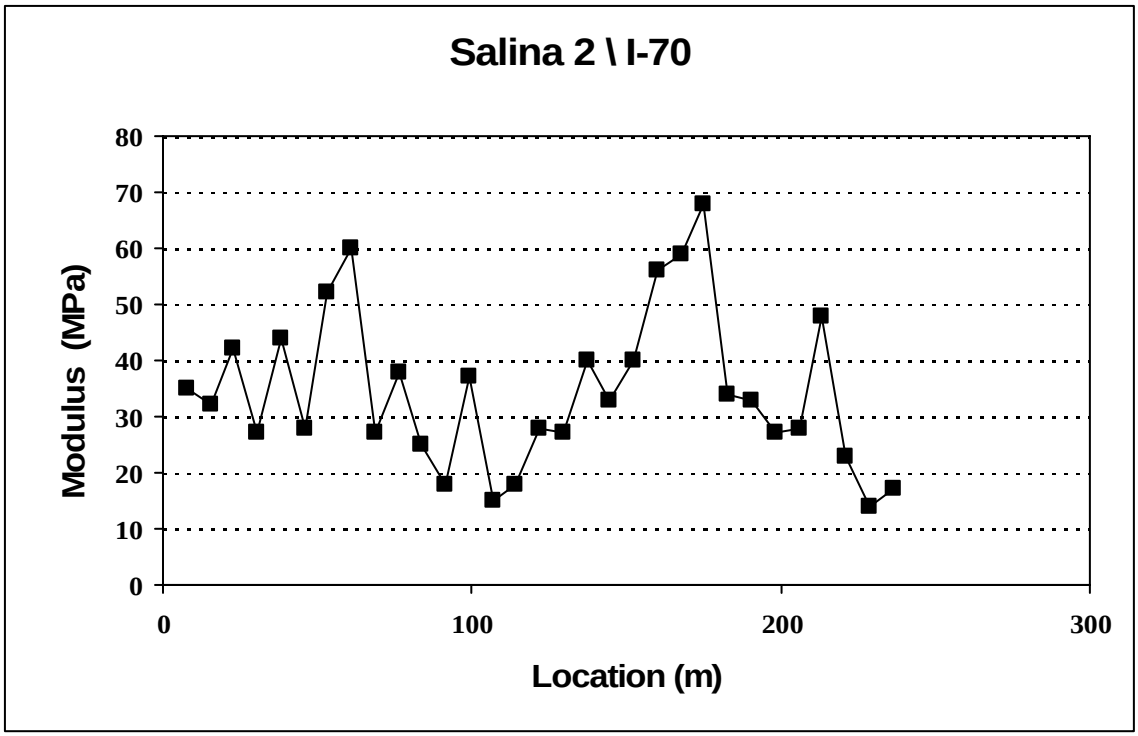

Figure 4.9: In-situ Measured Stiffness - Salina 2

4.3 Laboratory Resilient Modulus Test Results

Resilient modulus tests were preformed in the laboratory on the soil samples collected from eight of the nine test sections. For each test section, three moisture contents (-5%, OMC, +2% to +5%) and three compaction levels (90%, 95%, 100% ODD) were tested. Figures 4.10 through 4.17 display the results from the laboratory resilient modulus testing.

The effect of deviator stress on the resilient modulus varied between project soils. Of the eight soils tested, five soils showed an inverse relationship between the deviator stress and the resilient modulus. The Doniphan Co., Hill City, Manhattan, and Salina 2 soils' resilient modulus decreased with the progressive increase in deviator stress during testing. The Marysville resilient modulus decreased with increasing deviator stress only at OMC and +2% OMC. No consistent effect was noticed at -5%

OMC. Three of the soils tested showed no relationship between the deviator stress and the resilient modulus. Garden City, Sabetha, and Salina 1 did not display any consistent pattern.

The effect of compaction on resilient modulus varied with the project soil type and moisture level. Two of the eight soils tested, Hill City and Manhattan, exhibited little or no change in resilient modulus with increase in compaction level. All other soils showed varying effects of compaction based on the moisture content. The Marysville soil resilient modulus increased with compaction at -5% OMC. Marysville also showed a slight increase at OMC and no effect at +2% OMC. The Sabetha soil showed increases with compaction at all moisture contents, with the largest increase at OMC. The Salina 1 soil showed increases in resilient modulus with compaction at -5% OMC and OMC, but showed no pattern at +5% OMC. The Salina 2 soil resilient modulus increased at all moisture contents. The Doniphan Co. soil displayed no change at OMC or +3% OMC. However, a slight increase in resilient modulus was seen at -5% OMC between 90% and 95% compaction and a large increase between 95% and 100% compaction.

The effect of moisture content on the resilient modulus was similar between most of the soils tested. Of the eight soils tested, seven displayed decreasing resilient modulus with increasing moisture content. The Sabetha soil showed no consistent pattern; however the highest resilient modulus values were recorded at OMC moisture content.

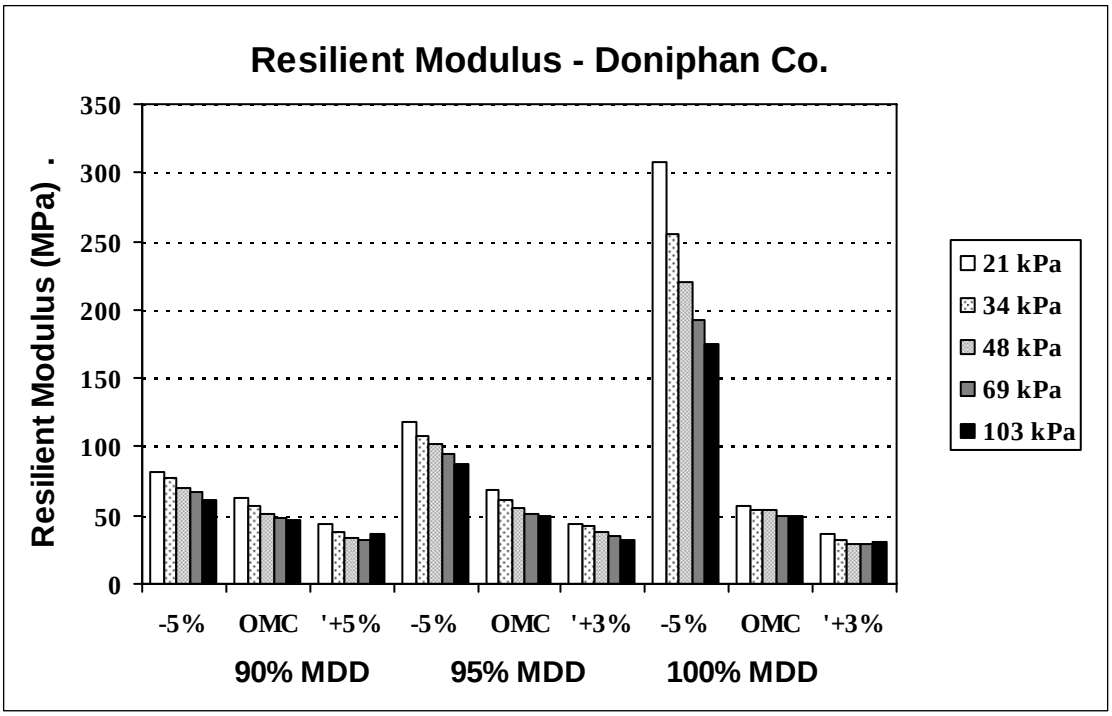

Figure 4.10: Laboratory Resilient Modulus - Doniphan soil

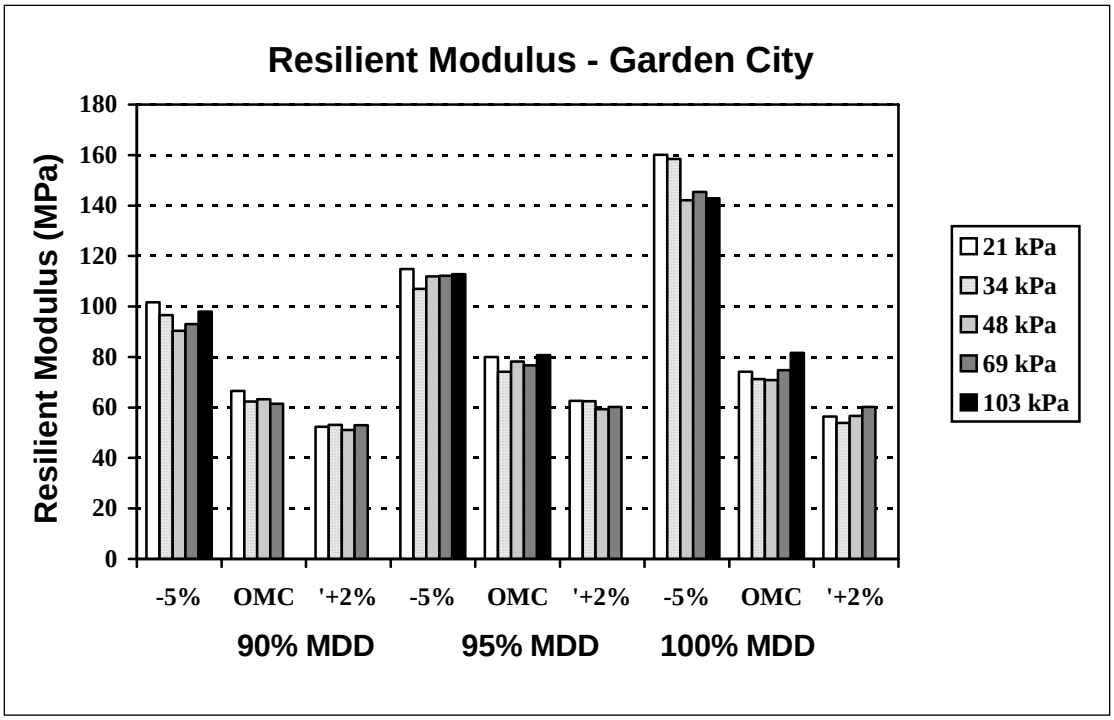

Figure 4.11: Laboratory Resilient Modulus - Garden City soil

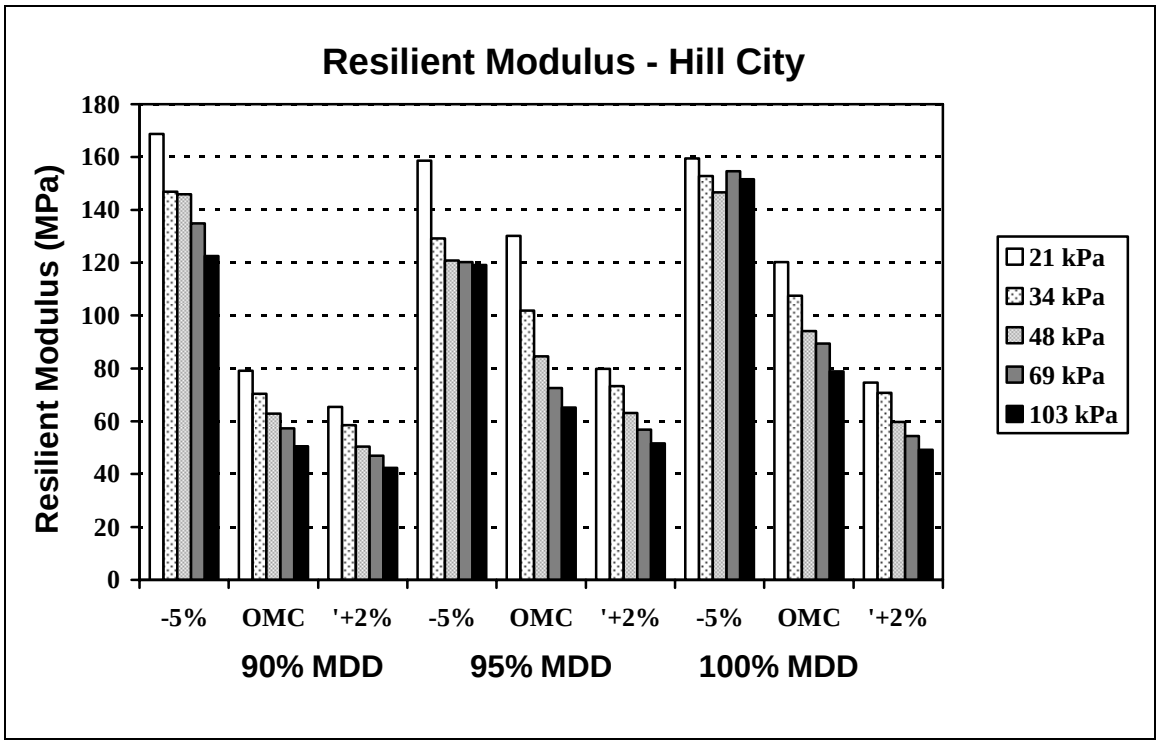

Figure 4.12: Laboratory Resilient Modulus - Hill City soil

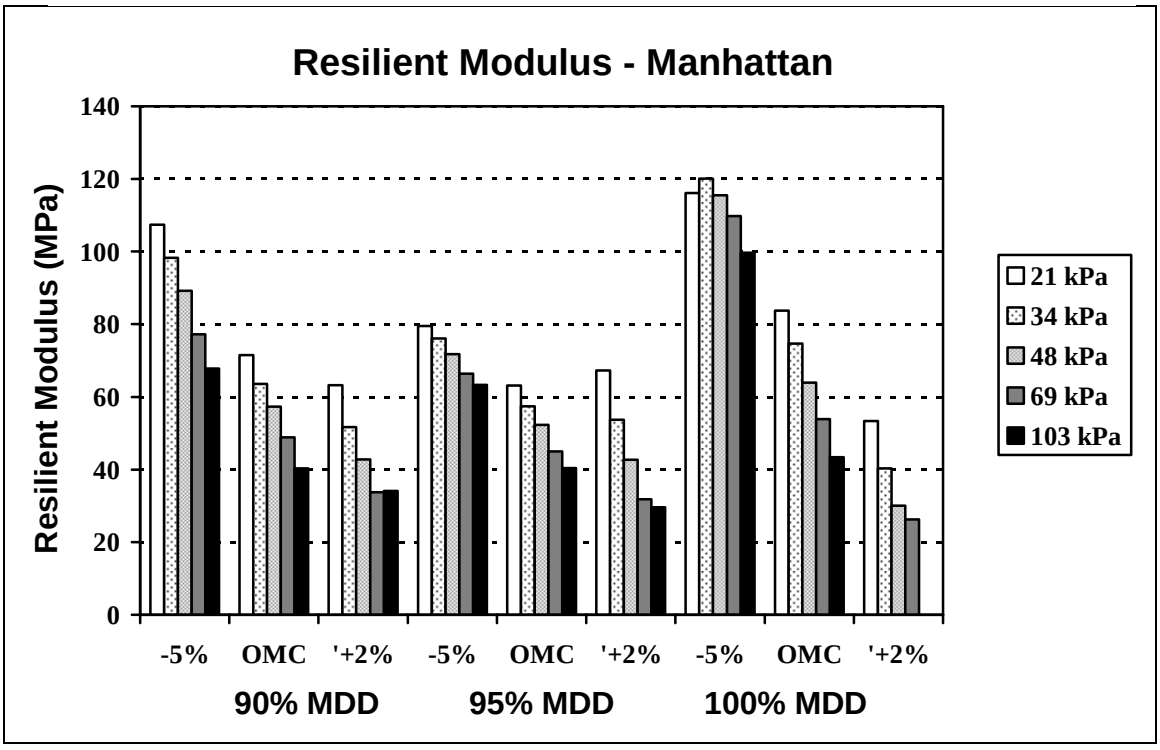

Figure 4.13: Laboratory Resilient Modulus – Manhattan soil

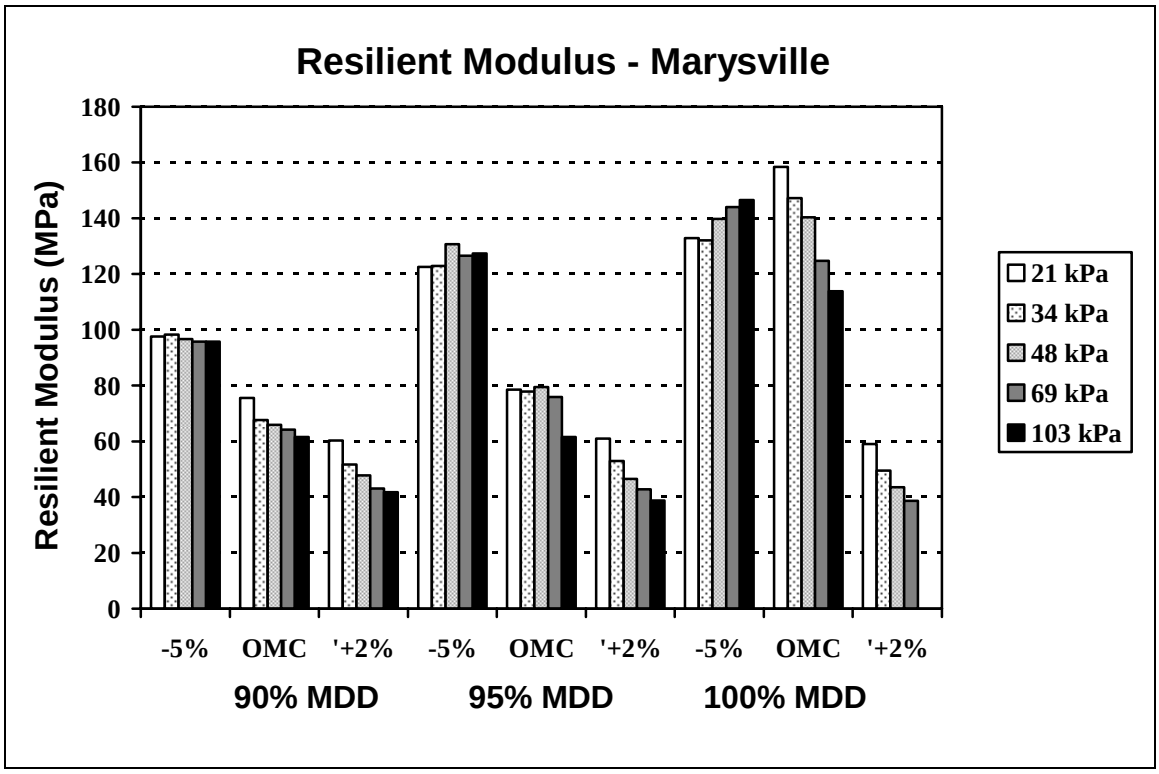

Figure 4.14: Laboratory Resilient Modulus - Marysville soil

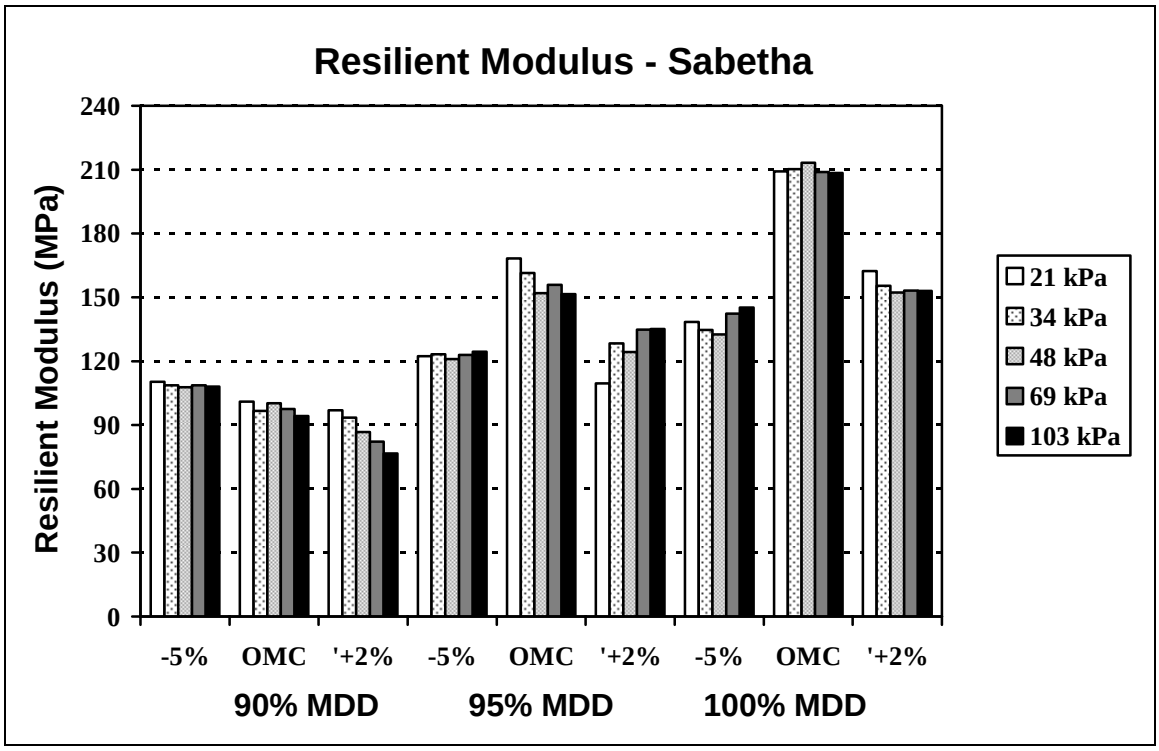

Figure 4.15: Laboratory Resilient Modulus – Sabetha soil

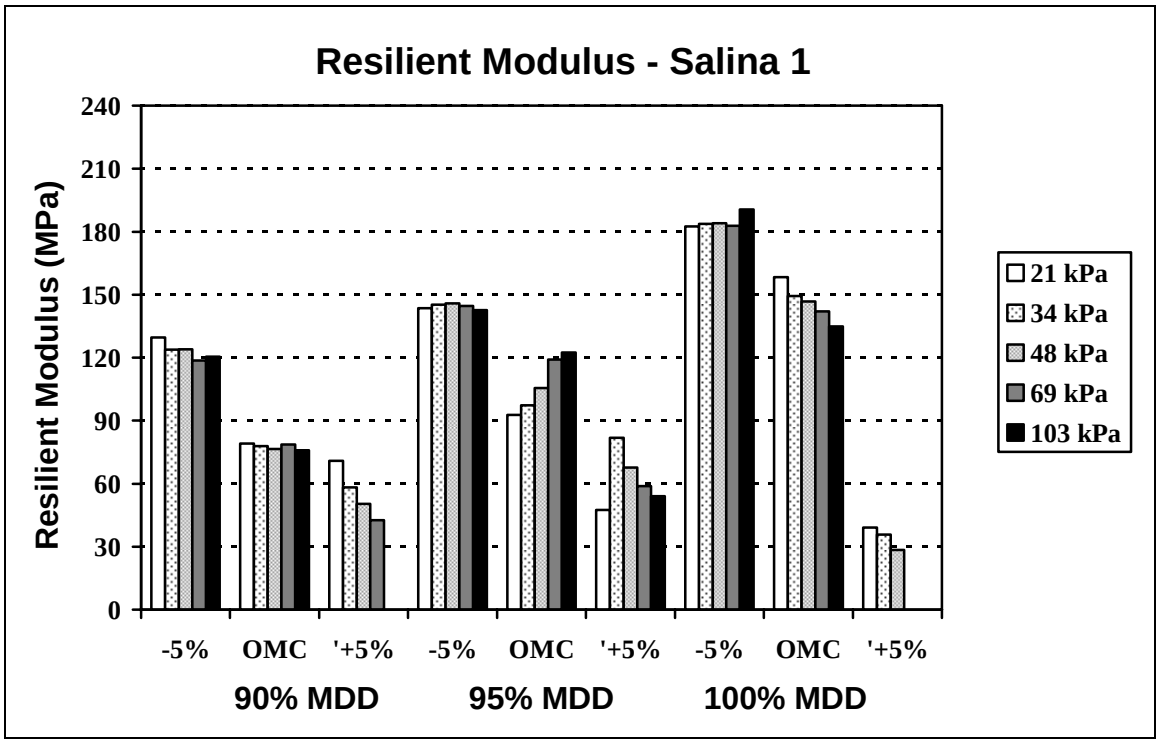

Figure 4.16: Laboratory Resilient Modulus - Salina 1 soil

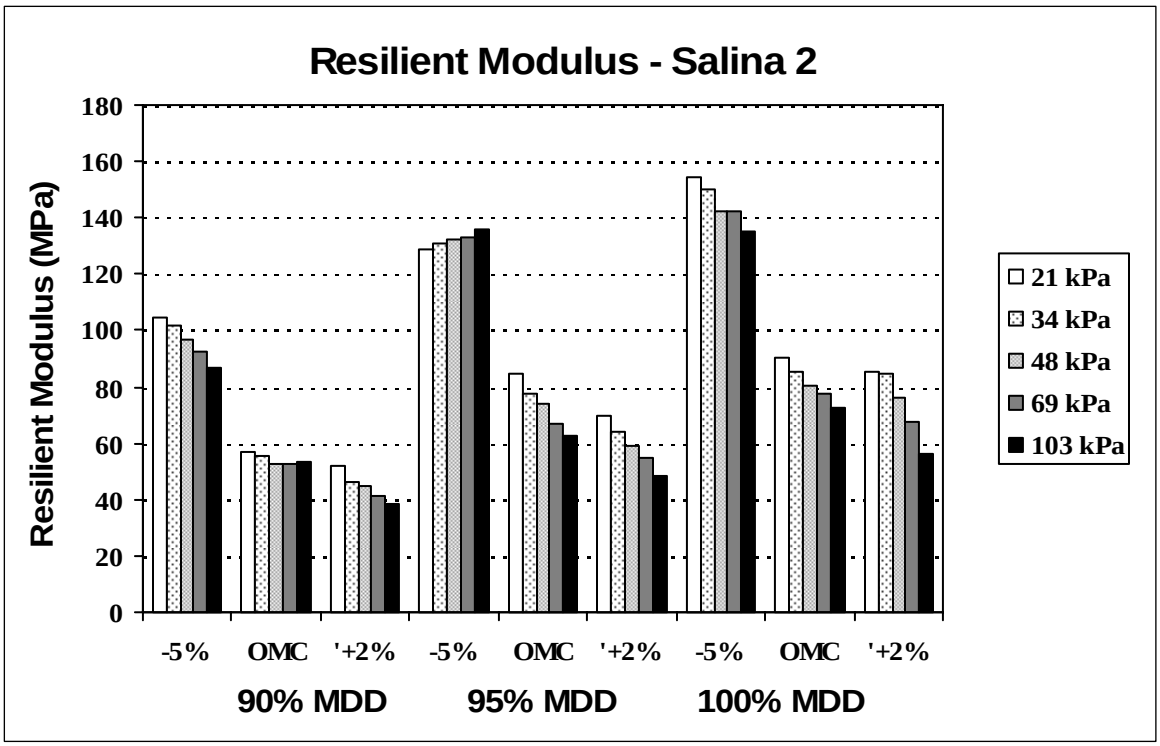

Figure 4.17: Laboratory Resilient Modulus - Salina 2 soil

4.4 Correlation of Laboratory Resilient Modulus with Moisture and Density

In order to develop a quality control scheme for the L-FWD stiffness measurements it is essential to investigate the correlation between the values of the L-FWD measured in-situ modulus and the modulus predicted for a half-space made of stress-sensitive soil loaded by a uniform distributed pressure over a circular area. The prediction of the in-situ moduli must be made based on the laboratory measure moduli and the in-situ moisture content and relative dry density, the ratio between the dry density and the maximum dry density obtained in the standard Proctor test.

4.4.1 Development of Non-Linear Constitutive Model for Clayey Soils

Two different regression models were used on eight of the nine test project soils. No model was developed for the Abilene soil, because the values of the in-situ moisture content and relative dry density were not available.

First, a constitutive model was created for each soil sample to relate the laboratory resilient modulus to the applied stresses. The constants of the model shown in Equation 4.4, were created for each soil for each of the nine moisture-density combinations using an error minimization technique in Excel Solver. The obtained constants of the constitutive model (K_1 and K_3) and R^2 values for each moisture-density combination are given in Tables 4.2 to 4.9.

$$M_r = K_1 * p_a * [(\tau_{oct} / p_a) + 1]^{K3} \qquad (4.4)$$

where,

M_r = Resilient modulus

K_1 and K_3 = regression constants

ρ_a = Pressure atmospheric

τ_{oct} = Octahedral Shear Stress $\tau_{oct} = [(\sigma_1-\sigma_2)^2 + (\sigma_1-\sigma_3)^2 + (\sigma_2-\sigma_3)^2]^{1/2} / 3$

Values for the coefficient of determination, R^2, above 0.80 were obtained for most cases. This indicates that the constitutive model is suitable to capture the stress-dependency behavior of the clayey soils studied in this project. In several instances, especially for the lowest density level and lowest moisture contents, the coefficient of determination was below 0.5. This suggests that, for these cases, the constitutive model may not represent well the stress- dependency behavior of the soil.

In a second stage, the general purpose finite element software ANSYS was used to model the deformation of a soil half-space under a static load distributed over a circular area. This was done to simulate the behavior of a stress-dependent soil during the Light FWD test.

The soil was modeled as an elastic but stress-dependent material. The two-parameter constitutive model given in Equation 4.4 was implemented in the ANSYS FEM model. The geometry of a half-space loaded by a circular plate is axis-symmetric. Therefore, for a better accuracy and reduced computation time, the mesh shown in Figure 4.18, made of axis-symmetric elements was built.

The rigid plate of the L-FWD was modeled as a circular steel plate with a modulus of elasticity of 200 GPa ($29*10^6$ psi). The vertical load was applied at the top of the rigid plate. The magnitude of the applied vertical load was 10 kN (2260 lbf); it corresponds to a uniformly distributed vertical stress of 135 kPa (20 psi). The values of the computed deflections at the center of the rigid loading plate are given in Tables 4.2 to 4.9, for each combination of moisture-density used in the laboratory resilient modulus tests.

The values of equivalent modulus for soil half-space were back-estimated from the values of the central deflections using the Boussinesq formula (Equation 4.1). The results of the half-space moduli back-estimation are also given in Tables 4.2 to 4.9.

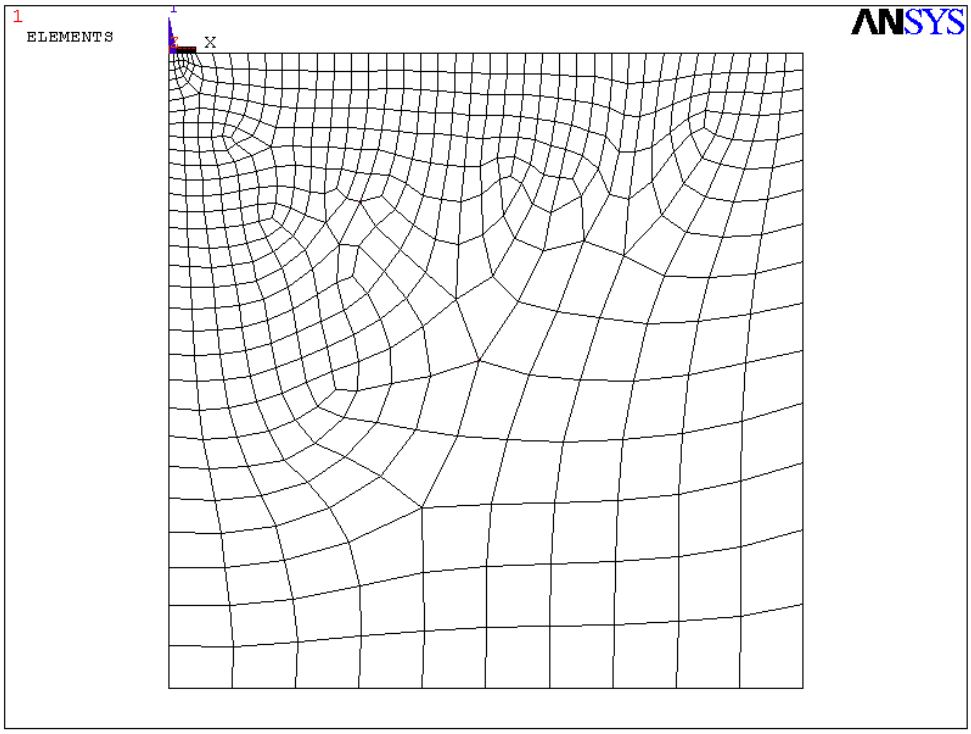

Figure 4.18: Axis-symmetric Mesh used for Modeling of the Soil Half-Space

Table 4.2: Back-estimated modulus of the soil half-space - Garden City soil

Relative Dry Density	Moisture content	K1	K3	R^2	Central deflection (mils)	Half-space modulus (MPa)
90%	OMC -5%	980.6	-0.0997	0.063	9.721	106.7
	OMC	1030.4	-3.3311	0.561	14.520	71.4
	OMC+2%	819.3	-3.1374	0.52	18.007	57.6
95%	OMC-5%	1112.8	0.019	0.974	8.447	122.7
	OMC	763.0	0.0953	0.993	12.209	84.9
	OMC+2%	982.3	-3.2705	0.581	15.153	68.4
100%	OMC-5%	1640.1	-0.406	0.993	6.028	172.0
	OMC	682.5	0.3877	0.990	13.189	78.6
	OMC+2%	859.1	-2.9732	0.472	17.064	60.8

Table 4.3: Back-estimated modulus of the soil half-space - Hill City soil

Relative Dry Density	Moisture content	K_1	K_3	R^2	Central deflection (mils)	Half-space modulus (MPa)	
90%	OMC-5%	1792.2	-1.0018	0.933	5.927	174.9	
	OMC	891.7	-1.5235	0.978	12.698	81.7	
	OMC+2%	733.9	-1.5213	0.949	15.423	67.2	
95%	OMC-5%	1582.0	-0.9052	0.799	6.637	156.2	
	OMC	1564.6	-2.5760	0.969	8.248	125.7	
	OMC+2%	910.5	-1.5571	0.983	12.486	83.0	
100%	OMC-5%	1566.1	-0.1039	0.859	6.090	170.3	
	OMC	1337.4	-1.4275	0.993	8.367	123.9	
	OMC+2%	856.0	-1.5038	0.972	13.189	78.6	

Table 4.4: Back-estimated modulus of the soil half-space - Marysville soil

Relative Dry Density	Moisture content	K_1	K_3	R^2	Central deflection (mils)	Half-space modulus (MPa)
90%	OMC -5%	986.4	-0.0845	0.736	9.647	107.5
	OMC	770.5	-0.6294	0.834	13.181	78.7
	OMC +2%	648.2	-1.2892	0.889	16.974	61.1
95%	OMC -5%	1226.1	0.1218	0.993	7.574	136.9
	OMC	872.3	-0.7027	0.874	11.745	88.3
	OMC+2%	681.0	-1.5735	0.943	16.729	62.0
100%	OMC-5%	1280.0	0.3642	0.998	7.051	147.0
	OMC	1752.3	-1.1245	0.999	6.154	168.5
	OMC+2%	951.2	-4.4048	0.831	17.352	59.8

Table 4.5: Back-estimated modulus of the soil half-space - Sabetha Soil

Relative Dry Density	Moisture content	K_1	K_3	R^2	Central deflection (mils)	Half-space modulus (MPa)
90%	OMC-5%	1099.3	-0.0514	0.425	8.623	120.2
	OMC	1021.1	-0.1875	0.612	9.434	109.9
	OMC+2%	1043.0	-0.8087	0.977	9.950	104.2
95%	OMC-5%	1213.0	0.0540	0.996	7.718	134.3
	OMC	1695.1	-0.3193	0.996	5.773	179.6
	OMC+2%	1111.9	0.5615	0.983	7.933	130.7
100%	OMC -5%	1315.7	0.2295	0.988	6.969	148.8
	OMC	2112.4	-0.0261	0.9998	4.474	231.8
	OMC+2%	1611.0	-0.1655	0.999	5.967	173.8

Table 4.6: Back-estimated modulus of the soil half-space - Salina 1 soil

Relative Dry Density	Moisture content	K_1	K_3	R^2	Central deflection (mils)	Half-space modulus (MPa)
90%	OMC-5%	1301.9	-0.2433	0.699	7.448	139.2
	OMC	793.5	-0.0991	0.430	12.013	86.3
	OMC+5%	1157.4	-4.6496	0.820	14.634	70.9
95%	OMC-5%	1454.1	-0.0323	0.997	6.503	159.4
	OMC	862.6	0.9520	0.988	9.774	106.1
	OMC+5%	661.6	-0.2915	0.694	14.740	70.3
100%	OMC -5%	1795.9	0.1250	0.999	5.169	200.6
	OMC	1635.6	-0.5017	0.9996	6.115	169.6
	OMC+5%	842.7	-7.0882	0.925	25.632	40.5

Table 4.7: Back-estimated modulus of the soil half-space - Salina 2 soil

Relative Dry Density	Moisture content	K_1	K_3	R^2	Central deflection (mils)	Half-space modulus (MPa)
90%	OMC-5%	1110.1	-0.6309	0.994	9.150	113.3
	OMC	569.7	-0.2092	0.490	16.952	61.2
	OMC+2%	554.5	-0.9957	0.959	19.144	54.2
95%	OMC-5%	1271.2	0.1724	0.9998	7.262	142.8
	OMC	919.9	-1.0370	0.997	11.597	89.4
	OMC+2%	771.3	-1.2054	0.998	14.119	73.4
100%	OMC-5%	1593.3	-0.4271	0.999	6.221	166.7
	OMC	956.0	-0.7327	0.998	10.756	96.4
	OMC+2%	1002.0	-1.3893	0.995	11.116	93.3

Table 4.8: Back-estimated modulus of the soil half-space - Doniphan soil

Relative Dry Density	Moisture content	K_1	K_3	R^2	Central deflection (mils)	Half-space modulus (MPa)
90%	OMC-5%	886.4	-0.9680	0.959	11.936	86.9
	OMC	668.8	-1.0571	0.921	15.992	64.8
	OMC+5%	420.1	-0.6186	0.327	24.144	42.9
95%	OMC -5%	1277.6	-1.0085	0.997	8.322	124.6
	OMC	747.3	-1.2090	0.933	14.579	71.1
	OMC+3%	483.5	-1.0457	0.962	22.090	46.9
100%	OMC -5%	3563.8	-2.0440	0.995	3.388	306.0
	OMC	587.7	-0.4738	0.914	16.960	61.1
	OMC+3%	346.6	-0.4868	0.881	28.813	36.0

Table 4.9: Back-estimated modulus of the soil half-space - Manhattan soil

Relative Dry Density	Moisture content	K_1	K_3	R^2	Central deflection (mils)	Half-space modulus (MPa)
90%	OMC-5%	1241.0	-1.5859	0.990	9.194	112.8
	OMC	851.9	-1.9234	0.998	13.963	74.3
	OMC+2%	758.9	-2.4599	0.898	16.758	61.9
95%	OMC-5%	852.2	-0.7991	0.996	12.163	85.3
	OMC	723.8	-1.5557	0.988	15.705	66.0
	OMC+2%	880.2	-3.2296	0.949	15.921	65.1
100%	OMC - 5%	1266.6	-0.5427	0.986	7.935	130.7
	OMC	1031.4	-2.2413	0.995	11.998	86.4
	OMC+2%	919.9	-5.5708	0.943	20.521	50.5

4.5 Prediction of In-Situ Modulus from Laboratory Measured Moduli

Once the equivalent modulus of the soil half-space was back-estimated for each moisture-density combination, a linear regression model was developed to relate the equivalent half-space modulus to the density and moisture content. The model, given by Equation 4.5, can be used to predict the in-situ modulus, EPRED, function of the in-situ soil relative dry density and moisture content (expressed as percent deviation from the optimum moisture content). This model can be used to predict the in-situ modulus for given in-situ moisture content and dry density values. The parameters of the regression model are given for each soil in Table 4.10.

$$E_{PRED} = a_0 + a_1*(RDD) + a_2*(MC - OMC) + a_3*(RDD)*(MC-OMC) \quad (4.5)$$

Where,

E_{PRED} = Regression Model Laboratory stiffness

a_0, a_1, a_2, and a_3 = regression constants

RDD = Relative Dry Density, the Dry Density as a percent of Maximum Dry Density

MC = Moisture Content, percent

OMC = Optimum Moisture Content, percent

Table 4.10: Regression Coefficients for the In-situ Moduli Prediction Model

Project		Regression Coefficients				R^2
		a_0	a_1	a_2	a_3	
Garden City	coefficient	-69.34	1.5833	78.982	-0.9407	0.963
	p-value	*0.388*	*0.095*	*0.020*	*0.013*	
Hill City	coefficient	-84.61	1.999	-47.41	0.3658	0.921
	p-value	*0.520*	*0.182*	*0.283*	*0.418*	
Marysville	coefficient	-286.75	3.9904	17.717	-0.2785	0.652
	p-value	*0.305*	*0.191*	*0.835*	*0.756*	
Sabetha	coefficient	-625.72	8.164	-77.367	0.832	0.691
	p-value	*0.045*	*0.021*	*0.353*	*0.343*	
Salina 1	coefficient	-167.24	2.833	78.648	-0.975	0.802
	p-value	*0.531*	*0.329*	*0.371*	*0.300*	
Salina 2	coefficient	-293.2	4.0225	12.194	-0.2338	0.972
	p-value	*0.006*	*0.002*	*0.582*	*0.333*	
Doniphan	coefficient	-376.25	4.8298	267.78	-2.996	0.878
	p-value	*0.251*	*0.175*	*0.019*	*0.015*	
Manhattan	coefficient	49.23	0.264	27.01	-0.3593	0.783
	p-value	*0.710*	*0.848*	*0.531*	*0.431*	

Table 4.10 gives the regression coefficients and their corresponding p-values, along with R-squared values obtained for the linear regression models. For a 95% confidence interval, the p-values indicate that the back-estimated stiffness of the Garden City soil appears to depend both on moisture content and dry density. The stiffness of Hill City, Marysville, Salina 1 and Manhattan soils seems to be unaffected by either moisture content or dry density level. The stiffness of the Sabetha and Salina 2 soils seems to be influences only by dry density; no linear relation with the moisture content exists. The Doniphan Co. soil was the only soil in which the stiffness depended on moisture alone.

Using the model developed from the in-situ half-space stiffness (Equation 4.5), the field stiffness of each soil was predicted using the in-situ measured dry density and moisture content, for the points for which the values were available. The predicted

stiffnesses are given in Tables 4.11 to 4.18. The values of the L-FWD measured stiffnesses are plotted relative to the predicted in-situ stiffnesses in Figures 4.19 to 4.26.

Table 4.11: Field Data and Predicted Stiffness - Doniphan

Doniphan Co.	Location	In-Situ Density (% ODD)	In-Situ Moisture (%OMC)	Stiffness (MPa)	Predicted Stiffness (MPa)
A-6/ CL	1	111.99	-11.5	17.9	943.4
	6	116.4	-8.5	21.3	873.9
	11	115.4	-11.6	27.0	1,085.2
	16	117.2	-11.2	17.0	1,123.1
	21	122.2	-7.9	53.5	990.6
	26	121.2	-8.8	72.4	1,047.9
	31	120.9	-9.4	16.7	1,095.2

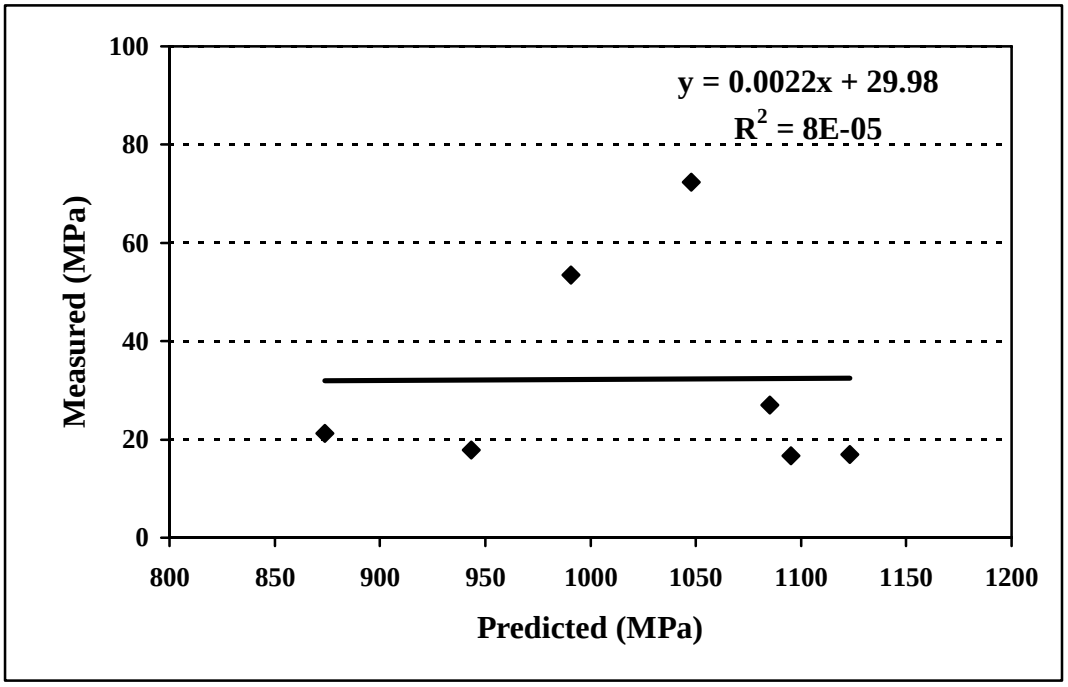

Figure 4.19: Measured vs. Predicted Stiffness - Doniphan Co.

The predicted in-situ stiffness of the Doniphan soil is 20 to 50 times higher than the measured stiffness. The most plausible reason for this difference and for the high values of the predicted moduli is that the soil was very dry during the L-FWD field tests; the in-situ moisture content was approximately 8 to 11 percent below the optimum moisture content for this soil, and about 4 to 6 percent below the lowest moisture content of the samples tested for resilient moduli in the laboratory. As indicated in Figure 4.19, there is no statistical correlation between the in-situ measured and predicted moduli for this soil.

Table 4.12: Field Data and Predicted Stiffness - Garden City

Garden City US-50	Location	In-Situ Density (% ODD)	In-Situ Moisture (%OMC)	Measured Stiffness (MPa)	Predicted Stiffness (MPa)
A-2-4/ SC-SM	1	95.2	-5.20	145	136.4
	6	98.7	-1.30	95	104.9
	11	95.7	-5.90	72	147.4
	16	99.7	-3.40	61	138.9
	21	96.5	-5.70	110	150.7
	26	97.4	-6.10	141	162.0
	31	93.3	-6.50	91	135.5
	36	97.7	-3.80	125	134.5

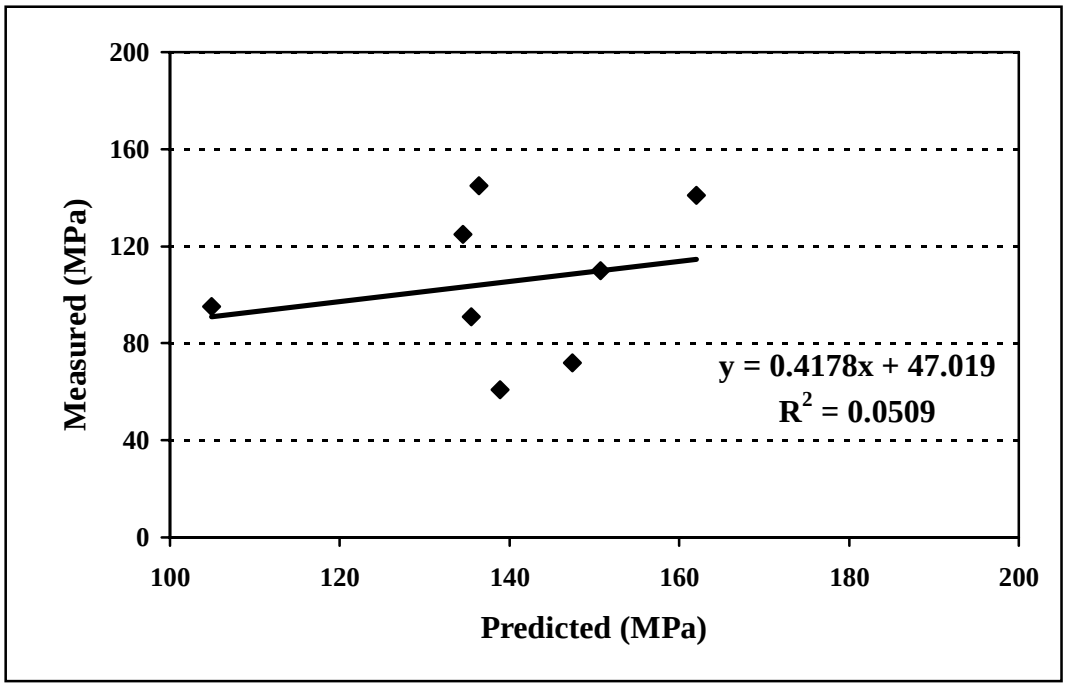

Figure 4.20: Measured vs. Predicted Stiffness - Garden City

The predicted in-situ stiffness of the Garden City soil is higher than the L-FWD measured stiffness. As indicated in Figure 4.20, there is no statistical correlation between the in-situ measured and predicted moduli for this soil.

Table 4.13: Field Data and Predicted Stiffness - Hill City

Hill City US-283	Location	In-Situ Density (% ODD)	In-Situ Moisture (%OMC)	Stiffness (MPa)	Predicted Stiffness (MPa)
A-6/ CL	1	104.4	-1.00	88	133.31
	6	93.1	-5.70	29	177.64
	11	103.5	-6.10	98	180.56
	16	101	-2.70	115	145.55
	21	103.7	-4.40	115	164.40
	26	101.1	-2.70	91	145.65
	31	106.6	-3.40	86	157.11
	36	102.9	-2.70	149	147.47

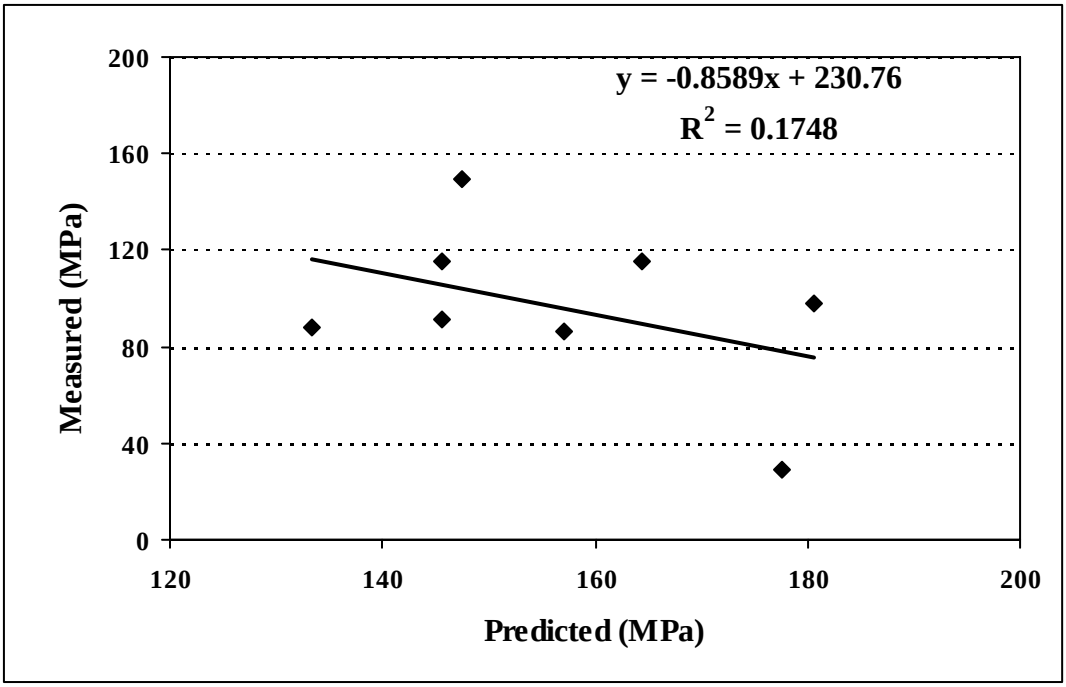

Figure 4.21: Measured vs. Predicted Stiffness - Hill City

The predicted in-situ stiffness of the Hill City soil is higher than the L-FWD measured stiffness. As indicated in Figure 4.21, there is a poor statistical correlation between the in-situ measured and predicted moduli for this soil.

Table 4.14: Field Data and Predicted Stiffness - Manhattan

Manhattan	Location	In-Situ Density (% ODD)	In-Situ Moisture (%OMC)	Stiffness (MPa)	Predicted Stiffness (MPa)
A-7-6/ CL	1	106	-11.9	22.6	209.0
	6	110	-8.9	34.1	189.6
	11	109	-12	18.2	223.8
	16	111	-11.6	37.4	227.8
	21	115	-8.3	58.0	198.3
	26	115	-9.2	45.3	211.2
	31	114	-9.8	37.0	216.0

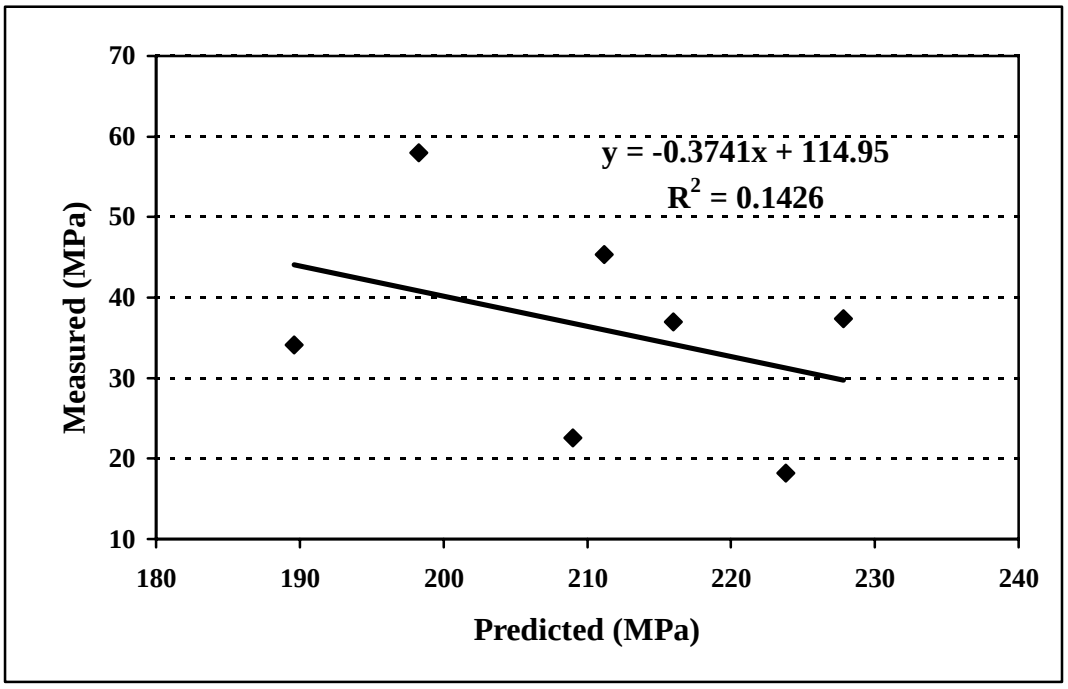

Figure 4.22: Measured vs. Predicted Stiffness - Manhattan

The measured in-situ stiffness of the Manhattan soil is lower than the predicted stiffness. As indicated in Figure 4.22, there is a poor statistical correlation between the in-situ measured and predicted moduli for the Manhattan soil. As for the Doniphan soil, the Manhattan soil was very dry during the L-FWD field tests; the in-situ moisture content was approximately 8 to 12 percent below the optimum moisture content, and about 4 to 6 percent below the lowest moisture content of the samples tested for resilient moduli in the laboratory.

Table 4.15: Field Data and Predicted Stiffness - Marysville

Marysville US-77	Location	In-Situ Density (% DD)	In-Situ Moisture (%MC-OMC)	Stiffness (MPa)	Predicted Stiffness (MPa)
A-4/ ML	5	101.3	-0.1	65	118.5
	10	96.6	-2.2	75	118.9
	15	102.5	-0.2	74	124.4
	20	101.4	1.2	63	105.2
	25	102.5	-1.2	30	135.2
	30	103.4	-4.1	29	171.3
	35	95.1	-2.3	64	112.9

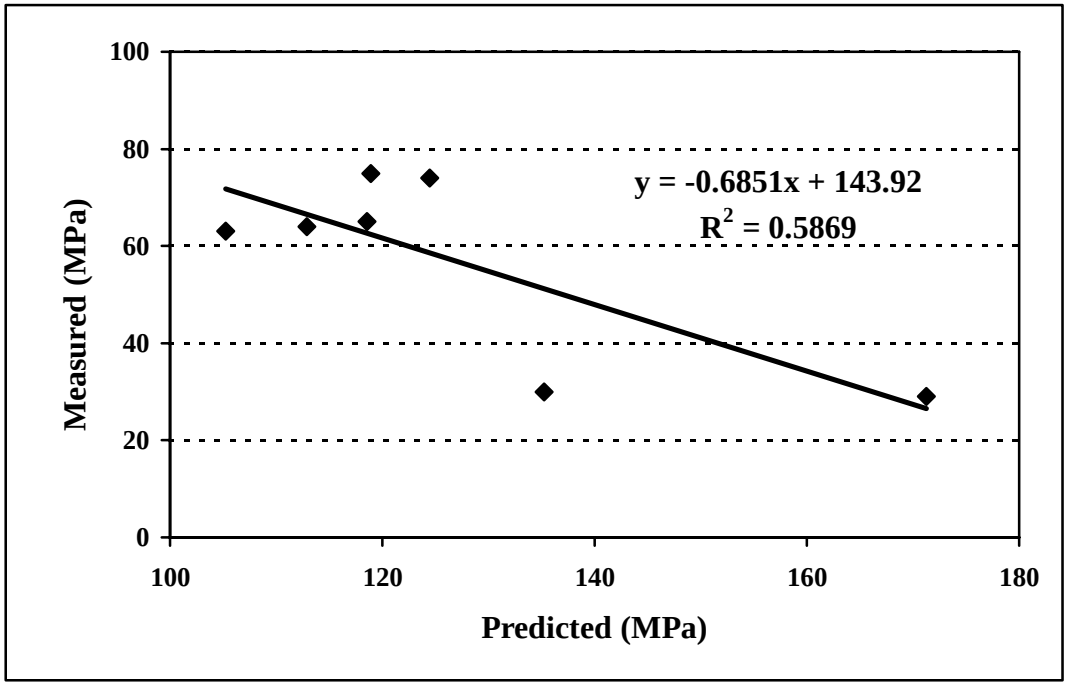

Figure 4.23: Measured vs. Predicted Stiffness - Marysville

The measured in-situ stiffness of the Marysville soil is lower than the predicted stiffness. As indicated in Figure 4.23, there is some negative statistical correlation between the in-situ measured and predicted moduli for this soil. When compared to the other soils, the in-situ moisture content for this soil was close to the optimum moisture content. Therefore, the prediction of stiffness is done more accurately since samples of

this soil were tested for resilient moduli in the laboratory at the optimum moisture content.

Table 4.16: Field Data and Predicted Stiffness - Sabetha

Sabetha US-75	Location	In-Situ Density (% ODD)	In-Situ Moisture (%OMC)	Stiffness (MPa)	Predicted Stiffness (MPa)
A-7-6/ CL	1	100.8	-3.5	47	174.31
	6	98.3	-2.4	41	166.10
	11	100.0	-4.0	35	167.17
	16	97.4	-1.0	22	165.75
	21	95.8	1.6	75	160.21
	26	94.2	1.9	44	145.33
	31	87.3	4.4	37	66.35
	36	92.6	2.2	65	129.65

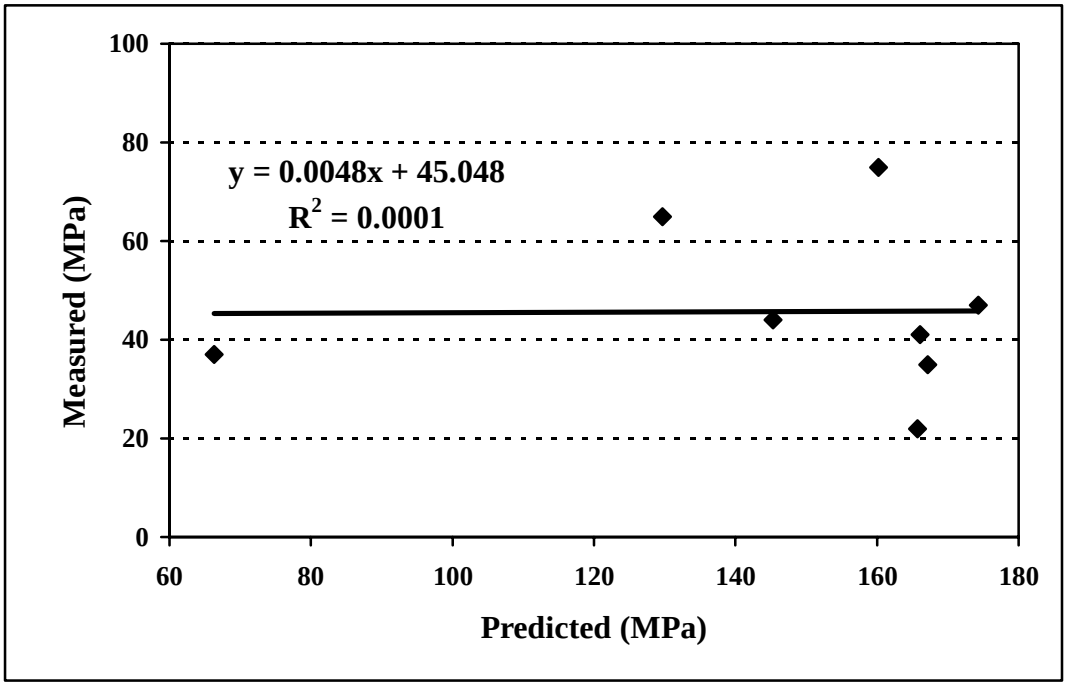

Figure 4.24: Measured vs. Predicted Stiffness - Sabetha

The predicted in-situ stiffness of the Sabetha soil is higher than the L-FWD measured stiffness. As indicated in Figure 4.24, there is no statistical correlation between the in-situ measured and predicted moduli for this soil.

The measured in-situ stiffness of the Salina 1 and Salina 2 soils is lower than the predicted stiffness. Figure 4.25 and 4.26 indicate that there is no statistical correlation between the in-situ measured and predicted moduli for these soils.

Table 4.17: Field Data and Predicted Stiffness - Salina 1

Salina I-70	Location	In-Situ Density (% ODD)	In-Situ Moisture (%OMC)	Stiffness (MPa)	Predicted Stiffness (MPa)
A-6/ CL	1	116.1	-0.5	38	178.95
	5	92.2	0.3	28	90.59
	10	97.1	-0.5	15	115.86
	15	93.3	2.6	53	65.06
	20	90.7	-1.5	47	104.39
	25	94.0	-0.7	29	108.16

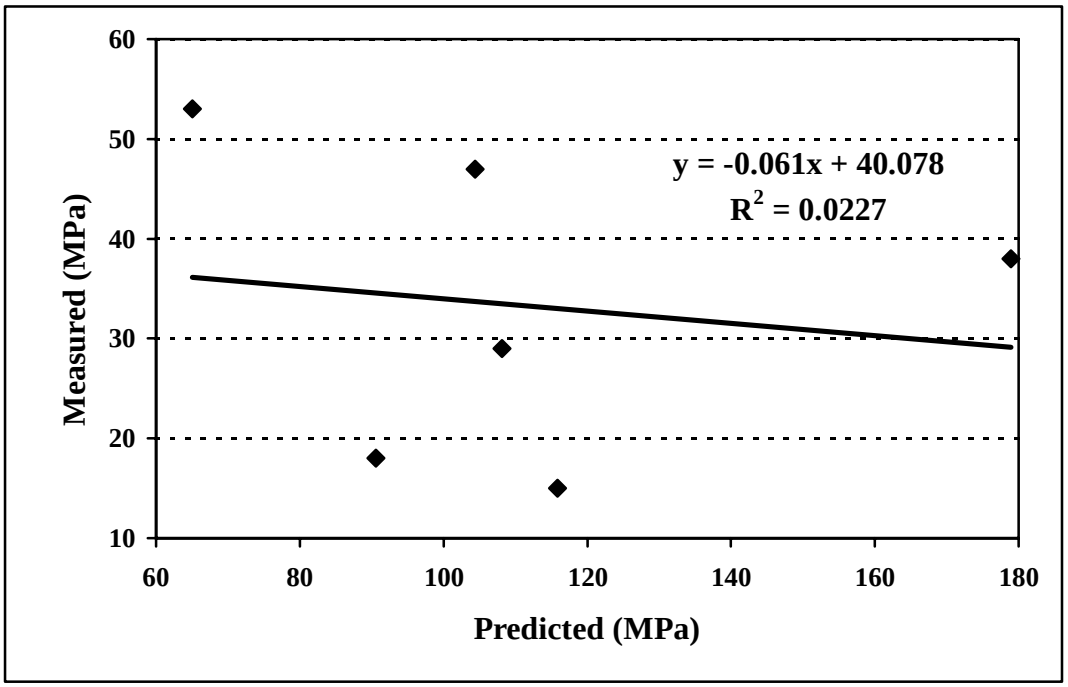

Figure 4.25: Measured vs. Predicted Stiffness - Salina 1

Table 4.18: Field Data and Predicted Stiffness - Salina 2

Salina 2 I-70	Location	In-Situ Density (% ODD)	In-Situ Moisture (%OMC)	Stiffness (MPa)	Predicted Stiffness (MPa)
A-7-6/ CL	1	101.5	-3.7	35	157.78
	6	96.4	1.0	28	84.22
	11	96.0	1.4	25	78.61
	16	98.3	5.6	28	41.79
	21	94.0	-1.5	56	99.59
	26	97.9	0.3	27	97.40
	31	100.3	-3.2	17	146.28

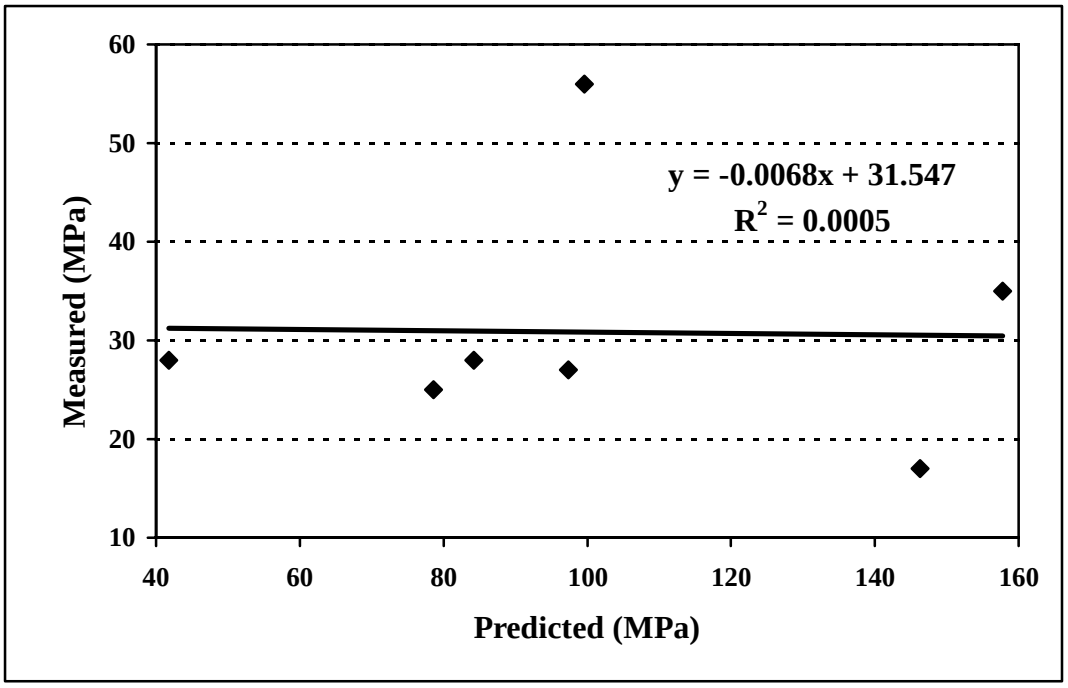

Figure 4.26: Measured vs. Predicted Stiffness - Salina 2

Overall, by looking at the results obtained for eight soils, it can be concluded that the in-situ soil stiffness measured by the L-FWD is in general lower than the predicted stiffness. Also, it can be concluded that there is a very poor statistical correlation between the in-situ measured and predicted moduli. Because of the lack of statistical correlation between the L-FWD in-situ measured stiffness and the in-situ stiffness predicted for a semi-infinite half-space of stress sensitive soil, no quality control schemes based on laboratory measured moduli could be developed in this study.

4.6 Correlation of In-Situ L-FWD Stiffness with GeoGauge Stiffness

The Geo-Gauge was used along with the L-FWD on three test sites to collect stiffness data. These project sites included Marysville, Manhattan, and Doniphan Co. As can be seen in Figure 4.27, there was little correlation between the L-FWD and the GeoGauge stiffness. The Marysville test site had an R^2 value of 0.1681 between the L-FWD and the GeoGauge stiffness; however, the stiffness values indicated an inverse relationship. The Manhattan test site had an R^2 value of 0.1945, and the Doniphan Co. test site had an R^2 value of 0.0980. Visually, the Doniphan Co. data appeared to have the most linear relationship; however, there were several out-lying points that decreased the R^2 value. When these out-lying data points are removed, the Doniphan Co. R^2 value is 0.6068.

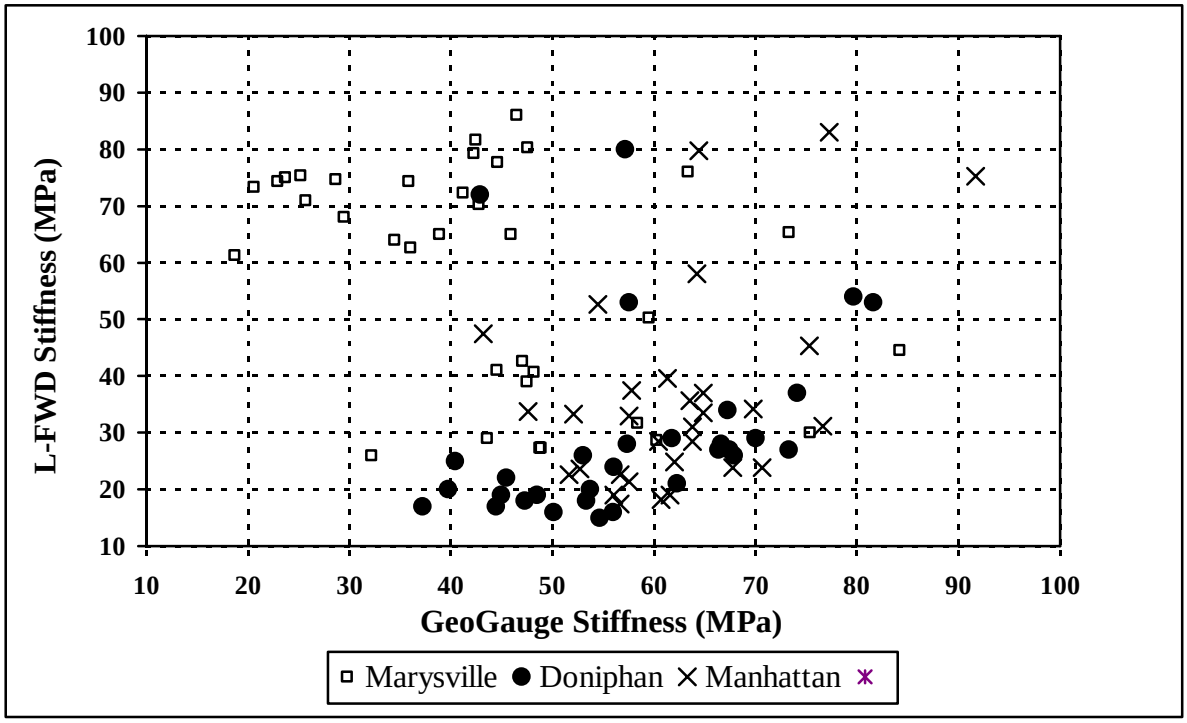

Figure 4.27: L-FWD vs. GeoGauge Stiffness

4.7 Correlation of In-Situ L-FWD Stiffness with FWD Stiffness

At the Doniphan Co. test site, the FWD was used in conjunction with the L-FWD to measure in-situ stiffness at the same test points. Figure 4.28 shows the correlation between the FWD and the L-FWD stiffness data. The graph shows a strong correlation between the stiffness values with an R^2 value of 0.836.

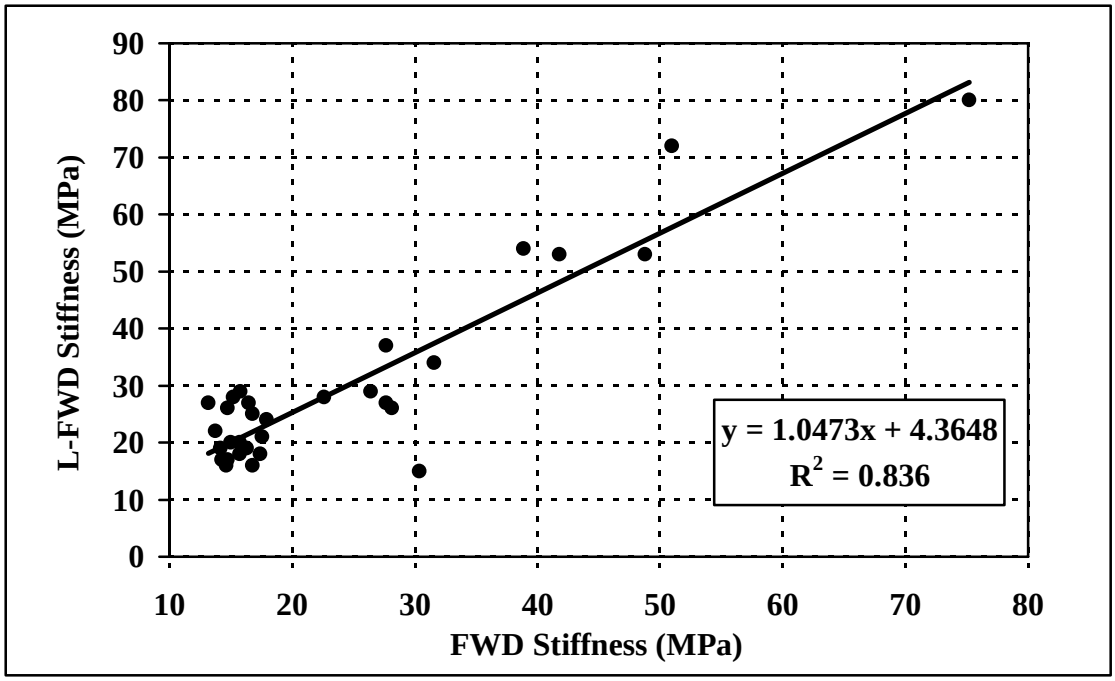

Figure 4.28 L-FWD vs. FWD Stiffness - Doniphan

4.8 Results from Additional Sensors on L-FWD

At the Abilene and Doniphan Co. test sites, L-FWD stiffness data was gathered with two additional geophones. Figures 4.29 and 4.30 show the stiffness values computed from the deflections measured by each of the three geophones. The Doniphan Co. test site exhibited similar stiffness results for the center-mounted geophone and the 250 mm offset geophone. The 500 mm offset geophone exhibited increased stiffness values with higher variability than either the center-mounted or 250

mm offset geophone. The Abilene test site showed progressively increasing stiffness values and variability as the offset distance increased. This indicates that the use of additional geophones does not improve the measurements of in-situ soil stiffness.

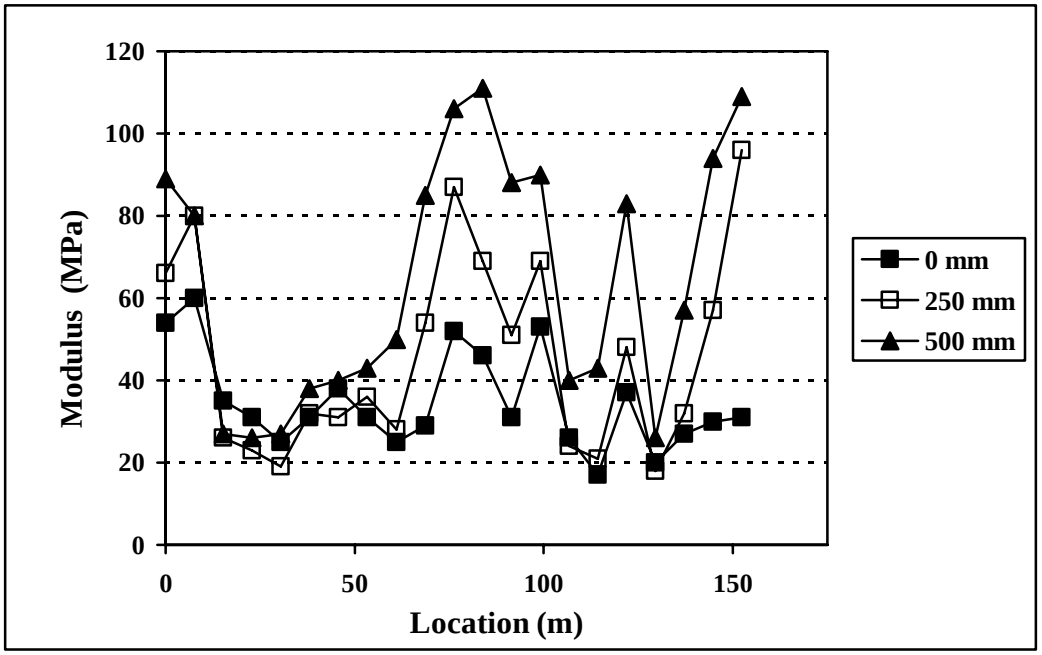

Figure 4.29: Stiffness Measured with Three Sensors - Abilene

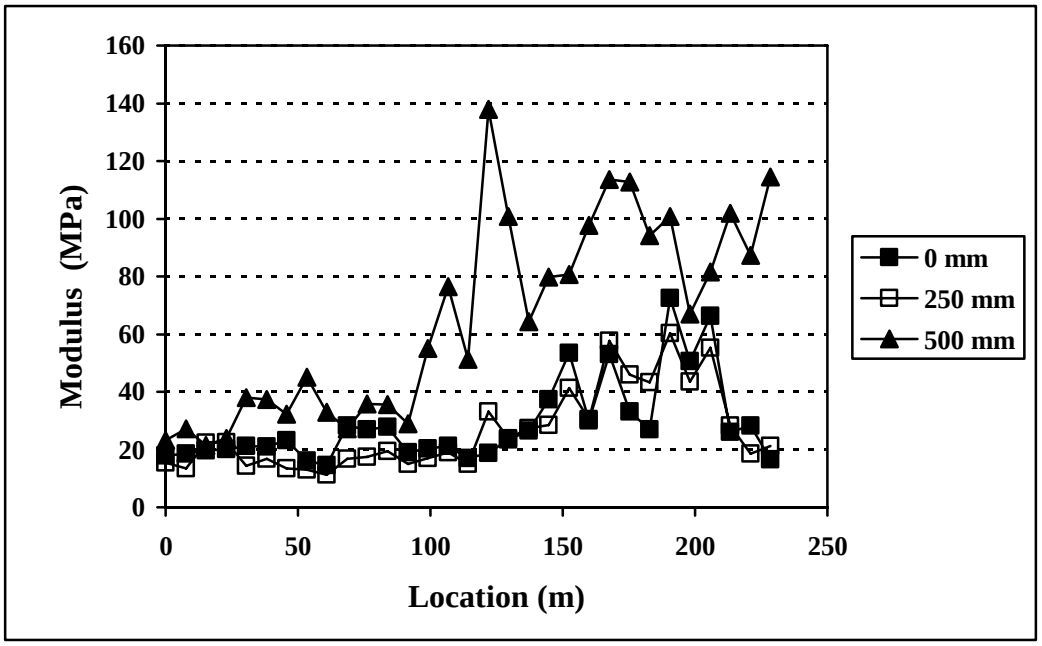

Figure 4.30: Stiffness Measured with Three Sensors - Doniphan

CHAPTER FIVE - CONCLUSIONS AND RECOMMENDATIONS

5.1 Conclusions

The objective of this study was to investigate the use of the Light Falling Weight Deflectometer (L-FWD) to measure in-situ soil stiffness and to investigate the feasibility of developing a stiffness based specification for embankment soil compaction quality control that uses the L-FWD measured stiffness.

To achieve this objective, soil stiffness values were measured at multiple locations along nine KDOT embankment projects using the Prima 100 L-FWD at more than twenty stations along each project. Density and moisture measurements were also performed at select L-FWD test stations. At the same stations where the L-FWD tests were performed, stiffness measurements were taken using the GeoGauge (on two projects) and the Falling Weight Deflectometer (on one project). Bulk soil samples were collected and remolded samples were then tested for resilient modulus in the laboratory at varying density and moisture contents. The resilient modulus tests were performed according to the AASHTO T 292-97 test protocol.

For each soil, and at each combination moisture content and dry density level used in the laboratory tests, a constitutive model was derived from the laboratory resilient modulus data to capture the stress-dependent behavior of the soil. The constitutive model was then implemented in a finite element model of a semi-infinite soil half-space to compute the deflection at the surface of the half-space for a circular load. An equivalent elastic modulus for the soil half-space was back-estimated with the Boussinesque formula, for each combination moisture content and dry density. A regression model was then developed to relate the equivalent elastic modulus of the soil

half-space to the dry density and moisture content of the soil. The regression model was used to predict the equivalent elastic moduli for the in-situ moisture contents and dry density values recorded during the field L-FWD tests. The predicted equivalent moduli were then compared to the moduli measured by the L-FWD.

The major findings of this research effort include:

- All soils exhibited a very high variability of the measured stiffness; the coefficient of variation ranged between 25.8 and 51.7 percent. Due to this high variability it is not possible to develop a quality control scheme for in-situ stiffness measurements based on a control test strip.
- The L-FWD was an effective test for determining soft spots along the test section. The measurements were repeatable, with the exception of the data recorded for silty soils (Marysville, Salina 2, and Doniphan Co. projects), for which it was observed that the soil consolidates and stiffens with the number of drops of the L-FWD weight.
- The in-situ stiffness predicted based on the laboratory determined resilient modulus did not have any correlation with the in-situ stiffness measured by the L-FWD. This lack of correlation may be due to:
    - For some moisture contents and dry density levels, the proposed constitutive model may not capture effectively the stress dependent behavior of the soil.
    - The prediction of the effective modulus of the soil half-space based on dry density and moisture content may not be accurate, especially if the

dry density and moisture content values are very different from the values used in the laboratory resilient modulus tests.

- The stress conditions the soils were subjected to during laboratory testing may not accurately replicate field stress conditions. In the laboratory test, the soil is uniformly subjected to deviatoric and volumetric stresses, while in the field, the soil near the L-FWD loading plate is subjected to higher stresses than the soil deeper in the embankment layer. Also, re-molding of laboratory samples do not replicate compaction conditions in the field, even though all the efforts were undertaken to ensure the proper compaction of the samples in the laboratory.
- In the field, the moisture content of the soil may vary within the testing area due to desiccation of the surface layer between the end of compaction and the time of stiffness testing. Also, the level of compaction of the soil may vary with depth.

- Because of the lack of statistical correlation between the L-FWD in-situ measured stiffness and the in-situ stiffness predicted for a semi-infinite half-space of stress sensitive soil, no quality control schemes based on laboratory measured moduli could be developed in this study.
- The L-FWD stiffness moduli values were compared to the stiffness moduli determined using other stiffness test methods. However, the L-FWD measured moduli showed little correlation with the GeoGauge measured moduli. The most plausible reasons are that the L-FWD and the GeoGauge

operate on different principles and that the GeoGauge applies much small stresses to the subgrade.

- On the Doniphan Co. project, where FWD and L-FWD tests were performed in parallel, it was found that the L-FWD moduli had good correlation with the moduli estimated from the FWD central deflection data using the Boussinesq equation. Possible reason for this good correlation are that L-FWD and FWD use the same loading and measuring principles and that the stresses applied to the embankment soil during the tests are similar.

5.2 Recommendations

The high variability of the stiffness modulus values prevents the development of a quality control scheme for the embankment compaction based on L-FWD measured stiffness on a control test strip. However, due to its portability and repeatability of the measurements, the L-FWD proved to be a useful tool for identifying soft spots. It is, therefore, recommended to use the L-FWD for identifying area where the soil is soft and it needs to be further compacted

When testing using the L-FWD it is recommended to use a two buffer configuration to increase the dampening of the impact load and to limit the moving of the machine during testing. It is also recommended that a smooth and level test area be provided to ensure contact between the loading plate and the test surface. This provides uniform loading and reduces machine movement during testing.

REFERENCES

Abu-Farsakh, M.Y., Alshibli, K., Nazzal, M. and Seyman, E. *Assessment of In-Situ Test Technology for Construction Control of Base Courses and Embankments Final Report*. Louisiana Department of Transportation and Development. 2004.

American Association of State Highway and Transportation Officials. *Standard Method of Test for Resilient Modulus of Subgrade Soils and Untreated Base/Subbase Material T 292-97.* AASHTO. Washington D.C. 2000.

American Association of State Highway and Transportation Officials. *Standard Specifications for Transportation Materials and Methods of Sampling and Testing Part 2*. 17th Ed. AASHTO. Washington, D.C. 1995.

Burczyk, James M., Ksaibati, Khaled, Anderson-Sprecher, Richard, and Farrar, Michael J. *Factors Influencing Determination of a Subgrade Resilient Modulus Value*. Transportation Research Record 1462, Transportation Research Board, National Research Council. Washington, D.C. 1994.

Caterpillar. *Caterpillar Performance Handbook*. 21st Edition. Caterpillar Inc. Peoria, Illinois. 1990.

Chen, J., Hossain, M., and LaTorella, T. 1995. *Use of Falling Weight Deflectometer and*
Dynamic Cone Penetrometer in Pavement Evaluation. Transportation Research Record
1655. Transportation Research Board, National Research Council. Washington, D.C. pp. 145-151. 1995.

Chua, K. M. and Lytton, R. L. *Dynamic Analysis Using the Portable Dynamic Cone Penetrometer*. Transportation Research Record 1192, Transportation Research Board, National Research Council. Washington, D.C. pp. 702-708. 1981.

Das, B.M. *Principles of Geotechnical Engineering*. Fourth Edition. PWS Publishing Company. Boston, MA. 1998.

De Beer, M. *Use of Dynamic Cone Penetrometer (DCP) in the Design of Road Structure*s. Geotechnics in African Environment. Balkema, Rotterdam. 1990.

Federal Highway Administration. *Geotechnical Aspects of Pavements*. Washington, D.C. 2005.

George, K.P. *Falling Weight Deflectometer for Estimating Subgrade Resilient Moduli Final Report*. Mississippi Department of Transportation. 2003.

George, K.P. and Uddin, W. *Subgrade Characterization for Highway Pavement Design Final Report*. Mississippi Department of Transportation. 2000.

Harrison, J.A. *Correlation of CBR and Dynamic Cone Penetrometer Strength Measurement of Soils*. Australian Road Research. Vol. 16. No.2. pp130-136. 1986.

Heukelom, W. and Klomp, A.J.G. *Dynamic Testing as Means of Controlling Pavements During and After Construction*. Proceedings of the First International Conference on Structural Design of Asphalt Pavement. University of Michigan. 1962.

Holtz, R.D. and W.D. Kovacs. *An Introduction to Geotechnical Engineering*. Prentice Hall. Englewood Cliffs, NJ. 1981.

http://www.durhamgeo.com. Accessed August 17th, 2005.

http://www.machinerytrader.com. Accessed May 18th, 2005.

http://www.k-state.edu/pavements/ Accessed April 2nd, 2006

Huang, Y. *Pavement Analysis and Design*. Prentice Hall. Englewood Cliffs, NJ. 2000.

Kansas Department of Transportation. *Standard Specifications for State Road and Bridge Construction*. Topeka, KS. pp. 184-186. 1990.

Kleyn, E. G. *The Use of the Dynamic Cone Penetrometer (DCP) Report 2/74*. Transvaal Roads Department, Pretoria. 1975.

Lenke, L. R.; McKeen, R. G.; and Grush, M. P. "Laboratory Evaluation of Geogauge for Compaction Control." *Transportation Research Board 1849*, TRB, National Research Council, Washington, D.C., 2003, pp.20- 30.

Livneh, M., and I. Ishai. *Pavement and Material Evaluation by a Dynamic Cone Penetrometer*. Proceedings of the Sixth International Conference on the Structural Design of Asphalt Pavement. Vol. 1. Ann Arbor, Michigan. pp. 665-674. 1987.

Li, Dingqing, and Selig, Ernest T. *Resilient Modulus for Fine Grained Subgrade Soils*. Journal of Geotechnical Engineering. Vol. 120. No. 6. pp. 939-957. 1994.

National Cooperative Highway Research Program, *Guide for Mechanistic-Empirical Design of New and Rehabilitated Pavement Structures Part 2 Design Inputs Chapter 2 Material Characterization. Transportation Research Board*, National Research Council, Washington, D.C., 2004

Pen, C. K. *An Assessment of the Available Methods of Analysis for Estimating the Elastic Moduli of Road Pavements*. Proceedings of the Third International Conference on Bearing Capacity of Roads and Airfields. Trondheim. 1990.

Powell, W. D., Potter, J. F., Mayhew, H. C., and Nunn, M. E. *The Structural Design of Bituminous Roads*. TRRL Report LR 1132. pp. 62. 1984.

Rollings, M.P. and Rollings, R.S. *Geotechnical Materials in Construction*. McGraw-Hill. New York, NY. 1996.

Smith, R. B., and Pratt, D. N. *A Field Study of In Situ California Bearing Ratio and Dynamic Cone Penetrometer Testing for Road Subgrade Investigation*. Australian Road Research. Vol. 13. No. 4. pp. 285-293. 1983.

Spangler, M.G. and R.L. Handy. *Soil Engineering Fourth Edition*. Harper and Row Publishers. New York, NY. 1982.

APPENDIX A - FIELD DENSITY AND MOISTURE CONTENT DATA

Table A1: Field Density and Moisture Content Results - Doniphan Co.

Doniphan Co.	Location	In-Situ Density (% ODD)	In-Situ Moisture (%OMC)
A-6/ CL	1	111.99	-11.5
	6	116.4	-8.5
	11	115.4	-11.6
	16	117.2	-11.2
	21	122.2	-7.9
	26	121.2	-8.8
	31	120.9	-9.4

Table A2: Field Density and Moisture Content Results - Garden City

Garden City US-50	Location	In-Situ Density (% ODD)	In-Situ Moisture (%OMC)
A-2-4/ SC-SM	1	95.2	-5.20
	6	98.7	-1.30
	11	95.7	-5.90
	16	99.7	-3.40
	21	96.5	-5.70
	26	97.4	-6.10
	31	93.3	-6.50
	36	97.7	-3.80

Table A3: Field Density and Moisture Content Results - Hill City

Hill City US-283	Location	In-Situ Density (% ODD)	In-Situ Moisture (%OMC)
A-6/ CL	1	104.4	-1.00
	6	93.1	-5.70
	11	103.5	-6.10
	16	101	-2.70
	21	103.7	-4.40
	26	101.1	-2.70
	31	106.6	-3.40
	36	102.9	-2.70

Table A4: Field Density and Moisture Content Results - Manhattan

Manhattan	Location	In-Situ Density (% ODD)	In-Situ Moisture (%OMC)
A-7-6/ CL	1	106	-11.9
	6	110	-8.9
	11	109	-12
	16	111	-11.6
	21	115	-8.3
	26	115	-9.2
	31	114	-9.8

Table A5: Field Density and Moisture Content Results - Marysville

Marysville US-77	Location	In-Situ Density (% ODD)	In-Situ Moisture (%OMC)
A-4/ ML	5	101.3	-0.1
	10	96.6	-2.2
	15	102.5	-0.2
	20	101.4	1.2
	25	102.5	-1.2
	30	103.4	-4.1
	35	95.1	-2.3

Table A6: Field Density and Moisture Content Results - Sabetha

Sabetha US-75	Location	In-Situ Density (% ODD)	In-Situ Moisture (%OMC)
A-7-6/ CL	1	100.8	-3.5
	6	98.3	-2.4
	11	100.0	-4.0
	16	97.4	-1.0
	21	95.8	1.6
	26	94.2	1.9
	31	87.3	4.4
	36	92.6	2.2

Table A7: Field Density and Moisture Content Results - Salina 1

Salina I-70	Location	In-Situ Density (% ODD)	In-Situ Moisture (%OMC)
A-6/ CL	1	116.1	-0.5
	5	92.2	0.3
	10	97.1	-0.5
	15	93.3	2.6
	20	90.7	-1.5
	25	94.0	-0.7

Table A8: Field Density and Moisture Content Results - Salina 2

Salina 2 I-70	Location	In-Situ Density (% ODD)	In-Situ Moisture (%OMC)
A-7-6/ CL	1	101.5	-3.7
	6	96.4	1.0
	11	96.0	1.4
	16	98.3	5.6
	21	94.0	-1.5
	26	97.9	0.3
	31	100.3	-3.2

APPENDIX B - FIELD RESILIENT MODULUS DATA

Table B1: Field Stiffness Modulus Results - Abilene

Point	Distance (m)	Modulus (MPa)	Point	Distance (m)	Modulus (MPa)
1	0.00	54	12	83.82	46
2	7.62	60	13	91.44	31
3	15.24	35	14	99.06	53
4	22.86	31	15	106.68	26
5	30.48	25	16	114.30	17
6	38.10	31	17	121.92	37
7	45.72	38	18	129.54	20
8	53.24	31	19	137.16	27
9	60.96	25	20	144.78	30
10	68.58	29	21	152.40	31
11	76.20	52			

Table B2: 3 Sensor Field Stiffness Modulus Results - Abilene

Point	Modulus (MPa)			Point	Modulus (MPa)		
	0-mm	250-mm	500-mm		0-mm	250-mm	500-mm
1	54	66	89	12	46	69	111
2	60	80	80	13	31	51	88
3	35	26	27	14	53	69	90
4	31	23	26	15	26	24	40
5	25	19	27	16	17	21	43
6	31	32	38	17	37	48	83
7	38	31	40	18	20	18	26
8	31	36	43	19	27	32	57
9	25	28	50	20	30	57	94
10	29	54	85	21	31	96	109
11	52	87	106				

Table B3: Field Stiffness Modulus Results - Doniphan Co.

Point	Distance (m)	Modulus (MPa)	Point	Distance (m)	Modulus (MPa)
1	0.00	18	17	121.92	19
2	7.62	19	18	129.54	24
3	15.24	20	19	137.16	27
4	22.86	20	20	144.78	37
5	30.48	21	21	152.40	54
6	38.10	21	22	160.02	30
7	45.72	23	23	167.64	53
8	53.24	16	24	175.26	33
9	60.96	15	25	182.88	27
10	68.58	28	26	190.50	72
11	76.20	27	27	198.12	51
12	83.82	28	28	205.74	66
13	91.44	19	29	213.36	26
14	99.06	20	30	220.98	28
15	106.68	21	31	228.60	17
16	114.30	17			

Table B4: GeoGauge Field Stiffness Modulus Results - Doniphan Co.

Point	Distance (m)	Modulus (MPa)	Point	Distance (m)	Modulus (MPa)
1	0.00	37	17	121.92	53
2	7.62	44	18	129.54	56
3	15.24	49	19	137.16	67
4	22.86	40	20	144.78	74
5	30.48	40	21	152.40	80
6	38.10	53	22	160.02	70
7	45.72	45	23	167.64	82
8	53.24	47	24	175.26	67
9	60.96	50	25	182.88	66
10	68.58	62	26	190.50	57
11	76.20	73	27	198.12	58
12	83.82	57	28	205.74	43
13	91.44	45	29	213.36	68
14	99.06	54	30	220.98	67
15	106.68	62	31	228.60	55
16	114.30	56			

Table B5: FWD Field Stiffness Modulus Results - Doniphan Co.

Point	Distance (m)	Modulus (MPa)	Point	Distance (m)	Modulus (MPa)
1	0.00	15	17	121.92	17
2	7.62	14	18	129.54	18
3	15.24	14	19	137.16	23
4	22.86	15	20	144.78	28
5	30.48	17	21	152.40	39
6	38.10	15	22	160.02	26
7	45.72	14	23	167.64	49
8	53.24	16	24	175.26	32
9	60.96	17	25	182.88	28
10	68.58	16	26	190.50	75
11	76.20	13	27	198.12	42
12	83.82	15	28	205.74	51
13	91.44	16	29	213.36	28
14	99.06	16	30	220.98	16
15	106.68	18	31	228.60	30
16	114.30	15			

Table B6: 3 Sensor Field Stiffness Modulus Results – Doniphan Co.

Point	Modulus (MPa)			Point	Modulus (MPa)		
	0-mm	250-mm	500-mm		0-mm	250-mm	500-mm
1	18	16	23	17	19	33	138
2	19	13	27	18	24	24	101
3	20	22	22	19	27	27	64
4	20	23	24	20	37	29	80
5	21	14	38	21	54	41	81
6	21	17	37	22	30	30	98
7	23	14	32	23	53	58	114
8	16	13	45	24	33	46	113
9	15	11	33	25	27	43	94
10	28	17	27	26	72	60	101
11	27	18	36	27	51	43	67
12	28	20	36	28	66	55	82
13	19	15	29	29	26	28	102
14	20	17	55	30	28	19	87
15	21	19	76	31	17	21	114
16	17	15	51				

Table B7: Field Stiffness Modulus Results - Garden City

Point	Distance (m)	Modulus (MPa)	Point	Distance (m)	Modulus (MPa)
1	7.62	145	19	129.54	60
2	15.24	99	20	137.16	69
3	22.86	57	21	144.78	110
4	30.48	62	22	152.40	113
5	38.10	75	23	160.02	74
6	45.72	95	24	167.64	111
7	53.24	74	25	175.26	114
8	60.96	137	26	182.88	141
9	68.58	78	27	190.50	87
10	76.20	99	28	198.12	125
11	83.82	72	29	205.74	90
12	91.44	111	30	213.36	80
13	99.06	137	31	220.98	91
14	106.68	70	32	228.60	132
15	114.30	84	33	236.22	126
16	121.92	61	34	243.84	101
17	7.62	145	35	251.46	102
18	15.24	99	36	259.08	125

Table B8: Field Stiffness Modulus Results - Hill City

Point	Distance (m)	Modulus (MPa)	Point	Distance (m)	Modulus (MPa)
1	7.62	88	22	167.64	99
2	15.24	103	23	175.26	123
3	22.86	64	24	182.88	132
4	30.48	56	25	190.50	58
5	38.10	137	26	198.12	91
6	45.72	29	27	205.74	56
7	53.24	105	28	213.36	103
8	60.96	58	29	220.98	127
9	68.58	70	30	228.60	100
10	76.20	58	31	236.22	86
11	83.82	98	32	243.84	96
12	91.44	64	33	251.46	81
13	99.06	48	34	259.08	86
14	106.68	77	35	266.70	97
15	114.30	55	36	274.32	149
16	121.92	115	37	281.94	133
17	129.54	60	38	289.56	136
18	137.16	35	39	297.18	72
19	144.78	114	40	304.80	181
20	152.40	42	41	312.42	93
21	160.02	115			

Table B9: Field Stiffness Modulus Results - Manhattan

Point	Distance (m)	Modulus (MPa)	Point	Distance (m)	Modulus (MPa)
1	0.00	23	17	121.92	83
2	7.62	31	18	129.54	75
3	15.24	17	19	137.16	34
4	22.86	19	20	144.78	36
5	30.48	31	21	152.40	58
6	38.10	34	22	160.02	33
7	45.72	24	23	167.64	80
8	53.24	29	24	175.26	34
9	60.96	40	25	182.88	53
10	68.58	23	26	190.50	45
11	76.20	18	27	198.12	19
12	83.82	33	28	205.74	48
13	91.44	24	29	213.36	25
14	99.06	21	30	220.98	29
15	106.68	24	31	228.60	37
16	114.30	37			

Table B10: GeoGauge Field Stiffness Modulus Results - Manhattan

Point	Distance (m)	Modulus (MPa)	Point	Distance (m)	Modulus (MPa)
1	0.00	57	17	121.92	77
2	7.62	64	18	129.54	92
3	15.24	57	19	137.16	48
4	22.86	62	20	144.78	64
5	30.48	77	21	152.40	64
6	38.10	70	22	160.02	58
7	45.72	68	23	167.64	64
8	53.24	64	24	175.26	65
9	60.96	61	25	182.88	54
10	68.58	52	26	190.50	75
11	76.20	61	27	198.12	56
12	83.82	52	28	205.74	43
13	91.44	53	29	213.36	62
14	99.06	58	30	220.98	60
15	106.68	71	31	228.60	65
16	114.30	58			

Table B11: Field Stiffness Modulus Results - Marysville 4 Buffer

Point	Distance (m)	Modulus (MPa)	Point	Distance (m)	Modulus (MPa)
1	0.00	32	19	274.32	26
2	15.24	41	20	289.56	63
3	30.48	29	21	304.80	75
4	45.72	41	22	320.04	70
5	60.96	65	23	335.28	65
6	76.20	71	24	350.52	45
7	91.44	73	25	365.76	30
8	106.68	75	26	381.00	74
9	121.92	78	27	396.24	76
10	137.16	75	28	411.48	27
11	152.40	61	29	426.72	65
12	167.64	86	30	441.96	29
13	182.88	43	31	457.20	39
14	198.12	79	32	472.44	50
15	213.36	74	33	487.68	68
16	228.60	82	34	502.92	72
17	243.84	27	35	518.16	64
18	259.08	80			

Table B12: Field Stiffness Modulus Results - Marysville 2 Buffer

Point	Distance (m)	Modulus (MPa)	Point	Distance (m)	Modulus (MPa)
1	0.00	28	6	76.20	31
2	15.24	20	7	91.44	19
3	30.48	30	8	106.68	23
4	45.72	18	9	121.92	37
5	60.96	39	10	137.16	47

Table B13: GeoGauge Field Stiffness Modulus Results - Marysville

Point	Distance (m)	Modulus (MPa)	Point	Distance (m)	Modulus (MPa)
1	0.00	58	19	274.32	32
2	15.24	48	20	289.56	36
3	30.48	44	21	304.80	24
4	45.72	45	22	320.04	43
5	60.96	39	23	335.28	73
6	76.20	26	24	350.52	84
7	91.44	21	25	365.76	75
8	106.68	29	26	381.00	23
9	121.92	45	27	396.24	63
10	137.16	25	28	411.48	49
11	152.40	19	29	426.72	46
12	167.64	46	30	441.96	60
13	182.88	47	31	457.20	47
14	198.12	42	32	472.44	60
15	213.36	36	33	487.68	29
16	228.60	42	34	502.92	41
17	243.84	49	35	518.16	34
18	259.08	48			

Table B14: Field Stiffness Modulus Results - Sabetha

Point	Distance (m)	Modulus (MPa)	Point	Distance (m)	Modulus (MPa)
1	7.62	47	19	144.78	70
2	15.24	115	20	152.40	40
3	22.86	48	21	160.02	75
4	30.48	80	22	167.64	34
5	38.10	90	23	175.26	30
6	45.72	41	24	182.88	87
7	53.24	50	25	190.50	68
8	60.96	25	26	198.12	44
9	68.58	36	27	205.74	76
10	76.20	17	28	213.36	101
11	83.82	35	29	220.98	81
12	91.44	55	30	228.60	71
13	99.06	47	31	236.22	37
14	106.68	48	32	243.84	105
15	114.30	57	33	251.46	37
16	121.92	22	34	259.08	52
17	129.54	52	35	266.70	60
18	137.16	57	36	274.32	65

Table B15: Field Stiffness Modulus Results - Salina 1

Point	Distance (m)	Modulus (MPa)	Point	Distance (m)	Modulus (MPa)
1	15.24	38	14	213.36	18
2	30.48	20	15	228.60	53
3	45.72	54	16	243.84	47
4	60.96	26	17	259.08	42
5	76.20	28	18	274.32	58
6	91.44	23	19	289.56	56
7	106.68	43	20	304.80	47
8	121.92	33	21	320.04	52
9	137.16	44	22	335.28	29
10	152.40	15	23	350.52	47
11	167.64	48	24	365.76	38
12	182.88	17	25	381.00	29
13	198.12	23			

Table B16: Field Stiffness Modulus Results - Salina 2

Point	Distance (m)	Modulus (MPa)	Point	Distance (m)	Modulus (MPa)
1	7.62	35	17	129.54	27
2	15.24	32	18	137.16	40
3	22.86	42	19	144.78	33
4	30.48	27	20	152.40	40
5	38.10	44	21	160.02	56
6	45.72	28	22	167.64	59
7	53.24	52	23	175.26	68
8	60.96	60	24	182.88	34
9	68.58	27	25	190.50	33
10	76.20	38	26	198.12	27
11	83.82	25	27	205.74	28
12	91.44	18	28	213.36	48
13	99.06	37	29	220.98	23
14	106.68	15	30	228.60	14
15	114.30	18	31	236.22	17
16	121.92	28			

APPENDIX C - LABORATORY RESILIENT MODULUS

Table C1: Laboratory Resilient Modulus- Doniphan Co.

Dry Density	Moisture Content	Deviator Stress				
		21 kPa	34 kPa	48 kPa	69 kPa	103 kPa
90%	-5%	81.50	78.00	70.40	66.40	61.80
	OMC	62.20	57.10	51.70	48.00	46.10
	+5%	43.30	37.60	33.60	31.80	36.80
95%	-5%	118.80	108.30	102.00	94.70	87.90
	OMC	69.20	61.70	55.60	51.20	49.10
	+3%	43.90	42.40	37.80	35.30	32.70
100%	-5%	307.40	255.80	220.90	191.90	174.40
	OMC	56.20	54.60	54.30	50.10	49.20
	+3%	35.80	31.50	28.50	28.90	30.80

Table B2: Laboratory Resilient Modulus - Garden City

Dry Density	Moisture Content	Deviator Stress				
		21 kPa	34 kPa	48 kPa	69 kPa	103 kPa
90%	-5%	101.60	96.56	90.32	92.99	97.98
	OMC	66.49	62.34	63.28	61.46	-
	+2%	52.31	53.10	51.05	53.01	-
95%	-5%	114.89	106.95	111.98	112.18	112.78
	OMC	79.99	74.17	78.17	76.72	80.76
	+2%	62.58	62.46	59.35	60.20	-
100%	-5%	160.06	158.51	142.15	145.45	142.80
	OMC	74.17	71.28	70.85	74.82	81.62
	+2%	56.41	53.81	56.62	60.20	-

Table B3: Laboratory Resilient Modulus - Hill City

Dry Density	Moisture Content	Deviator Stress				
		21 kPa	34 kPa	48 kPa	69 kPa	103 kPa
90%	-5%	168.72	146.81	145.83	134.90	122.59
	OMC	79.07	70.42	62.88	57.31	50.58
	+2%	65.42	58.55	50.50	46.97	42.32
95%	-5%	158.61	129.20	120.82	120.24	119.13
	OMC	130.15	101.90	84.55	72.54	65.17
	+2%	79.87	73.27	63.17	56.85	51.61
100%	-5%	159.39	152.74	146.61	154.60	151.63
	OMC	120.22	107.55	94.14	89.35	78.88
	+2%	74.65	70.75	59.74	54.40	49.18

Table B4: Laboratory Resilient Modulus - Manhattan

Dry Density	Moisture Content	Deviator Stress				
		21 kPa	34 kPa	48 kPa	69 kPa	103 kPa
90%	-5%	107.40	98.30	89.20	77.20	67.80
	OMC	71.50	63.60	57.30	48.90	40.30
	+2%	63.20	51.70	42.80	33.70	34.10
95%	-5%	79.50	76.10	71.80	66.40	63.30
	OMC	63.10	57.40	52.30	45.00	40.40
	+2%	67.30	53.70	42.70	31.80	29.60
100%	-5%	116.10	120.10	115.50	109.80	99.70
	OMC	83.70	74.70	63.90	53.90	43.40
	+2%	53.40	40.30	30.00	26.20	0.00

Table B5: Laboratory Resilient Modulus - Marysville

Dry Density	Moisture Content	Deviator Stress				
		21 kPa	34 kPa	48 kPa	69 kPa	103 kPa
90%	-5%	97.60	98.20	96.70	95.70	95.70
	OMC	75.60	67.70	65.90	64.20	61.60
	+2%	60.30	51.70	47.80	43.10	41.70
95%	-5%	122.60	122.90	130.70	126.60	127.40
	OMC	78.50	77.80	79.40	75.90	61.60
	+2%	61.00	53.00	46.50	42.80	38.80
100%	-5%	132.90	132.10	139.80	144.00	146.50
	OMC	158.50	147.20	140.30	124.70	113.90
	+2%	59.10	49.50	43.60	38.60	-

Table B6: Laboratory Resilient Modulus - Sabetha

Dry Density	Moisture Content	Deviator Stress				
		21 kPa	34 kPa	48 kPa	69 kPa	103 kPa
90%	-5%	110.30	108.60	107.70	108.70	108.00
	OMC	101.00	96.60	100.20	97.50	94.20
	+2%	97.00	93.50	86.70	82.20	76.70
95%	-5%	122.30	123.20	121.00	122.90	124.50
	OMC	168.30	161.40	152.00	155.90	151.50
	+2%	109.60	128.30	124.30	134.80	135.10
100%	-5%	138.40	134.60	132.50	142.30	145.20
	OMC	209.20	210.30	213.20	208.90	208.40
	+2%	162.30	155.40	152.30	153.10	153.00

Table B7: Laboratory Resilient Modulus - Salina 1

Dry Density	Moisture Content	Deviator Stress				
		21 kPa	34 kPa	48 kPa	69 kPa	103 kPa
90%	-5%	129.60	123.80	123.90	118.70	120.40
	OMC	79.10	77.80	76.50	78.70	75.90
	+5%	70.80	58.20	50.30	42.60	-
95%	-5%	143.50	145.20	145.90	144.60	142.60
	OMC	92.80	97.40	105.60	119.10	122.40
	+5%	47.45	81.85	67.68	58.89	54.02
100%	-5%	182.50	183.80	184.00	182.80	190.60
	OMC	158.30	149.30	146.70	142.10	134.90
	+5%	39.10	35.70	28.40	-	-

Table B8: Laboratory Resilient Modulus - Salina 2

Dry Density	Moisture Content	Deviator Stress				
		21 kPa	34 kPa	48 kPa	69 kPa	103 kPa
90%	-5%	104.60	101.60	96.80	92.80	86.70
	OMC	57.20	55.30	52.80	52.80	53.70
	+2%	51.80	46.40	45.10	41.10	38.30
95%	-5%	128.50	131.20	132.20	132.90	136.10
	OMC	84.70	77.90	74.20	66.90	62.50
	+2%	69.80	64.00	59.10	54.70	48.60
100%	-5%	154.20	150.30	142.40	142.00	135.30
	OMC	90.70	85.30	80.10	77.80	72.50
	+2%	85.10	84.50	76.30	67.80	56.30

K-TRAN

KANSAS TRANSPORTATION RESEARCH
AND
NEW - DEVELOPMENTS PROGRAM

A COOPERATIVE TRANSPORTATION RESEARCH PROGRAM BETWEEN:

KANSAS DEPARTMENT OF TRANSPORTATION

THE UNIVERSITY OF KANSAS

KANSAS STATE UNIVERSITY